SYNCHRONIZATION OF CONTINUOUS-TIME OSCILLATORS AND ITS CONTROL

by

Elif Köksal

B.S., Control Engineering, Istanbul Technical University, 2010

Submitted to the Institute for Graduate Studies in
Science and Engineering in partial fulfillment of
the requirements for the degree of
Master of Science

Graduate Program in M.S. in Electrical and Electronic Engineering
Boğaziçi University
2012

SYNCHRONIZATION OF CONTINUOUS-TIME OSCILLATORS AND ITS
CONTROL

APPROVED BY:

Assoc. Prof. Yağmur Denizhan ....
(Thesis Supervisor)

Prof. Işıl Bozma ....

Prof. Leyla Gören Sümer ....

DATE OF APPROVAL: 07.06.2012

ACKNOWLEDGEMENTS

ABSTRACT

SYNCHRONIZATION OF CONTINUOUS-TIME OSCILLATORS AND ITS CONTROL

In this thesis, synchronization of continuous-time oscillators with respect to the effects which are bases on the network structure the properties of the oscillators and its control are studied. In the context of synchronization, synchronization of the periodic oscillators in different network topologies is considered. It is observed that the topological properties of networks are crucial for synchronization. Then, similarity-dependent coupling approach is introduced and the effect of this formulation on synchronization is examined. Furthermore, synchronization in ensembles of chaotic oscillators is analyzed. In the control part, synchronization control is studied in ensembles of globally coupled chaotic oscillators. Two different control methods are proposed: time-delayed feedback and forcing with external periodic action. In the first one, the mean-field is fed back in a time-delayed manner to all oscillators. In the second one, cases are studied where an external periodic force is applied both to the mean-field and to all the oscillators individually. It is observed that depending on the control technique and related parameters, synchronization can be enhanced, suppressed or destroyed. Another contribution of this thesis is a basic user interface for studying synchronization of continuous-time oscillators in complex networks.

ÖZET

SÜREKLİ ZAMANLI OSİLATÖRLERİN SENKRONİZASYONU VE BUNUN KONTROLÜ

Bu tezde, sürekli zamanlı osilatörlerin ağ yapısına ve osilatör özelliklerinin etkileri bağlamında senkronizasyon ve senkronizasyonun kontrolü çalışılmıştır. Senkronizasyon kavramı altında, farklı ağ topolojilerindeki periyodik osilatörlerin durumu değerlendirilmiştir. Ağın topolojik özelliklerinin senkronizasyon için kritik olduğu gözlenmiştir. Ardında, benzerliğe dayalı bağlantı yaklaşımı tanıtılmış ve bu formülasyonun senkronizasyon üzerindeki etkisi incelenmiştir. Ek olarak, kaotik osilatör topluluklarının senkronizasyonu analiz edilmiştir. Kontrol başlığında, global olarak bağlanmış kaotik osilatörler topluluklarında senkronizasyon kontrolü çalışılmıştır. İki farklı kontrol yöntemi önerilmiştir: zaman-gecikmeli geribesleme ve harici periyodik kuvvet ile zorlama. İlkinde, ortak-alan tüm osilatörlere gecikmeli olarak geri beslenilmiştir. İkincisinde, periyodik bir kuvvetin dışarıdan hem ortak-alana hem de osilatörlerin her birine uygulandığı durumlar incelenmiştir. Kontrol yöntemine ve ilgili parametrelere bağlı olarak, senkronizayonun iyileştirilebildiği, bastırılabildiği veya ortadan kaldırılabildiği gözlenmiştir. Bu tezin bir başka katkısı da karmaşık ağlardaki sürekli zamanlı osilatörlerde senkronizasyon çalışmaları için hazırlanmış olan kullanıcı arayüzüdür.

TABLE OF CONTENTS

LIST OF FIGURES

LIST OF TABLES

LIST OF SYMBOLS

a_{ij}	Elements of the adjacency matrix
$\mathbf{A}$	Adjacency matrix
$coff_{S,T}$	Correlation coefficient between variables S and T
C	External periodic force amplitude
$\hat{\mathbf{C}}$	Coupling matrix
d_{ij}	Length of the shortest-path between node i and node j
D	Dimension of a regular lattice
$e(t)$	State difference
$f(.)$	Gauissian probability density function
$\mathbf{f}(.)$	Vector function representing dynamical system
F	Feedback signal
$\mathbf{F}$	Vector field
$\mathbf{h}$	Driving function
$\mathbf{I}$	Identity matrix
k_i	Degree of node i
k_{max}	Maximum node degree of a network
k_{min}	Minimum node degree of a network
K	Time-delayed feedback amplitude
l	Actual number of edges in a network
l_s	Average shortest-path length
L	Maximum number of edges in a network
m	Degree of new coming nodes
m_0	Initial number of nodes in the generation of scale-free networks
M	Dimension of a dynamical system
N	Number of nodes in a network
$\aleph$	Gaussian distribution representation
p	Connection probability

$\mathbf{p_{ij}}(.)$	Coupling function between node i and node j
$P(k)$	Scale-free degree distribution function in complex networks
$q(.)$	Averaged function of slow oscillating terms of Q
$Q_{ij}(.)$	2π-periodic function of the arguments of node i and node j
r	Bifurcation parameter of the Lorenz system
$S(.)$	Similarity function
T	Period of oscillation
v	Frequency of the external periodic force
$V(t)$	Ensemble deviation
$\mathbf{x}, \mathbf{y}, \mathbf{z}$	Vector representation of system states
x_i, y_i, z_i	States of the ith system
X	Mean-field
X_d	Time-delayed mean-field
w_i	Natural frequency of the ith oscillator/ Parameter of the ith chaotic Rössler oscillator
$\delta\mathbf{Z}$	Distance between two trajectories
Δw	Mismatch between natural frequencies or some other parameters
ε	Coupling strength
ε_{avg}	Average coupling strength
ε_c	Critical coupling strength
ε_{ij}	Coupling strength between node i and node j
Θ	Phase of a periodic external force
λ	Lyapunov exponent
μ	Mean of Gaussian distribution
ξ	Mapping representation
σ	Standard deviation of Gaussian distribution
τ	Delay time
ϕ_i	Phase of the ith oscillator
ψ	Phase difference

Ω_i (Mean) Observed frequency of the ith oscillator

LIST OF ACRONYMS/ABBREVIATIONS

AS	Almost Synchronization
BA	Barabasi-Albert
CE	Caenorhabditis Elegans
CS	Complete Synchronization
ER	Erdös-Rényi
GS	Generalized Synchronization
ILS	Intermittent Lag Synchronization
IPS	Imperfect Phase Synchronization
LS	Lag Synchronization
OGY	Ott-Grebogi-Yorke
OPF	Occasional Proportional Feedback
PS	Phase Synchronization
UPO	Unstable Periodic Orbit
WS	Watts-Strogatz
WWW	World Wide Web

1. INTRODUCTION

The word "synchronous" is a combination of two Greek word, $\chi\rho\acute{o}\nu\varsigma$ (*chronos*, meaning time) and $\sigma\acute{u}\nu$ (*syn*, meaning the same), that can be interpreted as "occurring or existing at the same time ", or "recurring or operating at exactly the same periods". Thus, the term "synchronization" is used to describe various phenomena in almost all branches, from engineering to social life, from natural sciences to psychology.

Synchronization, from dynamical systems' point of view, is the science of coupled oscillators, such as planets, pacemaker cells and so on. An oscillatory system rotates automatically that repeat itself over and overall again at more or less time intervals. Usually such systems are not isolated from their environment, but interact with other systems. Two or more oscillators are said to be coupled if there exists some mechanism which allows them influence each other. For example, fireflies interact via light signal, planets tug on each other via gravity, heart pacemakers transmit electrical currents. The result of the coupling between such oscillators, is often synchrony, i.e. the state when all oscillators, or at least a great portion of them, begin to move as one. Neurons fire together, bacteria colonize, tree crickets sing together, audiences applause rhythmically, biological clocks follow their daily cycles, a violinist play in unison with his neighbors.

Depending on the system, synchronization of an ensemble may introduce more robust performance or yield destructive effects in terms of achieving the target of the system. Thus control of synchronization is required for maintaining the collective behavior or heading it off.

The essence of this thesis is synchronization defined as *the adjustment of rhythms of oscillating systems due to an interaction among each other.* The aim of this thesis is to investigate synchronization phenomena for different types of oscillators, interacting in different manners, placed in various networks and endowed with the possibility of

influencing this collective behavior. The topics can be categorized into two groups: synchronization and synchronization control. Firstly, synchronization concept is investigated with respect to the effects which are bases on the network structure the properties of the oscillators. Then, the performance of different control techniques on influencing the synchronous behavior of the ensemble is studied.

In the second chapter, after presenting a historical background and different examples from various scientific fields, the basic concepts of synchronization are introduced, such as an oscillating object, notion of rhythm, interaction and adjustment of rhythms. In the third chapter, the tools used for qualifying the collective behavior and a user interface designed via MATLAB are given. The fourth chapter covers the experimental results. The fifth chapter, contains the discussion and conclusion of the whole study carried out.

2. THEORETICAL BACKGROUND OF SYNCHRONIZATION AND PROBLEM STATEMENT

Since the topic of this thesis combines several fields of investigation theoretical background of each of them will be provided here: After presenting graph representation and complex networks in a nutshell, some basic concepts related to dynamical systems will be given. Then, the phenomena of synchronization and its terminology will be introduced.

2.1. Graph Representation and Complex Networks

In real world, systems are typically composed of a large number of highly connected dynamical units. Coupled biological and chemical systems, neural networks, social interacting species, the Internet, and the World Wide Web (WWW), are only a few examples of such systems. The scientific desire to understand structural issues and dynamics running on networks generated a whole research field of *complex networks*. Complex networks are the networks the structure of which is irregular, complex and dynamically evolving in time with thousands or millions of nodes. With the possibility of assessing large databases, this area is very hot and continuing to develop [5].

Networks are generated in different domains by different dynamics with different number of nodes and with different number of edges. The structures of natural networks are result of evolution which provides optical functionality in some sense. Indeed, it has been shown that the coupling architecture has important consequences on the network functional robustness and response to the external perturbations. Network topology has a crucial role in determining the emergence of collective dynamical behavior, such as synchronization and spreading of epidemics, information and rumors. For example, from neural perspective, synchronization in neural networks are found to be correlated to many cognitive functions such as information transfer, perception, motor control and memory [6–8].

Networks are represented with graphs consist N *nodes* which are connected with L *edges*. Edge l_{ij} describes the connection between the node i and node j. The *adjacency matrix*, $\mathbf{A}$, is an $N \times N$ matrix with entries a_{ij}. If two node is connected $a_{ij} = 1$, otherwise $a_{ij} = 0$. k_i shows the number of edges going out of a node, namely *degree of a node*. Also some measurements are defined the characterization, e.g. *average shortest-path length*, $l_s = <d_{ij}>$ where d_{ij} is the length of the shortest path connecting node i and node j, and *clustering coefficient* for accounting the number of triangles.

During the construction of a real network, whatever the systems is, some common topological aspects exist, such as small-world property, scale-free degree distribution, correlations, and presence of clustering. Researchers try to understand real complex networks and model them via these common bases. Here, small world property and scale-free degree distribution will be introduced after mentioning random graphs.

The term *random graph* refers to the disordered nature of the arrangement of the links between different nodes. Erdös and Réyni proposed a model for generating random graphs with respect to some probabilistic methods [9] and they study the properties of graphs as a function of the increasing number of random connections. For such a network, called *Erdös-Réyni (ER) network*, topological properties depend on the connection probability between the nodes. They proposed that for large graphs the degree distribution can be well approximated by a Poisson distribution.

The first topological property to be introduced is the small-world property. In a D-dimensional regular lattice, the mean number of vertices to be transferred in order to reach an arbitrary node grows with the lattice size as $N^{1/D}$. Contrarily, in most of real networks, despite of their large sizes, there exist short-cuts between nodes which decrease the average shortest path length of the networks. Although, existence of short-cuts is an obvious mathematical property in random graphs, real networks are highly clustered compared to random network. The property of both having high clustering coefficient and small average shortest-path length value is called *small-world property*. *Watts-Strogatz (WS) network* is a network model with small-world property [4].

Another important topological property is the scale-free degree distribution. The datasets of real networks such as WWW and Internet show that the degree distribution is not homogeneous as random graphs but heterogeneous ruling by a power law degree distribution. This property is called *scale-free degree distribution property*. *Barabasi-Albert (BA) network* model is a network model based on two basic ingredients: growth and preferential attachment [10]. A scale-free degree distribution is an outcome of preferential attachment of the new coming nodes, where a node prefers to attach to the one with the highest connectivity. Scale-free degree distribution is associated with the existence of hubs in a network.

2.2. Some Basic Concepts and Methods Related to Dynamical Systems

A continuous-time dynamical system is represented in terms of differential equations of the form:

$$\dot{\mathbf{x}} = \mathbf{f}(\mathbf{x}). \tag{2.1}$$

In Equation 2.1, $\mathbf{x}$ is a M-dimensional *state vector*, $[x_1, x_2, \ldots, x_M]^T$ where x_i are the *states* of the system. Behavior of the system can be described completely by the time evolution of its states.

State space is a M-dimensional space whose coordinated are the states of the system. A *trajectory* is a curve in the state space representing a time solution of the system, $\mathbf{x}(t)$, starting with initial conditions $\mathbf{x}(0)$. *Phase portrait* is a geometric representation of the time solutions of the dynamical system starting from arbitrarily initial conditions. Phase portrait shows the overall picture of trajectories in the state space.

In dynamical systems, both "state" and "phase" are used to refer systems variables, such that state space is also known as phase space. It should be noted that, in this thesis, the term "state" is used for indicating the system variables as in the control

theory and the term "phase" is used for to describe angular component of the system states.

In physical sense, dissipation is related to dissipating the initial energy, eventually coming to a standstill. From the mathematical point of view, dissipation refers to shrinking state space (hyper) volume. The trajectories of a dissipative system move towards the *attractors* in the state space which characterize the typical behaviors of the system. An attractor can be of the following types: *equilibrium point, limit cycle, limit tori* or *strange attractor*.

There exist some metrics which are used for characterizing the stability of a dynamical system. One of them is *Lyapunov exponents* which describes the rate of separation of infinitesimally close trajectories. If the two nearby trajectories in the state space start off with an initial separation $\delta\mathbf{Z}_0$, then the divergence dynamics in one dimension can be written as in Equation 2.2, where λ is represents the Lyapunov exponent. Divergence corresponds to a positive Lyapunov exponent, whereas convergence is described with a negative exponent. If the two trajectories neither converge nor diverge from each other, the corresponding Lyapunov exponent is zero. A M-dimensional system has M Lyapunov exponents. If a system is dissipative, sum of the Lyapunov exponents of this system is negative.

$$\|\delta\mathbf{Z}(t)\| = \|\delta\mathbf{Z}_0\|e^{\lambda t} \tag{2.2}$$

The *method of Poincaré surface of section* is used, in general, to detect the existence of closed curves in the phase portrait of a dynamical systems and determine their stability. In this method a $(M-1)$-dimensional surface of section, the so-called Poincaré surface, is constructed in the phase portrait of the M-dimensional system with a direction of piercing. This surface is supposed to be placed transversal to the flow of the system. This powerful tool for detecting periodic orbits is also used to define the concept of *phase*, as it is done in this thesis.

Before moving on, a special type of dynamical systems, which have strange attractors, *chaotic systems* (dissipative chaotic systems), should be mentioned. The term "chaotic" refers to long-term behavior of a dynamical system which cannot be predicted even if there are no fluctuations of the system's parameters or influence of a noisy environment. Strogatz defined chaos (dissipative chaos) as "aperiodic long-term behavior in a deterministic system that exhibits sensitive dependence to initial conditions" [11]. This definition reveals the characteristic properties of chaotic systems: aperiodic behavior, deterministic and sensitivity to initial conditions.

- Having "aperiodic long-term behavior" is related to the existence of infinitely many *unstable periodic orbits* (UPOs) embedded within the strange attractor. Since all of the periodic orbits in the strange attractor is unstable, a chaotic trajectory does not settle down to any of them. On the other hand, it wanders incessantly in the vicinity of these orbits. Rich dynamics of a chaotic system is a result of UPOs.
- A chaotic system is a "deterministic" system, since it have no random parameters or noisy inputs.
- "Sensitive dependence on initial conditions" means that two trajectory in the state space of a chaotic systems starting from almost equal initial conditions eventually diverge from each other. Sensitivity to initial conditions is related to positive Lyapunov exponent(s) of a chaotic system. Furthermore, since a chaotic system is dissipative, sum of its Lyapunov exponents is negative.

2.2.1. Definition of the Phase

Consider a M dimensional ($M \geq 2$) nonlinear, dissipative, autonomous system which has a limit cycle with period T

$$\mathbf{x}(t) = \mathbf{x}(t + T) \qquad (2.3)$$

and the motion on this limit cycle Figure 2.1 is described by phase ϕ. Phase ϕ is a variable describing the angular part of the motion the limit cycle, which grows monotonically in the direction of motion and gains 2π during each rotation. The phase dynamics on the limit cycle is neutrally stable, i.e. phase perturbations are maintained without growing or decaying, which corresponds simply to a time shift on the limit cycle. Contrary to this, the amplitude of oscillations has a definite stable value. Besides, the phase of an oscillator can be considered as a variable that corresponds to the zero Lyapunov exponent.
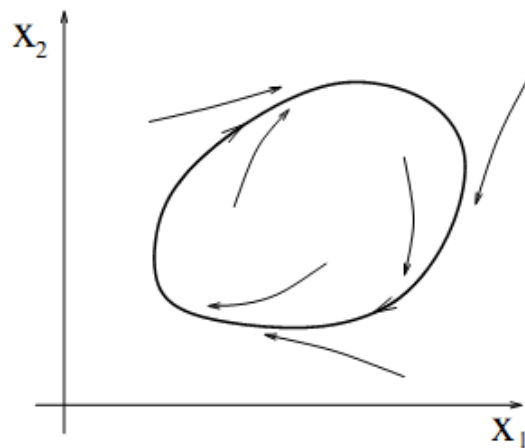
Figure 2.1. A stable limit cycle for two-dimensional dynamical system. Neighboring trajectories within the basin of attraction are attracted to the limit cycle.

Phase dynamics of a uniform oscillator (Figure 2.2) can be given as

$$\dot{\phi} = w_0. \tag{2.4}$$

where w_0 is the angular frequency on the limit cycle. Equation 2.4 has a time solution Equation 2.5 with the initial phase $\phi(0) = \phi_0$

$$\phi(t) = w_0 t + \phi_0. \tag{2.5}$$

For such an oscillator the phase grows monotonically and gains 2π over one period $T = \frac{w_0}{2\pi}$ (Figure 2.3).
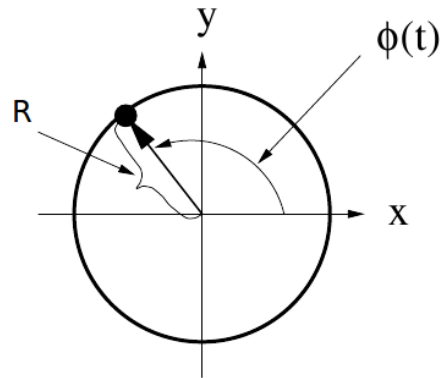
Figure 2.2. Phase portrait of a 2-dimensional uniform oscillator along the limit cycle with amplitude A and phase $\phi(t)$.

The limit cycle of the oscillator can be in an arbitrary shape (Figure 2.4), which is more general than the one in Figure 2.2. These types of oscillators are called *nonuniform oscillators*. The angular velocity of a nonuniform oscillator varies during one rotation on the limit cycle. For such an oscillator, the mean angular velocity, i.e. the frequency, can be calculated by introducing a reference line with a direction (Figure 2.5). As a particle moving on the limit cycle pierces this line, the monotonically increasing phase gains 2π at each of these piercings.

After the generalization for a 2-dimensional flows, one can introduce phase for a $M \geq 2$ dimensional nonuniform oscillators, e.g. relaxation oscillators, chaotic oscillators. For this case, Poincaré surface can be used to define phase of such motions. A suitable Poincaré surface with a direction of piercing in the phase portrait must be chosen such a way that the flow pierces it at each rotation. A limit cycle of an arbitrary shape or a chaotic flow crosses this surface and each successive piercing of the
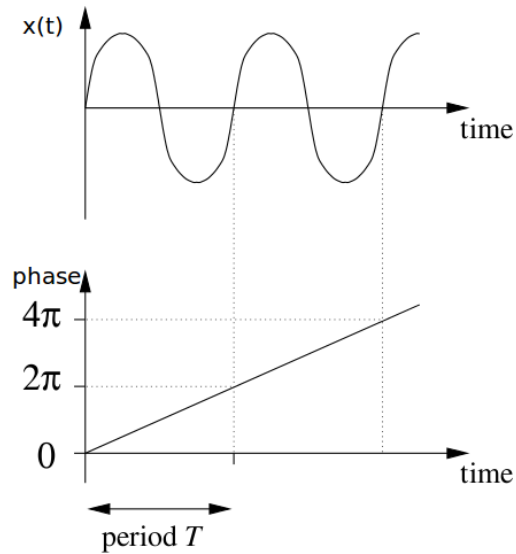
Figure 2.3. The phase of an periodic uniform oscillation grows uniformly in time and gains 2π at each period.

Poincaré surface can be associated with a phase shift of 2π. Furthermore; for the sake of convenience the phase can be assumed to be linear between successive piercings. This assumption gives phase as Equation 2.6, where t_n is the nth crossing time of the surface. Figure 2.6 shows a 2-dimensional Poincaré surface for a 3-dimensional flow.

$$\phi(t) = 2\pi \frac{t - t_n}{t_{n+1} - t_n} + 2\pi n, \qquad\qquad t_n \leq t \leq t_{n+1} \qquad\qquad (2.6)$$

Due to the neutral stability of the phase, phase and frequency of self-sustained oscillations can easily be changes by applying relatively small external inputs. This adjustment by external inputs is the essence of synchronization.

2.3. Synchronization

Synchronization results in a kind of cosmic balance that arises from our body to the universe as a whole. As stated before, synchronization is an adjustment of rhythms
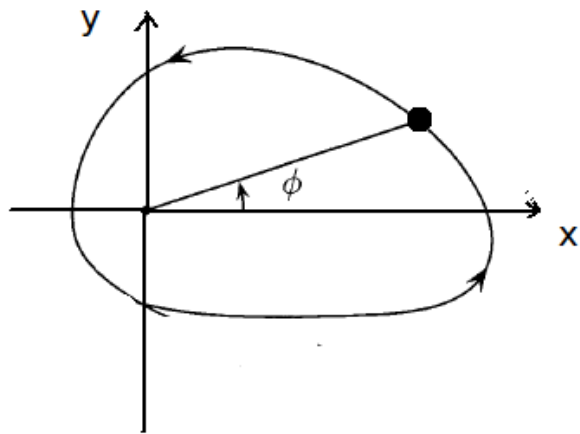
Figure 2.4. Phase portrait of a 2-dimensional nonuniform oscillator along the limit cycle with amplitude R and phase $\phi(t)$.
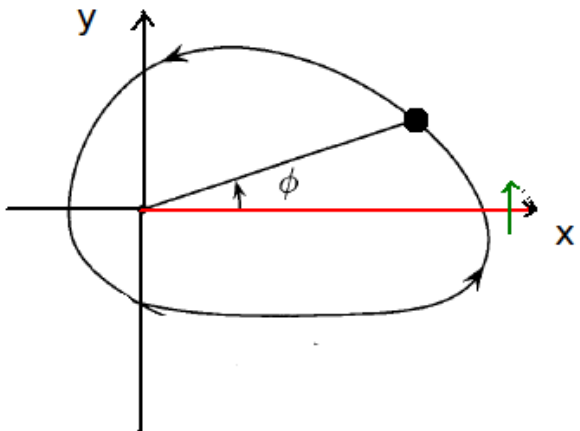
Figure 2.5. Reference line and its direction.
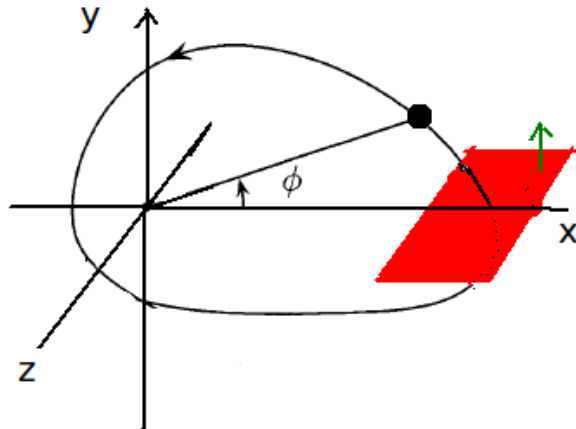
Figure 2.6. Reference surface and its direction.

of oscillating objects due to some weak interaction yielding a collective behavior.

The Dutch scientist Christiaan Huygens was the first one to describe the synchronization phenomenon scientifically. He observed that two pendulum clocks hanging on a common support always oscillate with the same rhythm (Figure 2.7). Although he became famous for his studies in optics and construction of the telescope, the invention and design of pendulum clocks was one of Huygens' most important contributions, which increased the accuracy of time measurements [1].

Huygens firstly mentioned his discovery in 1665 in a letter to his father [1]. During his illness, when he confined to bed for several days, he observed "... a wonderful effect that nobody could have thought before ...", the fact that the pendula of the two clocks hanging on the wall always swung together even if he moved them away from each other, or perturbed them. He claimed that the pendula keep their collective motion due to a sort of sympathy. He wrote in his own words as "...something so small is needed to keep them in eternal agreement...". He made many experiments thereafter, although he did not give exact description. But he explained qualitatively the effect of the "mutual synchronization"; the cause for the adjustment of the rhythms of two clocks had been an imperceptible motion of the beam.
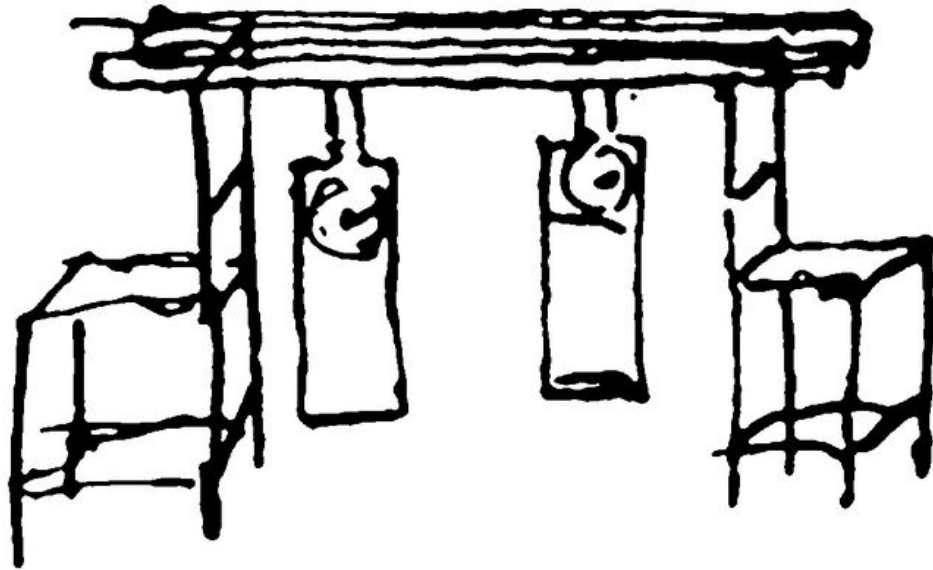
Figure 2.7. Huygens' drawing for his experiment done with pendulum clocks hanging on a common support.

In 1870s, William Strutt described an important issue of synchronization, namely *oscillation death* (quenching). He observed that if two distinct but similar organ pipes mutually interact with a strong coupling, one of the oscillations suppresses the other one.

In 1920s, radio and electrical engineering experiments accelerated the investigations of synchronization. In the experiments with two coupled triode generators, Eccles and Vincent showed the effect of the interaction via electrical current which was the vibration of two slightly different generators with a common frequency. Thereafter, Appleton and van der Pol pointed out the possibility of entrainment of a generator using a weak external signal [12, 13].

Synchronization of living systems is known for centuries. As early as the fourth century B.C., Androsthenes, scribe to Alexander the Great, noted that the leaves of certain trees opened during the day and closed at night. In 1729, French scientist Jean Jacques D´Ortous de Mairan found that even if heliotrope plants are kept in

total darkness, they will continue to open and close their leaves on schedule, which is the proof of having internal biological clocks and alternating its period according to sun light [14]. For human beings, in fact, the internal circadian period is different than 24-hours, as some experiments prove. If a person is completely isolated from sunlight, sound and temperature variations, the individual periods ranges from 13 to 65 hours [15]. But we are all locked to the 24-hours Earth's daily cycle and this entrainment regulates the society, everybody wakes up, eats, sleeps at nearly same times.

Synchronization is not restricted only two elements, but it is also a fundamental dynamical process in ensembles of coupled oscillators, like fireflies [16], glowworms [16], snowy tree crickets [17], bacterias [18], applauding audiences [19] and so on. In all these examples, not all of the entities are not identical oscillators, each firefly has its own natural frequency of firing, humans have different physical capabilities. But these oscillators, under necessary conditions, oscillates as one.

In 1917, Philip Laurent wrote an article in *Science* about his observations of the collective flashing of fireflies, thousands of fireflies blink on and off spontaneously [11]. By late 1960s, it was understood that each firefly has its own individual clock, which is one of the basic requirements of synchronization. John Buck and his colleagues made several laboratory experiments where a firefly was entrained by an artificial light. The researchers founded that an individual firefly can adjust itself to the cycle of the stimulus. In a large ensemble of such insects, each of them sends and receive optical signals, and shifts the others rhythm and has its own rhythm shifted by them. As a result, without any master, the whole ensemble blinks on and off in perfect harmony.

Another example for population synchrony is a group of people, an audience in a concert hall [19]. When the audience starts to applause, the sound is totally irregular, but as time goes by, the interaction via the common sound in the hall cause simultaneous clapping and finally the audience produce a regular performance. Néda *et al.* reported that such a collective behavior is typical in more homogeneous societies

like the East European, but occurs sporadically in West European and North American communities.

The reader will find further examples of synchronization in the next chapter. But before moving on, let us clarify what " weak interaction "is or how "strong" it should be. Huygens sensed the necessity of this " weak interaction "in his own words " something so small ". If the coupling is not "weak", it imposes too strong limitations on motion of two systems, like two clocks connected with a rigid body from their pendulums. In such a case, the whole system becomes nondecomposable. So synchronization is not a problem of a new unified system. The weak interaction of coupling should not qualitatively change the behavior either one of the interacting systems and should not deprive the systems of their individuality.

2.3.1. Synchronization of Periodic Oscillators

Systems to be synchronized are typically expected to exhibit self-sustained oscillations, i.e. they have to be autonomous dissipative systems with nondecaying stable oscillations [1]. Periodic self-sustained oscillators correspond to a limit cycle in the state space of the dynamical system. The phase ϕ can be introduced as the variable parameterizing the motion along this cycle (Section 2.2.1). The notion of phase has a key role in the theory of synchronization. Synchronization can be achieved by three different coupling schemes: (i) entrainment by an external force; (ii) mutual interaction; (iii) mean field coupling. In this section, mathematical description of synchronization of periodic oscillators will be introduced on the basis of these coupling types.

2.3.1.1. Synchronization of a Periodic System by External Force. Entrainment of a self-sustained periodic oscillator by an external force is the simplest case of synchronization. Many real world phenomena can be considered as a result of such a unidirectional effect: influence of the periodic movement of the Earth on organisms [20], entrainment of pulsatile insulin secretion by oscillatory glucose infusion [21], injection locking of a laser

array [22], periodically stimulated firefly [23], etc. In all these examples, each periodic oscillator is subject to a weak external influence and due to this unidirectional coupling the frequency of the driven oscillator is locked to frequency of the driving oscillator, yielding a synchronous motion. This phenomenon is called *frequency locking* [1].

In order to consider the effect of a small external periodic force on a self-sustained oscillator in Equation 2.1, let us describe the forced system as

$$\dot{\mathbf{x}} = \mathbf{f}(\mathbf{x}) + \varepsilon \mathbf{p}(\mathbf{x}, t) \tag{2.7}$$

where $p(x, t)$ is a periodic force with period T, i.e. $\mathbf{p}(\mathbf{x}, t) = \mathbf{p}(\mathbf{x}, t + T_0)$ has a period T_0. This force acts on the system proportional to a *coupling strength ε*. For the sake of simplicity, assume that the oscillator is a uniform periodic oscillators having a stable limit cycle with period $T = \frac{2\pi}{w}$ for $\varepsilon = 0$. The phase dynamics on this limit cycle can be given as in Equation 2.4.

The phase description of the entrained oscillator in Equation 2.7 by a periodic force with phase Θ and frequency $w_0 = \frac{2\pi}{T_0}$ with coupling strength $\varepsilon \neq 0$ [24], can be stated in the form

$$\begin{aligned} \dot{\phi} &= w + \varepsilon Q(\phi, \Theta) \\ \dot{\Theta} &= w_0 \end{aligned} \tag{2.8}$$

where Q is the 2π-periodic coupling function of its arguments which depends on the phases of the oscillator and the external force. This function can be represented as a double Fourier series as

$$Q(\phi, \Theta) = \sum_{l,k} a_{l,k} e^{ik\phi + il\Theta}. \tag{2.9}$$

Substitution of time solutions of periodic oscillators in Equation 2.5 in Equation 2.9

yields

$$Q(\phi, \Theta) = \sum_{l,k} a_{l,k} e^{i(k\phi_0 + l\Theta_0)} e^{i(kw + lw_0)t}. \tag{2.10}$$

The coupling function Q in Equation 2.10 includes both fast oscillating $e^{i(k\phi_0 + l\Theta_0)}$ and slow oscillating $e^{i(kw + lw_0)t}$ terms. The latter are related with the resonance condition

$$kw + lw_0 \approx 0 \tag{2.11}$$

which can cause to large shifts of the phase, and is critical for the dynamics [1]. When Equation 2.10 is averaged leaving the resonant terms to preserve the fundamental dynamics, the relation between w_0 and w is obtained. If the simplest case is considered with $w_0 \approx w$, only the terms with $k = -l$ are resonant. The averaged equation is obtained as

$$\sum_{l=-k} a_{l,k} e^{i(k\phi + l\Theta)} = \sum_k a_{-k,k} e^{i(k\phi - k\Theta)} = q(\phi - \Theta) \tag{2.12}$$

where q is a 2π periodic function of $(\phi - \Theta)$. Substituting q in Equation 2.8, the phase dynamics of a forced uniform oscillator is obtained as

$$\begin{aligned} \dot{\phi} &= w + \varepsilon q(\phi - \Theta) \\ \dot{\Theta} &= w_0. \end{aligned} \tag{2.13}$$

The effect of the external force on the driven oscillator depends on the phase difference $(\phi - \Theta)$. Thus, in order to derive the synchronization condition and determine the frequency locking region, it is meaningful to define a new variable, namely the phase difference between the oscillators as follows

$$\psi = \phi - \Theta. \tag{2.14}$$

The time derivation of ψ is obtained as

$$\dot{\psi} = -(w_0 - w) + \varepsilon q(\psi). \tag{2.15}$$

When a 2π-periodic function q is considered in the simplest form as $q = \sin(.)$, Equation 2.15 is called *the Adler equation* [25]:

$$\dot{\psi} = -(w_0 - w) + \varepsilon \sin(\psi). \tag{2.16}$$

When the driven oscillator adjusts its rhythm to the external force, i.e. frequency locking, the phase difference remains constant ($|\phi - \Theta| = |\psi| = constant$). Equation 2.16 allows the derivation of the conditions for the regime of synchronization, where the first derivative of Equation 2.14 is zero.

$$|\dot{\phi} - \dot{\Theta}| = |\dot{\psi}| = 0 \tag{2.17}$$

Equation 2.17 gives the stability region of Equation 2.16 and this region is often called the *synchronization region*, or *Arnold tongue*, which is

$$\varepsilon q_{min} < w - w_0 < \varepsilon q_{max} \tag{2.18}$$

and corresponds to phase locking in Equation 2.19 and frequency locking in Equation 2.20

$$\phi = wt + \psi_e \tag{2.19}$$

$$< \dot{\phi} >= \Omega = w \tag{2.20}$$

where ψ_e is the constant phase difference between the oscillators and Ω is the *observed frequency* of the driven oscillator. By looking at Equation 2.18, it is meaningful to

conclude that there exists a region the width of which is a the function of frequency mismatch $w_0 - w$ and the coupling strength ε. Within this region the phase ϕ just follows the phase of forcing Equation 2.19. Figure 2.8 demonstrates the Arnold tongue and synchronization plateau.
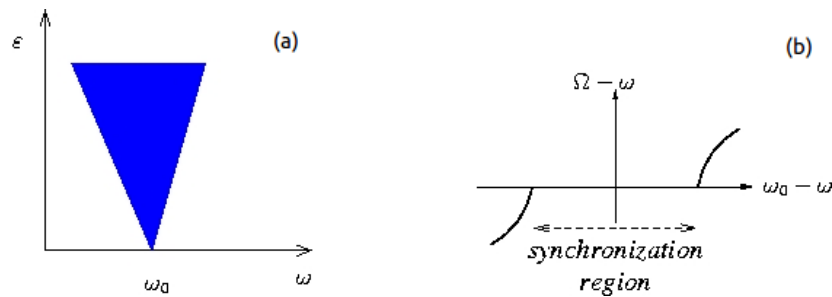
Figure 2.8. From [1]. (a) Schematic view of the Arnold tongue; (b) dependence of the observed frequency on the external frequency.

Figure 2.9 shows the dynamics of the phase difference ψ in Equation 2.16 as a function of the coupling strength ε. If ε is large enough, ψ remains constant. In the vicinity of the critical value of ε (or the critical frequency mismatch value), ψ remains constant for some time intervals and then increases by 2π; these events are called *phase slips*. Between these slips the oscillator is nearly locked by the external force and during the slip it makes one more rotation with respect to the external force. This phenomenon is called the *beat phenomenon*. As one can see in Figure 2.9 higher coupling strengths result in longer time lapse between phase slips. Eventually for large enough coupling strengths, phase slips are eliminated and synchronization steps in.

If the natural frequency of the oscillator and the external force fulfill $mw_0 \approx nw$ condition, then the dynamics of the phase difference $\psi = m\phi - n\Theta$ is described by a generalized equation similar to Equation 2.15 as

$$\dot{\psi} = -(nw - mw_0) + \varepsilon\bar{q}(\psi). \tag{2.21}$$

In this case, entrainment occurs with the observed frequency equal to a rational multiple
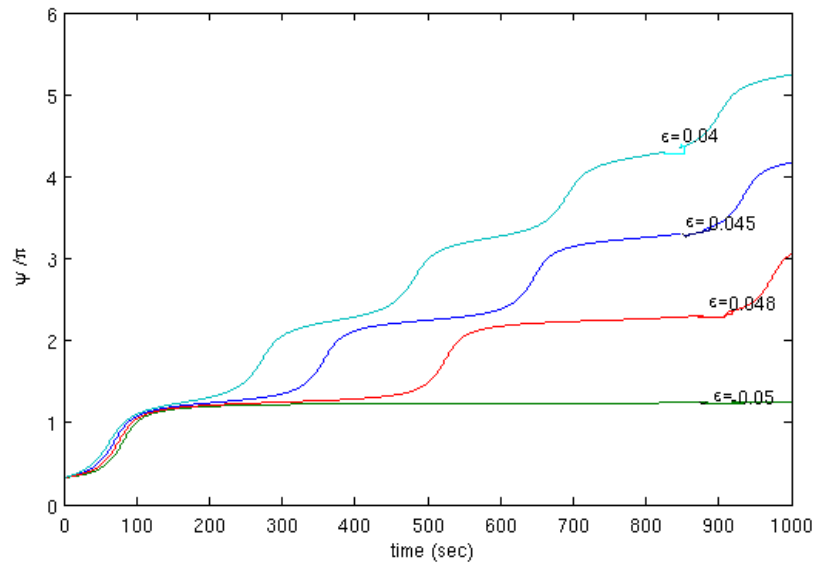
Figure 2.9. The dynamics of the phase difference Equation 2.16 for different coupling
strengths ε and for $w_0 = 1.1$, $w = 1$.

of forcing frequency, $\Omega = \frac{n}{m}w$, and phase $m\phi = mwt + \psi_e$, namely *higher order synchronization (locking)*. Figure 2.10 demonstrates the Arnold tongue for higher order frequency locking.
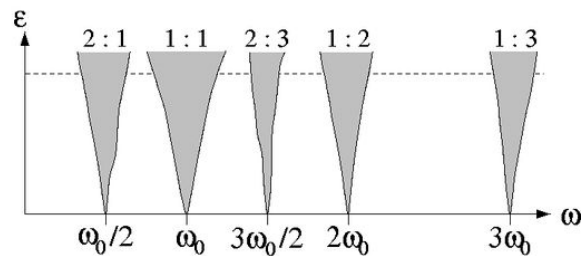
Figure 2.10. From [1]. Schematic view of the Arnold tongue for higher order locking.

2.3.1.2. Synchronization of Ensembles of Coupled Periodic Systems. The other widely studied case in the context of synchronization is collective dynamics of large ensembles of self-sustained periodic oscillators. Collective dynamics are observed in locally and globally coupled oscillating objects: interacting pendulum clocks [1], interacting organ pipes [1], biological oscillators [26], flashing fireflies [16], chemical oscillators [24], a large applauding audience [19]. In those examples, as a consequence of bidirectional

interaction, periodic oscillators with different natural frequencies act at a common frequency. It appears then as a collective coherent mode in a group of nonidentical systems and as Wiener [27] posed "...thousands of neurons or fireflies or crickets can suddenly fall into step with one another, all firing or flashing or chirping at the same time...".

Two mutually interacting nonidentical periodic oscillators construct a fundamental building block for the case of many mutually coupled systems. To describe the phase dynamics of two coupled self-sustained oscillators with a basic approach similar to Section 2.3.1.1 will be studied. In order to analyze the effect of bidirectional coupling of two nonidentical self-sustained oscillators in Equation 2.1, it is possible to construct a basic model as

$$\dot{\mathbf{x}}_1 = \mathbf{f}_1(\mathbf{x}_1) + \varepsilon_{12}\mathbf{p}_1(\mathbf{x}_1, \mathbf{x}_2)$$
$$\dot{\mathbf{x}}_2 = \mathbf{f}_2(\mathbf{x}_2) + \varepsilon_{21}\mathbf{p}_2(\mathbf{x}_2, \mathbf{x}_1). \tag{2.22}$$

where the autonomous dynamics $\mathbf{f}_i(\mathbf{x}_i)$ are influenced by the interaction function $\mathbf{p}_i(\mathbf{x}_i, \mathbf{x}_j)$ proportional to the coupling strength ε_{ij}. Without coupling, for the sake of simplicity, one can assume that each system has a stable limit cycle with frequencies w_1 and w_2, respectively, as described in Equation 2.4, and phase dynamics in the vicinity of these limit cycles is as follows:

$$\dot{\phi}_1(\mathbf{x}_1) = w_1$$
$$\dot{\phi}_2(\mathbf{x}_2) = w_2. \tag{2.23}$$

A model of two mutually coupled periodic oscillators can be represented similar

to Equation 2.8,

$$\dot{\phi}_1 = w_1 + \varepsilon_{12}Q_1(\phi_1, \phi_2)$$
$$\dot{\phi}_2 = w_2 + \varepsilon_{21}Q_2(\phi_2, \phi_1) \tag{2.24}$$

with 2π-periodic coupling functions Q_{ij} which can be represented as double Fourier series

$$Q_1(\phi_1, \phi_2) = \sum_{k,l} a_1^{k,l} e^{ik\phi_1 + il\phi_2}$$
$$Q_2(\phi_2, \phi_1) = \sum_{l,k} a_2^{l,k} e^{ik\phi_2 + il\phi_1}. \tag{2.25}$$

By replacing the time solutions of Equation 2.23 in Equation 2.25

$$Q_1(\phi_1, \phi_2) = \sum_{k,l} a_1^{k,l} e^{i(k\phi_{1(0)} + l\phi_{2(0)})} e^{i(kw_1 + lw_2)t}$$
$$Q_2(\phi_2, \phi_1) = \sum_{l,k} a_2^{l,k} e^{i(k\phi_{2(0)} + l\phi_{1(0)})} e^{i(kw_1 + lw_2)t} \tag{2.26}$$

one obtains fast oscillating $e^{i(k\phi_{i(0)} + l\phi_{j(0)})}$ and slow oscillating $e^{i(kw_i + lw_j)t}$ terms that satisfy the resonance condition

$$kw_1 + lw_2 \approx 0. \tag{2.27}$$

If it is assumed that the natural frequencies are nearly in resonance with $nw_1 \approx mw_2$, then all the terms of the Fourier series with $k = nj$, $l = -mj$ are resonant and contribute to the averaged equations

$$q_1(n\phi_1 - m\phi_2) = \sum_j a_1^{nj,-ml} e^{ij(n\phi_1 - ml\phi_2)}$$
$$q_2(n\phi_2 - m\phi_1) = \sum_j a_2^{nj,-ml} e^{ij(m\phi_2 - nl\phi_1)}. \tag{2.28}$$

Finally, with the acceptance of equivalent coupling strengths $\varepsilon_1 = \varepsilon_2 = \varepsilon$, Equation 2.24 is put into the following form

$$\dot{\phi}_1 = w_1 + \varepsilon q_1(n\phi_1 - m\phi_2)$$
$$\dot{\phi}_2 = w_2 + \varepsilon q_2(m\phi_2 - n\phi_1). \tag{2.29}$$

For two bidirectionally coupled systems like in the case of a driven periodic oscillator, the mutual influence of the oscillators depends on the phase difference. Thus, it is useful to define phase difference as a variable in Equation 2.30 and obtain its time derivative as in Equation 2.31, where $q(\psi) = nq_1(\psi) - mq_2(-\psi)$.

$$\psi = n\phi_1 - m\phi_2 \tag{2.30}$$
$$\dot{\psi} = -(mw_2 - nw_1) + \varepsilon q(\psi) \tag{2.31}$$

Since Equation 2.31 has the same form as in Equation 2.15, it can again be stated that when the oscillators synchronize the phase difference remains constant ($|n\phi_1 - m\phi_2| = |\psi| < constant$) implying that $\dot{\psi} = 0$ and Equation 2.31 has a stable equilibrium point ψ_e. The observed frequencies of the oscillators are

$$\Omega_{1,2} = <\dot{\phi}_{1,2}> = w_{1,2} + \varepsilon q_{1,2}(\pm\psi_e), \tag{2.32}$$

and rational multiple of each other

$$\frac{\Omega_1}{\Omega_2} = \frac{m}{n}. \tag{2.33}$$

The simplest case of coupled oscillators is 1:1 resonance, when the natural frequencies are almost equal to each other ($w_1 \approx w_2$) meaning $n = m = 1$. If the

coupling is assumed to be symmetric, i.e. $q_1(\psi) = q_2(\psi)$ and taken as $q = \sin(.)$, the corresponding basic model for the phase difference dynamics of two mutually coupled periodic oscillators obtained as

$$\dot{\psi} = -(mw_2 - nw_1) + \varepsilon \sin(\psi)). \tag{2.34}$$

In the synchronous status, oscillators move with a constant phase shift $\psi_e = \phi_1 - \phi_2$. ψ_e varies with respect to the sign of ε. If $\varepsilon < 0$, two oscillators attract each other and *in-phase* synchronous motion is observed since $-\pi/2 < \psi_e < \pi/2$. Figure 2.11 demonstrates two coupled identical oscillators for different coupling values. For $\varepsilon = -0.1$ in-phase motion is observed with $\psi_e = 0$, while for $\varepsilon = 0.1$ out-of-phase motion occurs with $\psi_e = \pi$.
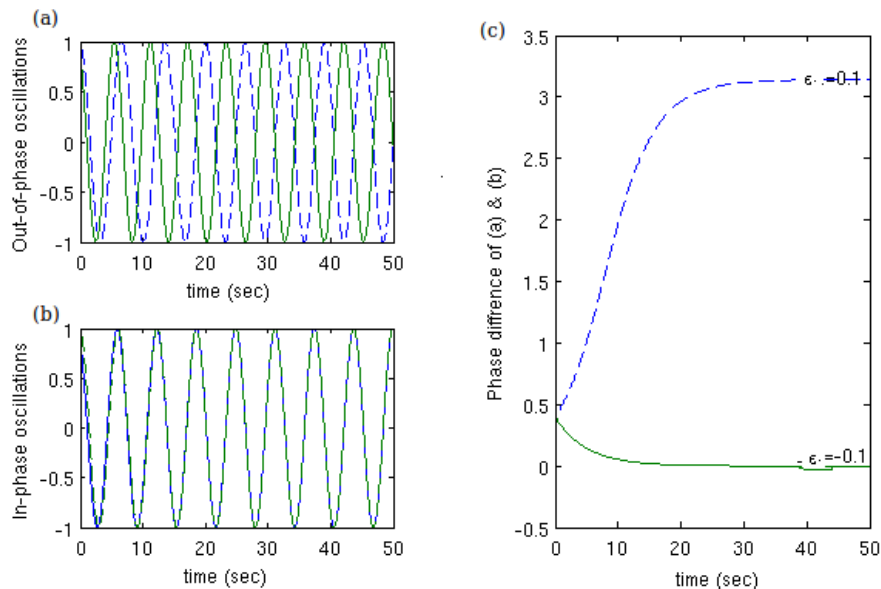
Figure 2.11. Synchronous motion of two coupled identical oscillators with $w_1 = w_2 = 1$ (a) Out-of-phase motion for $\varepsilon = 0.1$; (b) In-phase motion for $\varepsilon = -0.1$; (c) ψ_e of the processes (a) and (b).

Generalized form of N locally coupled nonidentical $M \geq 2$ dimensional periodic

systems as in Equation 2.1 can be stated as

$$\dot{\mathbf{x}}_i = \mathbf{f}_i(\mathbf{x}_i) + \sum_{j=1}^{N} a_{ij}\varepsilon_{ij}\mathbf{p}_{ij}(\mathbf{x}_i, \mathbf{x}_j) \tag{2.35}$$

where $\mathbf{p}_{ij} : \Re^M \to \Re^M$ coupling function between the ith and j^{th} oscillators, a_{ij} are the elements of $N \times N$ dimensional adjacency matrix A of the network, and ε_{ij}s are the coupling strengths between i^{th} and j^{th} oscillators. The generalized phase representation in the vicinity of the limit cycle of a periodic oscillator in a locally coupled network can be stated as

$$\dot{\phi}_i = w_i + \sum_{j=1}^{N} a_{ij}\varepsilon_{ij}Q(\phi_i, \phi_j). \tag{2.36}$$

Kuramoto proposed an all-to-all connected purely sinusoidal coupling [24] and came up with Equation 2.37, one of the most studied equations of globally interacting oscillators.

$$\dot{\phi}_i = w_i + \frac{\varepsilon}{N} \sum_{j=1}^{N} \sin(\phi_j - \phi_i) \tag{2.37}$$

where the factor $1/N$ is incorporated to ensure a good behavior of the model in the thermodynamic limit, i.e. as $N \to \infty$. What he prosed is important for representing and understanding the phenomenon of collective synchrony, i.e. synchrony extending to a whole population, or to a large portion of it. An equivalent representation of all-to-all coupling is the *mean field* approach, where each oscillator in the ensemble is driven by a force that is proportional to the sum of the outputs of all the oscillators in the set (Figure 2.12). To generalize this both to periodic and chaotic oscillators, one can denote these outputs, representing the oscillating quantity, as $x_i(t)$, where $i = 1, \ldots, N$ is the index of an oscillator, and N is the number of elements in the ensemble. For instance, x can be variation of light intensity like in a population of flashing fireflies or the acoustic field of an applauding crowd. The effect of the rest of

the set on each individual oscillator is represented with εX, where X stands for the mean field in Equation 2.38 and ε for the coupling strength.

$$X = N^{-1} \sum_{i=1}^{N} x_i \tag{2.38}$$

Synchronization of flashing in a population of fireflies [28], applause in a large audience [19], menstrual cycles of mammals living together [29], glycolytic oscillations in a population of yeast cells [30] are only a few examples for mean field coupling.
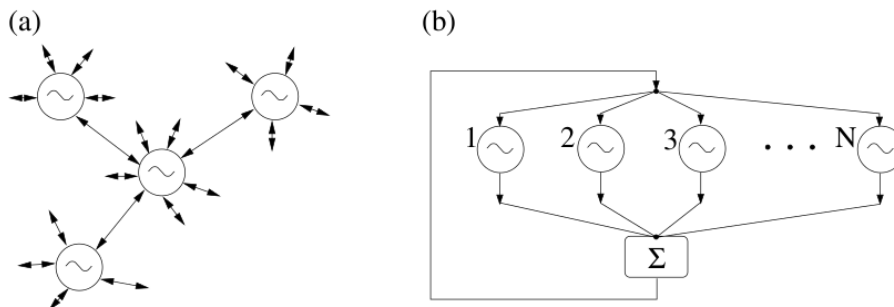
Figure 2.12. From [1]. (a) Each oscillator mutually interacts with others in an all-to-all coupled ensemble; (b) An equivalent representation of globally coupled oscillators where each of them is driven by a mean field that is generated by all set.

2.3.2. Synchronization of Chaotic Systems

In dynamical systems theory, the term chaotic is used to define a group of deterministic systems that exhibit aperiodic behavior and that exhibit sensitive dependence on initial conditions. As these properties, chaotic self-sustained oscillators introduce a richer and variety of forms of synchronization than periodic oscillators. Thus, synchronization of chaotic systems needs to be studied separately from the case of periodic oscillators.

Here, again, *synchronization of chaotic systems* refers to a process wherein two

(or many) chaotic self-sustained oscillators (identical or nonidentical) adjust a property of their rhythms, which ranges from complete agreement of trajectories to locking of phases, due to forcing or coupling. In the context of synchronization of coupled chaotic systems, several cases depending on the identity of coupled systems and coupling type, have been studied: complete or identical synchronization (CS) [31, 32], phase synchronization (PS) [33, 34], imperfect phase synchronization (IPS) [2], lag synchronization (LS) [35], intermittent lag synchronization (ILS) [35], generalized synchronization (GS) [36], and almost synchronization (AS) [37].

In this section, firstly, synchronization of coupled identical chaotic systems will be investigated, then the cases, except for AS, for nonidentical systems will be introduced.

2.3.2.1. Synchronization of Identical Chaotic Systems. As stated before, the most characteristic property of chaotic systems is their sensitivity to initial conditions. As a consequence, if two identical chaotic systems start from almost equal initial conditions, as time goes by, they track totally different trajectories and produce uncorrelated time solutions which remain in the basin of the same strange attractor. Nevertheless, with a proper coupling structure, it is possible to drive these systems onto the same chaotic trajectory [31, 32].

In the context of coupled identical chaotic systems, synchronization refers to the equality of the system states, namely *complete synchronization* (CS). CS is introduced by [32] as a state when two state trajectories converge to the same values and continue in such a relation further in time. In other words, when two chaotic oscillator completely synchronize, they "forget" their initial conditions. Reference [38] defines CS as follows:

Definition Complete synchronization of two identical chaotic systems represented with their phase plane trajectories $\mathbf{x}(t)$ and $\mathbf{y}(t)$, respectively, takes place when for

all $t > 0$, for the relation fulfilled as

$$\lim_{t \to \infty} \parallel \mathbf{x}(t) - \mathbf{y}(t) \parallel = 0.$$

Complete synchronization can be achieved by either unidirectional (drive-response) coupling or bidirectional coupling. In unidirectional coupling, the driver affects the states of the responding system, while the reverse does not occur. On the contrary, in the bidirectional case, both systems' states alter as a consequence of coupling. Under this classification, there exit several coupling schemes [32, 39–42].

One of the unidirectional coupling configurations is introduced by Pecora and Carroll, a method also referred to as the Pecora-Carroll method [32]. In this configuration a chaotic system is separated into two subsystems; drive and response. One subsystem evolves freely and drives the other one. As a result of this chaotic force, the response system follows exactly the driver; similar to the case of a periodic oscillator driven by an external force (Section 2.3.1.1). Communication techniques, which utilize chaos, take the advantages of the drive-response configuration [41].

In order to describe the essentials of Pecora-Carroll configuration, one can consider a chaotic system as follows

$$\dot{\mathbf{z}} = \mathbf{F}(\mathbf{z}) \tag{2.39}$$

where $\mathbf{z} = \{z_1, z_2, ..., z_n\}$ is a M-dimensional state vector, with $\mathbf{F}$ defining a vector field $\mathbf{F} : \Re^M \to \Re^M$. Under the assumption of Equation 2.39 to be *drive decomposable*, it can be separated three subsystems, referring *driver* and *response* systems,

$$\left. \begin{aligned} \dot{\mathbf{u}} &= \mathbf{f}(\mathbf{u}, \mathbf{v}) \\ \dot{\mathbf{v}} &= \mathbf{g}(\mathbf{u}, \mathbf{v}) \end{aligned} \right\} driver,$$

$$\dot{\mathbf{w}} = \mathbf{h}(\mathbf{u}, \mathbf{w}) \left.\right\} response,$$

where $\mathbf{u} = \{u_1, u_2, ..., u_n\}$, $\mathbf{v} = \{v_1, v_2, ..., v_k\}$, $\mathbf{w} = \{w_1, w_2, ..., w_l\}$ and $M = n + k + l$. The evolution of response system is under the control of the driver systems via chaotic driving signal $\mathbf{u}$ and, by definition, if CS is achieved the response system will track the same trajectory as the driver does. Moreover, [32] show that in CS all Lyapunov exponents of the response system are negative.

An example for the Pecora-Carroll method is given in [43], where two identical Lorenz systems is considered. The first system is the driver and the second system (the response) is driven by the driver's x state.

$$\left.\begin{aligned}\dot{x} &= 16(y - x) \\ \dot{y} &= -xz + 45.92x - y \\ \dot{z} &= -xy - 4z\end{aligned}\right\} driver,$$

$$\left.\begin{aligned}\dot{y'} &= -xz' + 45.92x - y' \\ \dot{z'} &= -xy' - 4z'\end{aligned}\right\} response.$$

As shown in Figure 2.13, the response system forgets its initial conditions and tracks the driver.

As stated above, unidirectional coupling is not the only way of achieving CS. Mutually coupled identical systems can also synchronize completely. In general, two mutually coupled identical chaotic systems can be represented as [28]

$$\dot{\mathbf{x}} = \mathbf{f}(\mathbf{x}) + \hat{\mathbf{C}}(\mathbf{y} - \mathbf{x})^T$$
$$\dot{\mathbf{y}} = \mathbf{f}(\mathbf{y}) + \hat{\mathbf{C}}(\mathbf{x} - \mathbf{y})^T. \tag{2.40}$$

In Equation 2.40, $\mathbf{x}$ and $\mathbf{y}$ represent the M-dimensional state vectors, with $\mathbf{f}$ defining
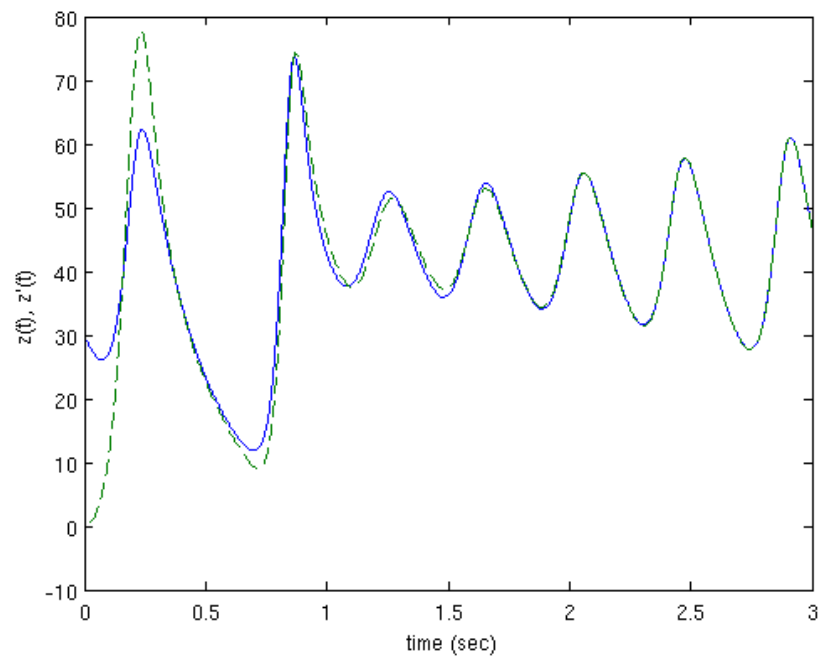
Figure 2.13. CS of two identical unidirectionally coupled Lorenz systems. Solid line represents $z(t)$ and dashed line represents $z'(t)$ of the given example.

a vector field $\mathbf{f} : \Re^M \to \Re^M$. $\hat{\mathbf{C}}$ is the $M \times M$ dimensional coupling matrix. When CS is achieved, the systems follow a common chaotic trajectory ($\mathbf{x} = \mathbf{y}$) without adhering to their initial conditions.

An example of CS in bidirectionally coupled chaotic oscillators is constructed again for two identical Lorenz systems as Equation 2.41 for a particular case where $\hat{\mathbf{C}} = \varepsilon\mathbf{I}$. Figure 2.14 shows the synchronous behavior. As expected from the definition, the difference between the states approaches to zero.

$$\dot{x}_{1,2} = 16(y_{1,2} - x_{1,2}) + \varepsilon(x_{2,1} - x_{1,2})$$

$$\dot{y}_{1,2} = -x_{1,2}z_{1,2} + 40x_{1,2} - y_{1,2} + \varepsilon(y_{2,1} - y_{1,2})$$

$$\dot{z}_{1,2} = -x_{1,2}y_{1,2} - 4z_{1,2} + \varepsilon(z_{2,1} - z_{1,2}) \tag{2.41}$$
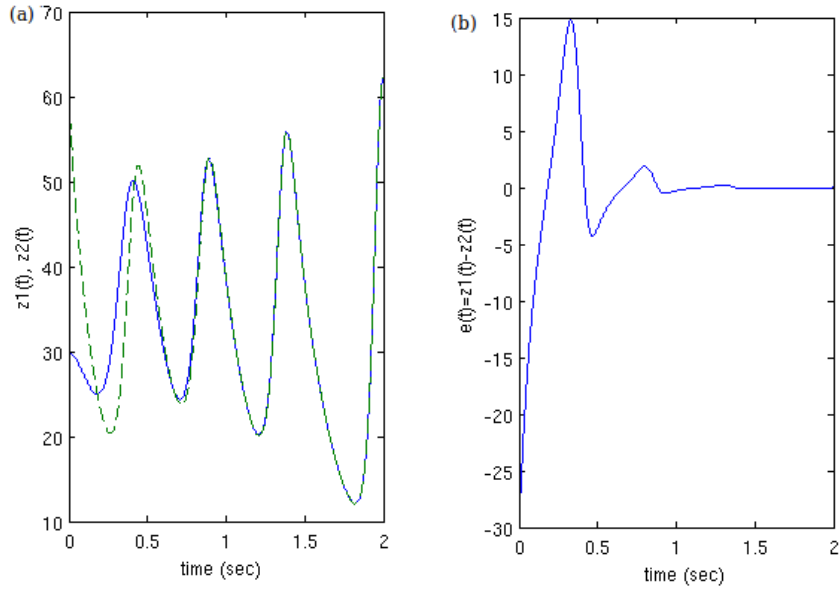
Figure 2.14. CS of two identical bidirectionally coupled Lorenz systems for $\varepsilon = 3$.(a) Solid line represents $z_1(t)$ and dashed line represents $z_2(t)$; (b) state difference $e(t) = z_2 - z_1$ of the given example.

2.3.2.2. Synchronization of Nonidentical Chaotic Systems. Completely identical synchronization may not occur in nonidentical chaotic systems, since there does not exist a synchronization manifold such as $\mathbf{x} = \mathbf{y}$ because of parameter mismatches and structural differences [28]. Pazo *et al.* [44] investigated different synchronization scenario by increasing the coupling strength between the oscillators from zero up to a specific value, beyond which oscillations start being suppressed (quenching). It is shown that, if the coupling strength between the systems is increased, firstly the weakest degree of synchronization, the so-called *phase synchronization* occurs, where the phases of interacting chaotic systems (or the phase of a system and phase of an external force) are locked to each other, while the amplitudes remain uncorrelated. If the periods of UPOs embedded in the chaotic oscillator are scatted over a wide range, *imperfect phase synchronization* is observed where synchronization epochs are interrupted by intermittent phase slips. If the coupling strength is increased further, the states of the chaotic oscillators become correlated with a proper shifting of time, a situation called *lag synchronization*. Between PS and LS, systems most of the time exhibit LS, but intermittent bursts of local nonsynchronous behavior may occur in correspondence with unlocked UPOs. For a stronger coupling, the time lag approaches to zero, and two nonidentical chaotic systems become almost completely synchronized.

The term *generalized synchronization* is used as a generalization of CS [36,41]. In this case, the states of two nonidentical chaotic systems ($\dot{\mathbf{x}} = \mathbf{f_1}(\mathbf{x})$, $\dot{\mathbf{y}} = \mathbf{f_2}(\mathbf{y})$) coupled with a strong enough coupling strength converge to a synchronization subspace of the combined phase space of the two systems ($\mathbf{x}, \mathbf{y}$). Because the systems are nonidentical, this synchronization subspace has generally a more complicated relationship that $\mathbf{x} = \mathbf{y}$.

Although the synchronization of chaotic oscillators can be observed in terms of some characteristic changes in the Lyapunov exponents of the combined systems, the more practical method of phase dynamics is used for the sake of simplicity. As stated in Section 2.2.1 phase of a chaotic flow can be obtained by constructing an appropriate Poincaré surface of section (Figure 2.15). With this method, the phase $\phi(t)$ is obtained

as Equation 2.6 and a *mean frequency w* can be defined for a chaotic oscillator (Equation 2.42), although the Poincaré return times are nonuniform as opposed to the case of a periodic oscillator.

$$w = <\dot{\phi}> \tag{2.42}$$
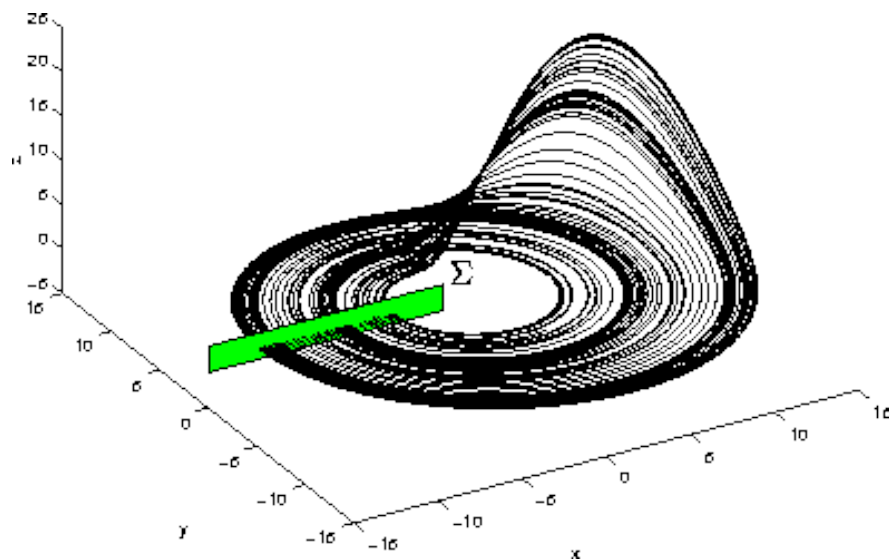
Figure 2.15. A single trajectory of Rössler chaotic system with a Poincaré surface (green plane $\sum$).

Phase Synchronization of Chaotic Systems.   PS of chaotic oscillators is similar to the notion of synchronization in periodic oscillators described in Section 2.3.1. Details of PS are investigated within the scope of bifurcation theory [45], and UPOs [44, 46]. As a consequence of the interaction with a periodic or a chaotic oscillator, it is possible to suppress the irregularity of the Poincaré return times of the chaotic system. If the mean observed frequencies of the oscillators coincide, one can speak of frequency locking, similar to periodic oscillators.

The effect of PS in chaotic systems can be explained on the example of a Rössler chaotic oscillator driven by a periodic external force as

$$\dot{x} = -y - z + \varepsilon \sin(vt)$$

$$\dot{y} = x + 0.04y$$

$$\dot{z} = 0.2 + z(x - 10)$$

$$(2.43)$$

where v is the frequency of the periodic motion and ε is the coupling strength. [46] states that as the UPOs construct the skeleton of a chaotic system, PS can be represented in terms of individual phase locking of these orbits. If v and ε are within the entrainment region given as in Equation 2.18 of each UPO, PS is obtained for the whole system (Figure 2.16).
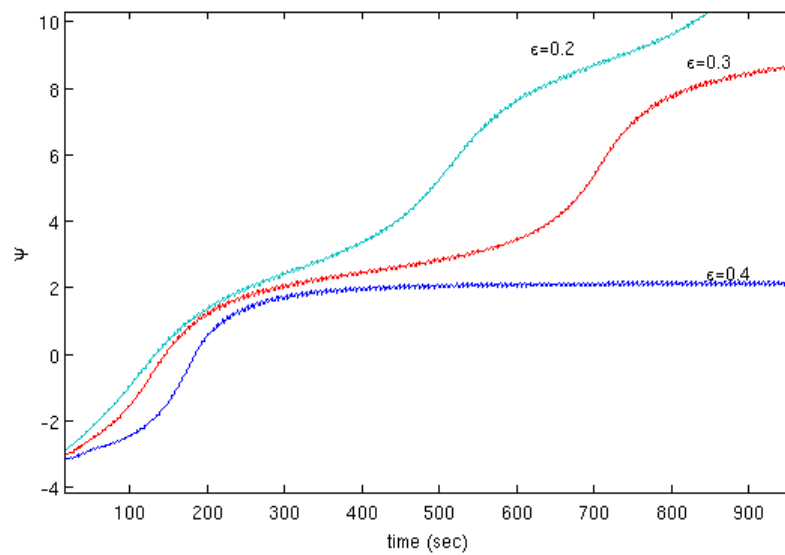
Figure 2.16. Phase difference ψ between the periodic external force and the chaotic Rössler system in Equation 2.43. As coupling strength ε increases, chaotic oscillator synchronizes with the external force.

PS in periodically forced chaotic oscillators is also observed experimentally, e.g. the frequency entrainment of a chaotic electronic oscillator [47], chaotic gas discharge by periodic forcing [48].

PS is also possible in mutually coupled chaotic oscillators. Generalized representation of N locally and mutually coupled chaotic M-dimensional systems can be given as in Equation 2.44 similar to Equation 2.35, with M-dimensional vector fields $\mathbf{F}_i$, the coupling functions $\mathbf{p}_{ij} : \Re^M \to \Re^M$, elements of adjacency matrix a_{ij} and the coupling. strengths ε_{ij}.

$$\dot{\mathbf{x}}_i = \mathbf{F}_i(\mathbf{x}_i) + \sum_{j=1}^{N} a_{ij}\varepsilon_{ij}\mathbf{p}_{ij}(\mathbf{x}_i, \mathbf{x}_j) \tag{2.44}$$

To study the effects of mutual coupling on PS, one can consider the example of two mutually coupled nonidentical Rössler chaotic oscillators in Equation 2.45, which again demonstrates similar properties to bidirectionally coupled periodic oscillators. Without synchronization the phase difference between them increases ($|\phi_1 - \phi_2| \to \infty$). But with a proper coupling strength and a coupling scheme, this difference remains constant ($|\phi_1 - \phi_2| < constant$), therefore the systems oscillate with a common mean frequency ($| < \dot{\phi}_1 > - < \dot{\phi}_2 > | = |w_1 - w_2| = 0$), while the amplitudes remain uncorrelated and chaotic (Figure2.17, Figure 2.18).

$$\dot{x}_{1,2} = -(w_0 \pm \Delta w)y_{1,2} - z_{1,2} + \varepsilon(x_2 - x_1)$$
$$\dot{y}_{1,2} = (w_0 \pm \Delta w)x_{1,2} + 0.15y_{1,2}$$
$$\dot{z}_{1,2} = 0.2 + z_{1,2}(x_{1,2} - 10) \tag{2.45}$$

Figure 2.17 shows the transition to synchronization regime as the coupling strength increases. Two nonidentical Rössler oscillators with a parameter mismatch $\Delta w = 0.02$ oscillate at a common frequency for $\varepsilon = 0.04$, which is very small compared with the

one in CS. Thus, PS represents a weak degree of synchronization in contrast to CS.
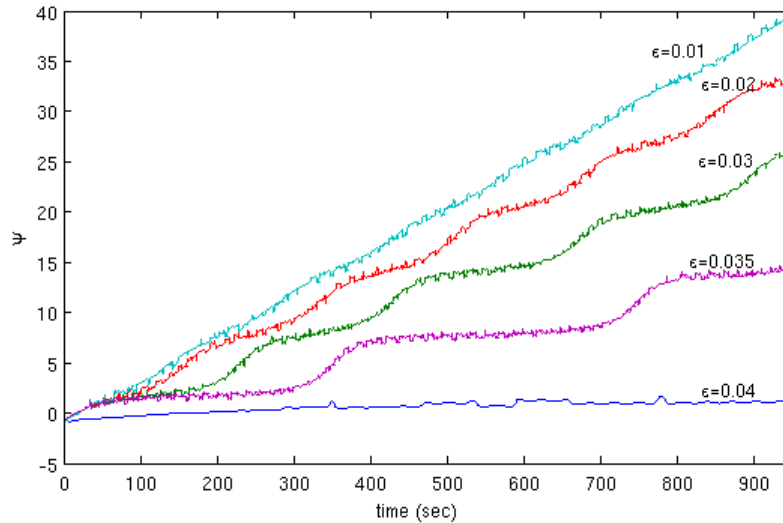
Figure 2.17. Phase differences ψ of Equation 2.45 for different coupling strengths ε. $w_0 = 0.995$, $\Delta w = 0.02$.

[28, 44, 46] state that PS of chaotic oscillators is a result of entrainment of the frequencies of UPOs by a periodic or a chaotic oscillator. PS is possible when UPOs of the systems are locked and have the same frequency ratio. It is underlined that the distribution of the natural frequencies of UPOs play an important role. For example, in the Rössler oscillators given above in Equations 2.43 and 2.45, this variation is rather small, therefore it is easy to synchronize them by a weak forcing with a period close to their mean frequencies. Because there exists an intersection region of the Arnold tongue of each UPO and it is possible to find a suitable coupling strength and forcing frequency within this region. [44, 49] state that this is a generally valid fact for chaotic systems whose chaotic attractors of which emerge from a phase-doubling bifurcation sequence. However, for such chaotic oscillators with widely distributed UPO frequencies, an external effect may not be able to lock all the UPOs. In this case or when a weak coupling strength is suggested for a period-doubling oscillator, phase drifts occur while the trajectory of the chaotic oscillator is passing near the unlocked
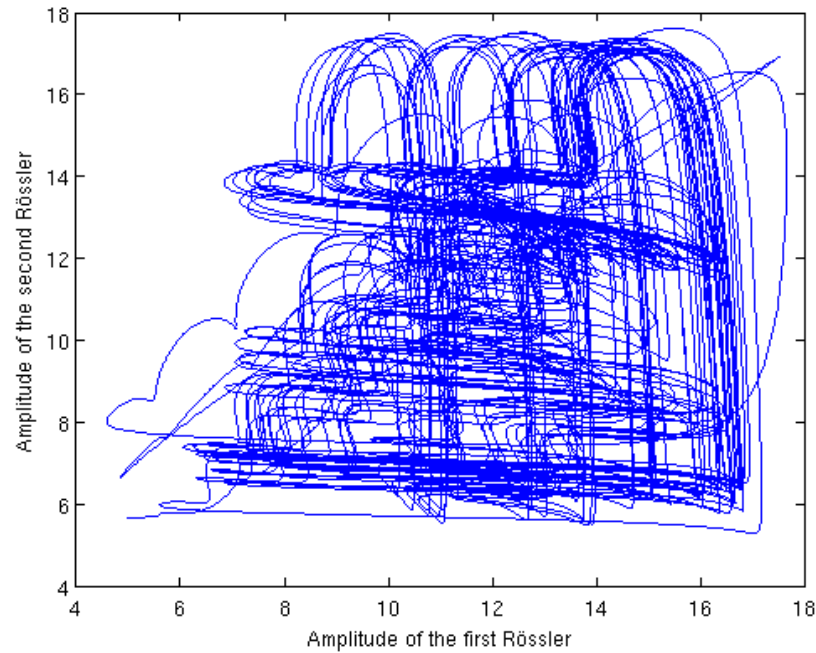
Figure 2.18. Amplitudes of Equation 2.45 for the phase synchronized case at $\varepsilon = 0.04$.

UPOs and an *imperfect phase synchronization* (IPS) is observed.

[2, 49] have studied an example of a periodically driven Lorenz oscillator (Equation 2.46) to show PS and IPS. For a chaotic Lorenz system, r is the critical parameter. If $r = 210$, chaotic oscillations emerge from a period-doubling bifurcation, and Equation 2.46 can synchronize to a periodic force with a frequency close to its mean frequency. But if $r = 28$ frequencies of the UPOs are widely distributed, and there exist certain unstable orbits which are not locked. These unlocked orbits cause the phase slips in the phase difference dynamics and make synchronization plateau disappear (Figure2.19, Figure 2.20).

$$\dot{x} = 10(y - x)$$
$$\dot{y} = rx - y - xz$$
$$\dot{z} = xy - 2.667z + \varepsilon cos(\Omega t) \tag{2.46}$$

Lag Synchronization of Chaotic Systems. Mutually coupled chaotic oscillators can adjust their time scales with relatively weak coupling, which corresponds to PS. For stronger coupling strengths oscillators can also track nearly the same chaotic trajectory with a time shift. This behavior is called *lag synchronization* [35]. In this case, not only the phases but also the amplitudes become correlated with a time delay τ, i.e. $\mathbf{x}_1(t) \approx \mathbf{x}_2(t + \tau)$. [44] claims that the onset of LS is preceded by the disappearance of UPOs which are geometrically incapable of LS.

Considering the previous example of two mutually coupled nonidentical Rössler chaotic oscillators in Equation 2.45, under the usage of stronger enough coupling strength ε, the relation between the states can be written as follows

$$x_1(t) \approx x_2(t + \tau_0), \qquad y_1(t) \approx y_2(t + \tau_0), \qquad z_1(t) \approx z_2(t + \tau_0). \qquad (2.47)$$

To characterize LS, similarity function $S(\tau)$ has been introduced in Equation 2.48 and $S(\tau_0) = 0$ gives the lag time τ_0. In Figure 2.21, $S(\tau)$ is plotted for different coupling values of Equation 2.45. Note that for the strengths providing PS, $S(\tau)$ has a minimum above zero. Increase in the coupling strength yields a decrease in τ and minimum of $S(\tau)$ goes down to zero. For example, if $\varepsilon = 0.14$, minimum value of $S(\tau)$ reaches zero for τ_0 and the whole system undergoes a transition to LS. Figure 2.22 shows the states x_1, x_2 and the amplitudes of the oscillators in the case of LS.

$$S^2(\tau) = \frac{< (x_2(t + \tau) - x_1(t))^2 >}{\sqrt{< x_1^2(t) >< x_1^2(t) >}} \qquad (2.48)$$

One should note that further increase in the coupling strength lets the time lag in Equation 2.45 approach to zero. With vanishing τ_0, the two nonidentical oscillators tend to be synchronized almost completely, i.e. $x_1(t) \approx x_2(t)$.
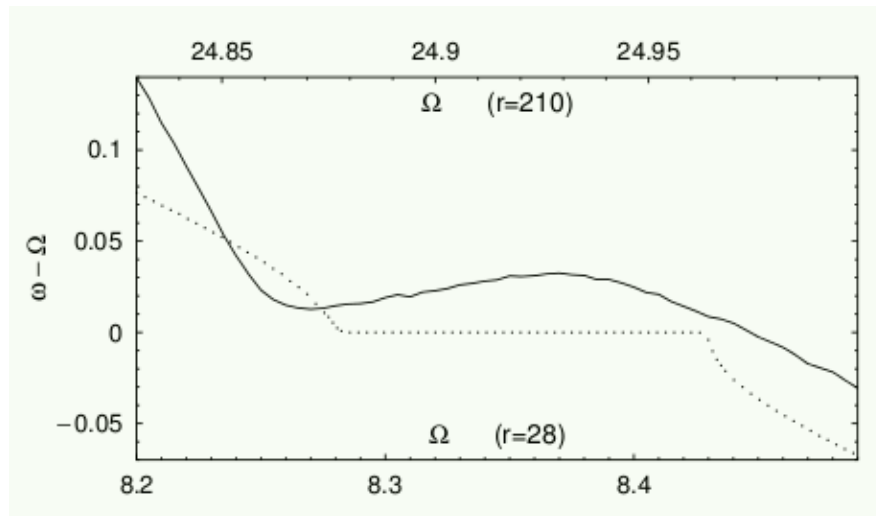
Figure 2.19. From [2]. PS and IPS in Equation 2.46; solid line: $r = 28, \varepsilon = 6$; dotted line: $r = 210, \varepsilon = 3$.
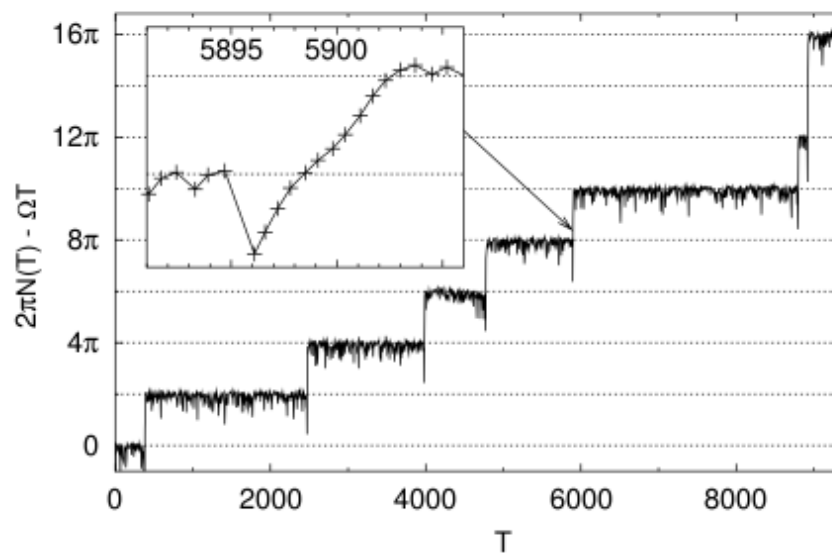
Figure 2.20. From [2]. Phase slips of IPS in Equation 2.46 for $r = 28, \varepsilon = 6$.
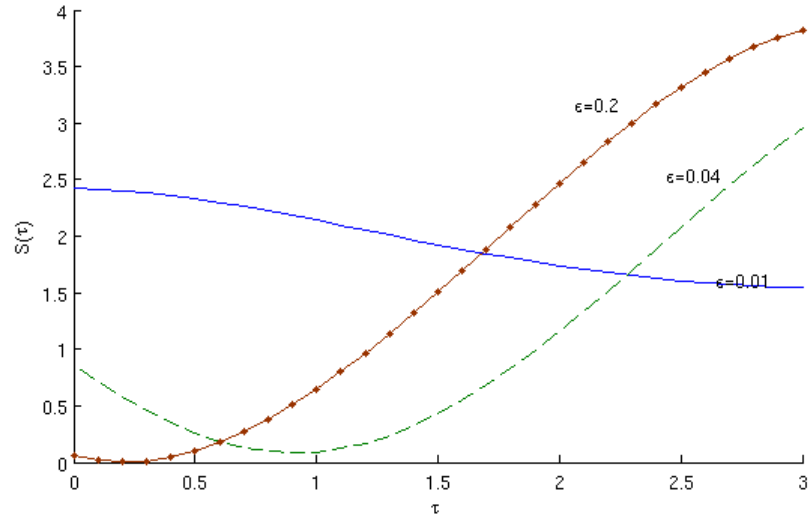
Figure 2.21. Similarity function $S(\tau)$ obtained for two coupled Rössler oscillators (Equation 2.45) for different values of the coupling strength ε. In PS regime ($\varepsilon = 0.04$), $min(S(\tau)) \neq 0$ when LS is obtained ($\varepsilon = 0.14$), $min(S(\tau)) = 0$.
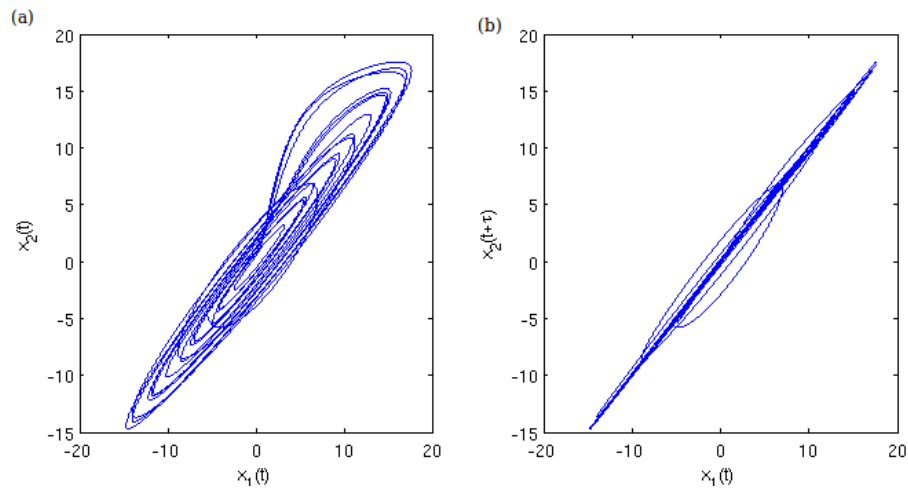
Figure 2.22. LS of Equation 2.45 for $\varepsilon = 0.2$. (a) $x_1(t)$ vs $x_2(t)$ shows systems do not completely synchronize; (b) $x_1(t)$ vs $x_2(t + \tau_0)$ shows LS exits between the systems for $\tau_0 = 0.21$.

Intermittent lag synchronization occurs during the transition from PS to LS, where LS of the oscillators is interrupted by intermittent burst of large synchronization error $x_1(t) - x_2(t + \tau_0)$ [28]. The reason of ILS is explained in terms of the changes in the Lyapunov exponents of whole system. In PS of two mutually coupled 3-dimensional chaotic oscillators, one of the two zero Lyapunov exponents becomes negative. When the coupling strength is increased, before LS, one of the two positive Lyapunov exponents also becomes negative. With this change, ILS is observed for the coupling strengths within this region.

Generalized Synchronization of Chaotic Systems. In Section 2.3.2.1 it is claimed that coupled identical systems can lock to a common chaotic trajectory in the state space ($\mathbf{x}_i = \mathbf{x}_j$) and CS is achieved. But this situation is not valid is the coupled systems are nonidentical. Thus, the synchronization concept needs to be generalized for the asymmetric case. [36, 50] introduce *generalized synchronization* concept for unidirectionally coupled nonidentical chaotic systems in Equation 2.49, where $\mathbf{F} : \Re^n \to \Re^n, \mathbf{G} : \Re^m \to \Re^m$ and the driving function $\mathbf{h} : \Re^n \to \Re^m$ If GS is satisfied, there exists a transformation $\xi : \mathbf{x} \to \mathbf{y}$ which maps drivers trajectories into the ones of response $\mathbf{y}(t) = \xi(\mathbf{x}(t))$.

$$\dot{\mathbf{x}} = \mathbf{F}(\mathbf{x})$$
$$\dot{\mathbf{y}} = \mathbf{G}(\mathbf{y}, \mathbf{h}(\mathbf{x})) \tag{2.49}$$

[50] also introduces necessary and sufficient conditions for GS in Equation 2.49 and expresses that GS is about the asymptotic stability of the response systems. The response system is asymptotically stable if $\lim_{t \to \infty} \|\mathbf{y}(t, \mathbf{x}(\mathbf{0}), \mathbf{y_1}(\mathbf{0})) - \mathbf{y}(t, \mathbf{x}(\mathbf{0}), \mathbf{y_2}(\mathbf{0}))\| = 0$, where $(\mathbf{x}(\mathbf{0}), \mathbf{y_1}(\mathbf{0}))$ and $(\mathbf{x}(\mathbf{0}), \mathbf{y_2}(\mathbf{0}))$ are two initial conditions for the system in Equation 2.49 in the basin of the synchronization attractor. In other words, if the chaotic driving signal provides the oblivion of initial conditions of the response, there exists a mapping $\mathbf{y}(t) = \xi(\mathbf{x}(t))$. This property leads to a nice approach for detecting

GS by generating a replica of the response system $(\mathbf{y}' = \mathbf{G}(\mathbf{y}', \mathbf{h}(\mathbf{x})))$. In this framework, it is concluded that GS is satisfied if $\mathbf{y}(t)$ and $\mathbf{y}'(t)$, which start from different initial conditions, synchronize completely.

[51] construct a system in which a Lorenz oscillator and its replica are driven by a Rössler oscillator in Equation 2.50. Figure 2.23 visualizes the CS between the Lorenz and its replica as an evidence for GS between the Rössler and the Lorenz.

$$\dot{x}_1 = -\lambda(x_2 - x_3)$$
$$\dot{x}_2 = \lambda(x_1 + 0.2x_2)$$
$$\dot{x}_3 = \lambda(0.2 + x_3(x_1 - 5.7))$$
$$\dot{y}_1 = 10(y_2 - y_1)$$
$$\dot{y}_2 = 28y_1 - y_2 - y_1y_3 + \varepsilon x_2$$
$$\dot{y}_3 = y_1y_2 - \frac{8}{3}y_3$$
$$\dot{\mathbf{y}'} = f(\mathbf{y}) \qquad\qquad\qquad (2.50)$$

2.3.3. Synchronization Control

Synchronization in an ensemble of oscillators is crucial for brain functions, communication, chemical reactions, predator-prey systems and so on. Controlling of this collective rhythm is important in order to reach the desired motion in the ensemble, e.g. influencing the phase or frequency, enhancement or suppression of the synchronization. For instance, the enhancement of synchronous behavior may be desired for obtaining a more robust behavior of the whole system. Such a requirement is crucial for the of failure of cardiac or neural pacemakers. On the other hand, extremely strong synchronization may have destructive effects on some brain functions. For example, neurons located in the thalamus and basal ganglia fire in an uncorrelated manner under healthy conditions [52], whereas the Parkinsonian tremor is a result of the synchronization of
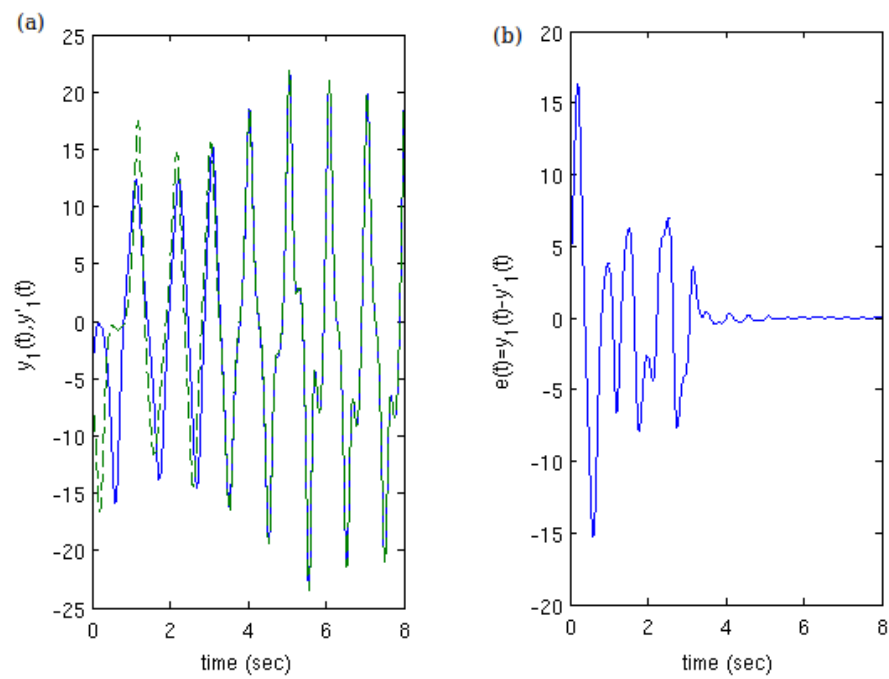
Figure 2.23. CS of driven Lorenz systems for $\lambda = 6, \varepsilon = 50$ (Equation 2.50).(a) Solid line represents $y_1(t)$ and dashed line represents $y_1'(t)$; (b) state difference $e(t) = y_1 - y_1'$.

these neurons. Thus, for such cases, the suppression of synchronization may be crucial. Some techniques are presented for enhancing or desynchronizing oscillatory networks, e.g. using phase resetting principles [53, 54], delayed feedback stimulation [55–57] or demand-controlled method [52].

In order to control synchronization in an ensemble of chaotic oscillators, researchers not only have introduced new methods but also have adapted some techniques have been used to control single chaotic systems. Due to the rich dynamics of chaotic systems, there are different methods for control and stabilization of chaos, e.g. changing the systems parameters, applying a damper, time-delay feedback method (Pyragas' method), stabilizing UPOs (the Ott-Grebogi-Yorke (OGY) method), occasional proportional feedback (OPF). Even synchronization can be considered as a control method of chaotic systems [58], which allows the suppression of the sensitivity to the initial conditions or the modification of the phase of the oscillator. The interaction between the oscillators certainly increases the complexity of the overall systems, however, some of these techniques can still give successful outcomes.

Time-delayed feedback method is one of the most studied techniques to control synchronization. This technique has originally been introduced by Pyragas [59], therefore also called *Pyragas' method*. It is based on stabilizing one of the UPOs embedded in a chaotic attractor by feeding back the delayed version of one of the observed system states in continuous time. Equations 2.51 and 2.52 show the original formalism for this control approach.

$$\dot{y} = P(y, \mathbf{x}) + F(t)$$

$$\dot{\mathbf{x}} = Q(y, \mathbf{x}) \tag{2.51}$$

$$F(t) = K[y(t - \tau) - y(t)] \tag{2.52}$$

In Equation 2.51 and Equation 2.52, $y(t)$ represents the output state and the vector $\mathbf{x}$ the remaining states of the dynamic system. Time delay shown by τ is chosen

equal to the period of the UPO to be stabilized, and K denotes the amplitude of the feedback signal $F(t)$. Delayed feedback control algorithm has been applied successfully in experiments in various domains such as electronics, mechanics, and pathological brain rhythms [60].

Rössler chaotic system in Equation 2.50 is considered to illustrate the Pyragas' method (Equation 2.53). An approximate period of period-one UPO $\mathbf{x_0}(t) = \mathbf{x_0}(t+T)$ embedded in its chaotic attractor is $T \approx 5.9$. Figure 2.24 and 2.25 show the successful stabilization of the period-one UPO by time-delayed feedback with $\tau = T = 5.9$.

$$\dot{x}_1 = -(x_2 - x_3)$$
$$\dot{x}_2 = (x_1 + 0.2x_2) + F(t)$$
$$\dot{x}_3 = 0.2 + x_3(x_1 - 5.7)$$
$$F(t) = K(x_2(t - \tau) - x_2) \tag{2.53}$$

The technique presented above can be applied to a drive-response configuration in Equation 2.50 as in Equation 2.54. Here, chaotic motion of the Lorenz oscillator is controlled by a time-delayed feedback control via a chaotic Rössler system. Here, the frequency of the synchronous motion is effected by this control input, that is equal to $T = 5.9$ sec.

$$\dot{x}_1 = -\lambda(x_2 - x_3)$$
$$\dot{x}_2 = \lambda(x_1 + 0.2x_2) + F(t)$$
$$\dot{x}_3 = \lambda(0.2 + x_3(x_1 - 5.7))$$
$$\dot{y}_1 = 10(y_2 - y_1)$$
$$\dot{y}_2 = 28y_1 - y_2 - y_1y_3 + \varepsilon x_2$$
$$\dot{y}_3 = y_1y_2 - \frac{8}{3}y_3$$
$$F(t) = K(x_2(t - \tau) - x_2) \tag{2.54}$$
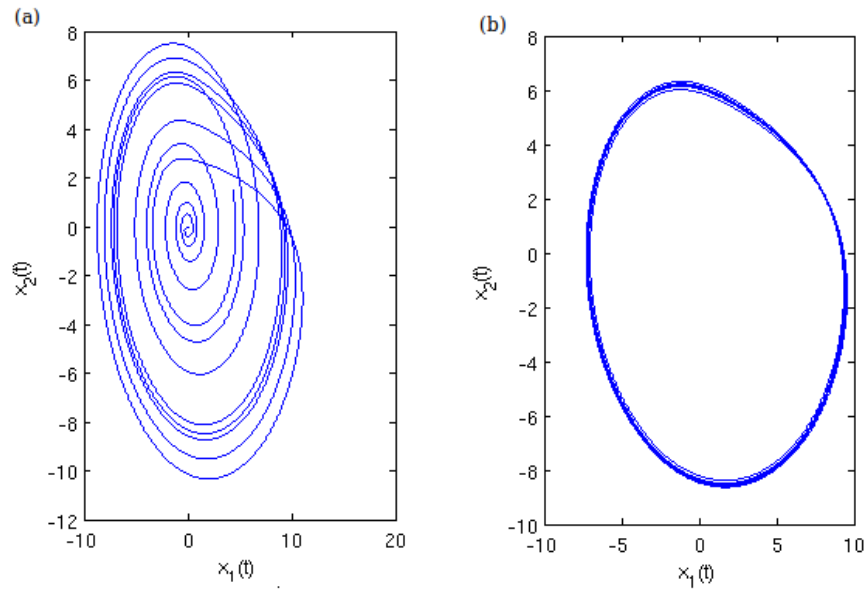
Figure 2.24. $x_1 - x_2$ phase portrait of Equation 2.53. (a) Without control input; (b) in the post-transient regime with control input $F(t)$ for $K = 0.2$ and $\tau = 5.9$.
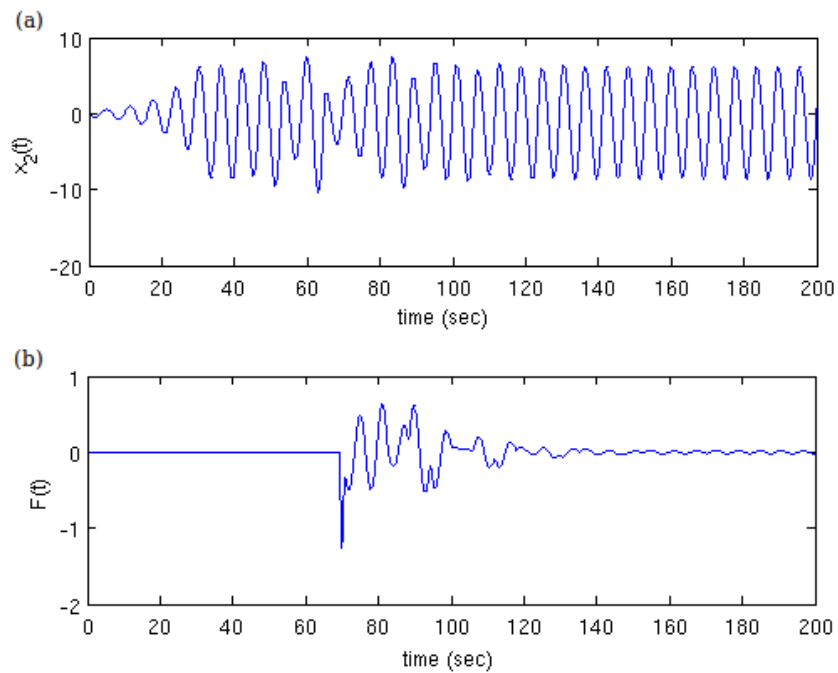
Figure 2.25. (a) Dynamics of the output signal x_2; (b) continuous control input $F(t)$. Control is switched on at $t = 70$ sec.

Time-delayed feedback control is applied both theoretically and experimentally to both locally and globally coupled ensembles of periodic and chaotic oscillators [55, 61]. Beside this method, some other control methods are applied for controlling synchronization. [62] investigate the synchronization control in a nonlinearly coupled oscillators by a periodic force. An automatic control method introduced in [63] is applicable to both coupled periodic and chaotic oscillators.

2.4. Problem Statement

The concept of this thesis can be divided into two: (i) investigation of impacts of different factors on synchronization; (ii) controlling synchronization.

Firstly, two fundamental points associated with synchronizability are investigated; network structure and individual properties of the oscillators. In this thesis, three types of artificial networks having different topological properties (Erdős-Rényi, Watts-Strogatz and Barabasi-Albert networks) are compared with a natural network (the neural network model of a soil roundworm) on basis of how much they support synchronization of the oscillators as nodes.

The second factor on synchronization is individual properties of the oscillators. Different synchronization scenarios are observed for periodic oscillators (phase and frequency locking) and chaotic oscillators (complete synchronization, phase synchronization... etc.) depending on the coupling strengths and coupling functions. A coupling scheme depending on the similarity of the the natural frequencies of the interacting systems is presented and its effect on synchronization is studied. To eliminate the randomness in network-structural sense, only globally (all-to-all) coupled networks of oscillators are considered and because of technical limitations small size networks are considered.

Synchronization control which is crucial in many applications is studied on an ensemble of mean-field-coupled chaotic oscillators. Basically, two different approaches
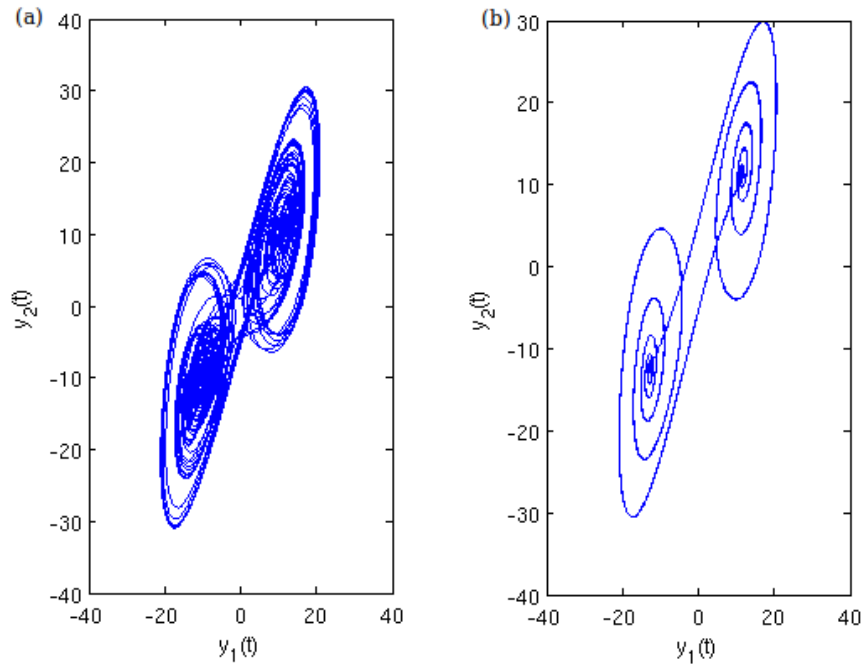
Figure 2.26. $y_1 - y_2$ phase portrait of Equation 2.54. (a) Without control input; (b) in the post-transient regime with control input $F(t)$ for $K = 0.2$, $\tau = 5.9$ and $\lambda = 1$.
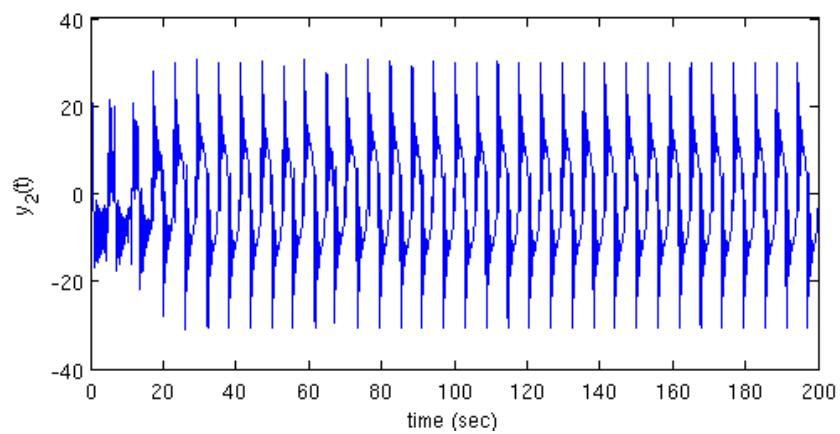
Figure 2.27. Dynamics of the y_2 in Equation 2.54. Control is switched on at 70 sec.

are studied; time-delayed mean-field feedback control and applying external periodic force. The performance of these techniques are investigated on basis of influencing synchronous state of the ensemble.

3. ANALYSIS TOOLS

In this chapter some indirect analysis methods of synchronization are presented: power spectral density analysis, variance analysis on the ensemble and the correlation coefficient. Those methods are useful especially when directly identifying phase is not possible or its dynamics is hard to analyze. Additionally, the user interface prepared for the simulation of oscillators networks will be presented.

3.1. Power Spectral Density Analysis

For a given signal, the power spectrum gives a plot of the portion of a signal's power (energy per unit time) within each frequency bin. The peak in this plot occurs at the dominant frequency value of the signal. Power spectrum analysis presented as a tool for detecting synchronization in [64] can be useful even for the cases where the coupled oscillators are structurally distinct.

A direct way to track the collective behavior between coupled oscillators is to define phase for each oscillator properly, then to look for horizontal plateaus in the phase difference, as it is done in the previous sections. However, assigning phase for some oscillators, is not an easy task. Phase of a periodic oscillator can be obtained by constructing a Poincaré surface in the state space of the system. Contrarily, if the oscillator under consideration is an aperiodic one, like a chaotic system, assigning a Poincaré surface is not so simple. An inadequate choice of the Poincaré surface leads to wrong measurements and errors in phase calculation. To avoid confusion, power spectral analysis can be executed for an appropriate observed state of the oscillator. This analysis can be performed both on numerical solutions of system models and experimental results.

Let us consider two mutually coupled Rössler chaotic oscillators in Equation 2.45 as an example for power spectral density analysis. Typically, the power spectrum of

a chaotic system has a board-band component and a peak at the mean frequency of oscillations. It should be kept in mind that in case of phase synchronization, the coupled systems oscillate at the same mean observed frequency. Figure 3.1 demonstrates how the peaks of the power spectra of the oscillators converge to each other and finally overlap.
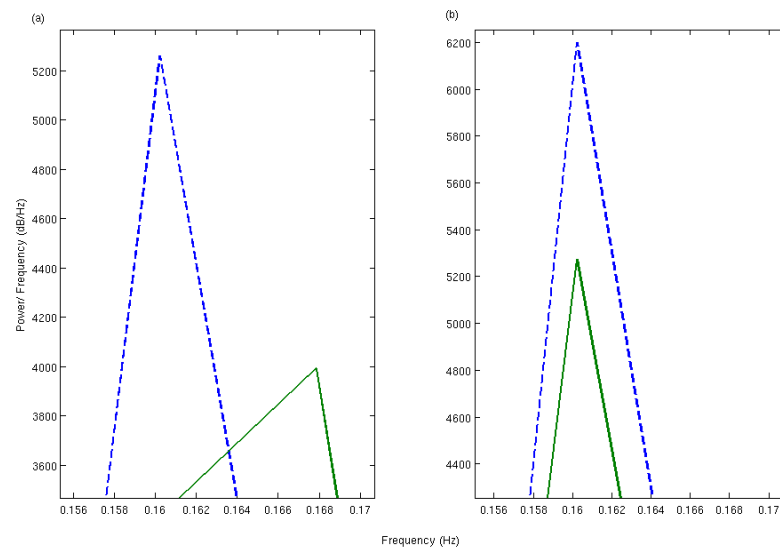
Figure 3.1. Power spectra of coupled Rössler oscillators in Equation 2.45 (a) before phase synchronization; (b) after phase synchronization is achieved.

Power spectrum analysis of the mean field of a mean-field-coupled network also gives an idea about whether the synchronization state is achieved. As Figure 3.2 shows for the mean-field-coupled Rössler oscillators in Equation 2.45, with increasing in the coupling strengths the power spectrum becomes narrower and a sharp peak shows up at the mean frequency when the ensemble achieves phase synchronous behavior for $\varepsilon = 0.2$.

In this thesis, in all experiments with chaotic oscillators, power spectral analysis is used for assigning the mean observed frequencies.
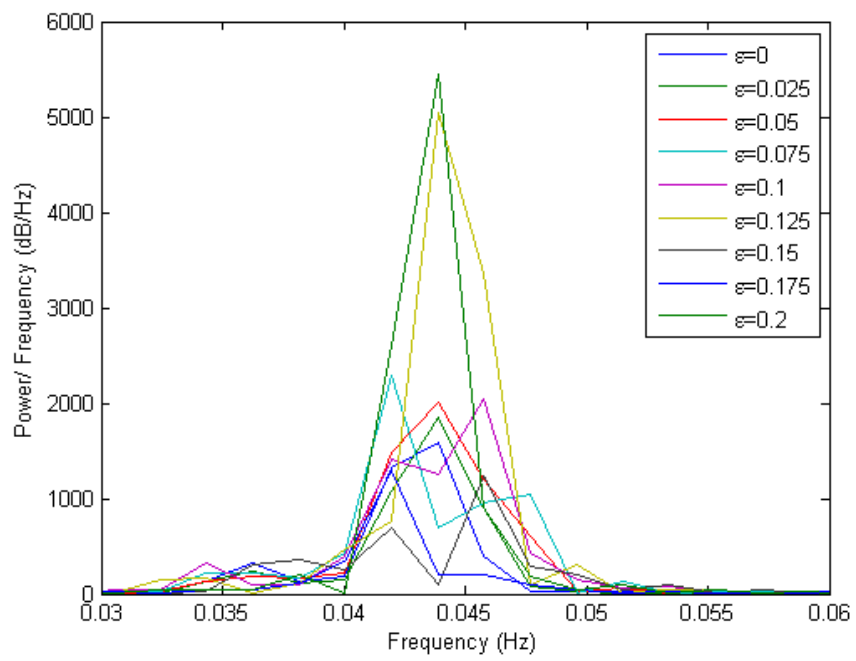
Figure 3.2. Evaluation of power spectrum of the mean field of coupled Rössler oscillators in Equation 2.45 for different coupling strengths.

3.2. Ensemble Deviation and Correlation Factor

Another strategy of detecting synchronization of mean-field-coupled systems is by means of analyzing the ensemble variance [65]. Here, ensemble deviation refers to the largest absolute deviation of the mean field oscillations from zero. The ensemble deviation of synchronized oscillators is larger than that of unsynchronized oscillators. Figure 3.3 and Figure 3.4 shows the asynchronous and synchronous states of two mutually coupled identical periodic uniform oscillators.

Is this thesis, inspired by mean field variance, *ensemble deviation* is used for quantifying the synchronization of coupled identical oscillators. Ensemble deviation is the mean of the difference between the mean field and each of the oscillators which can be calculated as in Equation 3.1. If the oscillators completely synchronize, this difference approaches zero, since the oscillators' states follow the same trajectory within the state space of the overall system.

$$V(t) = \sqrt{\frac{\sum_i^N (X(t) - x_i(t))}{N}} \tag{3.1}$$

In some cases, such as complete synchronization and lag synchronization, the correlation between the states can be used as an indirect measurement. The correlation coefficient between two variables S and T consisting of n samples, also known as Pearson's correlation coefficient, is formulated as in Equation 3.2, where s_i and t_i are the samples, $\bar{S}$ and $\bar{T}$ are the mean values, σ_S and σ_T are the standard deviations of S, T vectors. This coefficient ranges between $[-1, 1]$ (Figure 3.5). The meaning of the value of this correlation coefficient in given in Table 3.1.

$$corr_{ST} = \frac{\sum_i^n (s_i - \bar{S})(t_i - \bar{T})}{(n-1)\sigma_S \sigma_T} \tag{3.2}$$
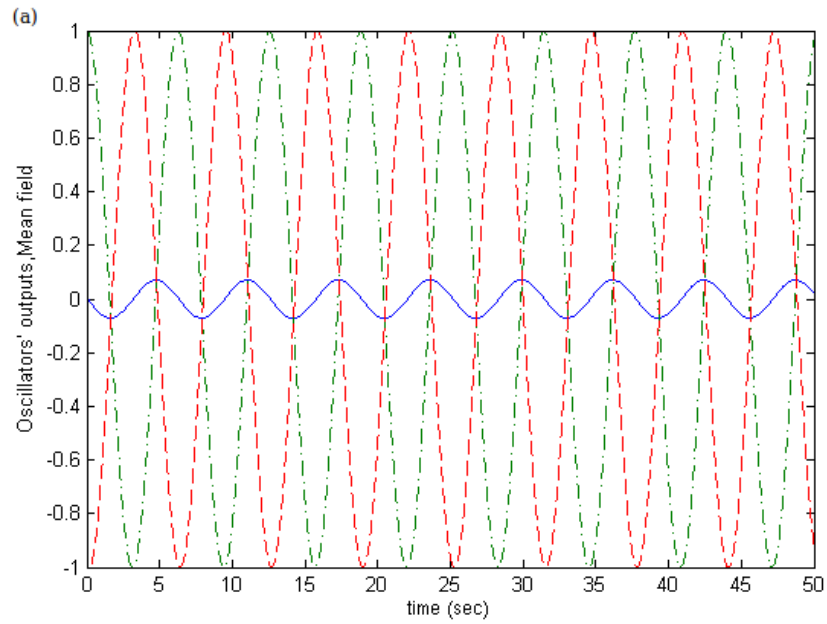
Figure 3.3. Two mean-field-coupled periodic oscillators (dash and dash-dot lines) and their mean (solid line) for asynchronous behavior.
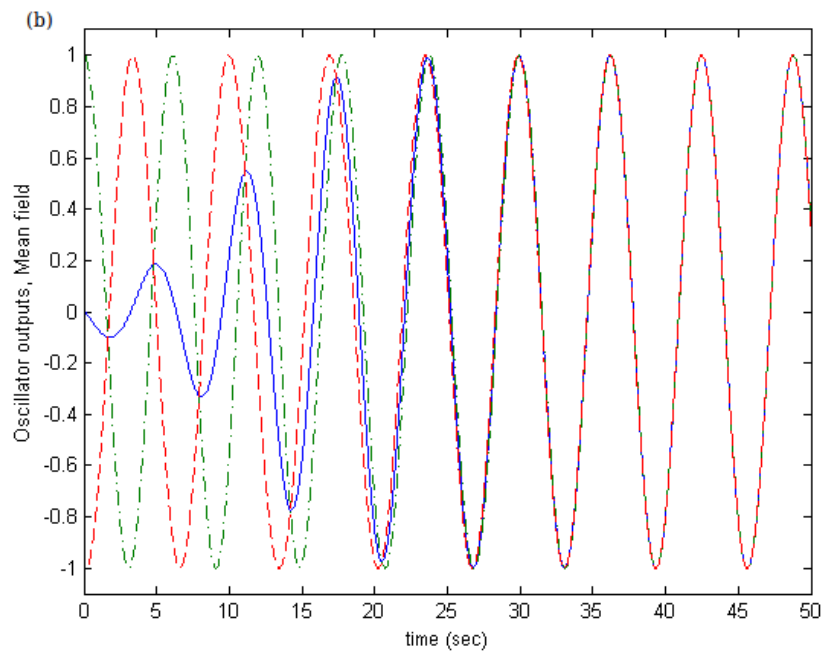
Figure 3.4. Two mean-field-coupled periodic oscillators (dash and dash-dot lines) and their mean (solid line) for synchronous behavior.
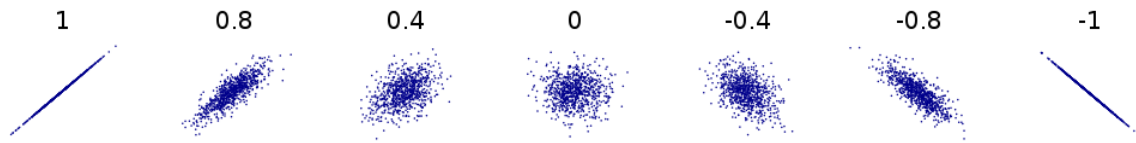
Figure 3.5. Variation of correlation coefficient between different pairs of variables.

Table 3.1. Ranges of the correlation coefficient and their respective meanings.

Correlation	Negative	Positive
None	(-0.1,0]	[0,0.1)
Small	(-0.3,-0.1]	[0.1, 0.3)
Medium	(-0.5,-0.3]	[0.3, 0.5)
Strong	[-1,-0.5]	[0.5, 1]

3.3. An Interface for Coupled Oscillators In Complex Networks

For investigating the collective behavior of coupled oscillators on basis of simulations a user-friendly interface has been designed as part of this thesis (Figure 3.6).

The interface enables the user to:

- investigate behaviors of forced or coupled oscillators of three different types, and combine them as well,
- assign natural frequencies and some specific parameters of the oscillators as Gaussian distributed random or predefined variables,
- choose among predefined topology types or work on his own network,
- edit the coupling matrix, i.e. delete existing edges or add new ones,
- specify the effect type of interacting oscillators.

After assigning the simulation time and running the system, a new table pop ups demonstrating the natural and observed frequencies of the oscillators, besides they are
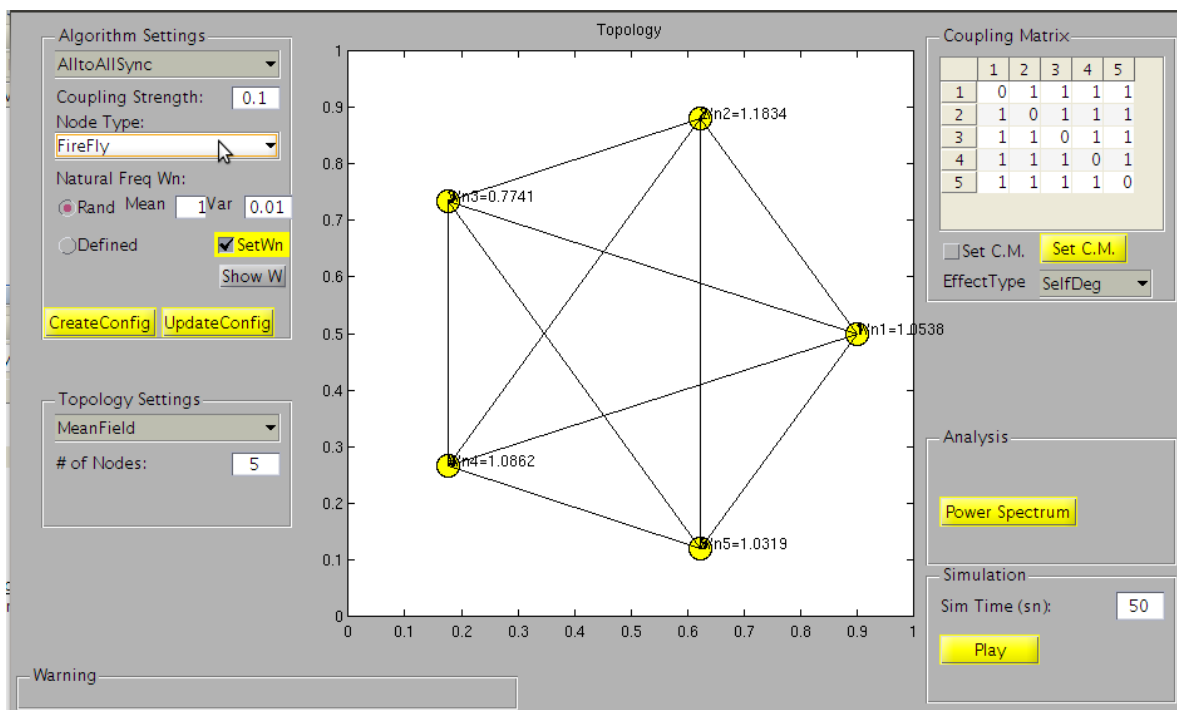
Figure 3.6. User interface designed for simulations of synchronization in oscillator networks.

showed in the main figure. Finally, the numerical time solutions of the oscillators are exported in the workspace, so the user can plot or examine them separately. At the same time, the obtained numerical results can be analyzed by already existing power spectral density analysis.

The user manual for this simple interface is given in Appendix C.

4. EXPERIMENTS AND RESULTS

4.1. Synchronization

In this section, synchronization in complex networks, similarity-dependent coupling scheme and synchronization of chaotic Rössler systems will be presented.

4.1.1. Synchronization in Complex Networks

One of the questions to be answered is the effect of network topology on synchronization behavior. For this purpose, a well-studied model of neural network of soil nematode Caenorhabditis elegans (C. elegans) is studied and compared with other artificially created networks, e.g. Erdös-Rényi (ER), Watts-Strogatz (WS) and Barabasi-Albert (BA), having same number of nodes and edges. For the sake of simplicity, the nodes are considered to be uniform periodic oscillators and only unweighted and undirected graphs are studied.

C. elegans is a free-living, transparent roundworm (nematode), about 1 mm in length, which lives in temperate soil environments. Researches in the molecular and developmental biology of c. elegans begun in 1974 and since then it has been used extensively as a model organism. C. elegans has a relatively simple nervous system consisting 302 neurons and all the connections of its neuronal network are well known. The nervous system is separated into two units as follows. First, the pharyngeal nervous system is composed of 20 cells. Second, the somatic nervous system consists of the rest neurons. The long processes from the somatic neurons construct bundles; the nerve ring, the ventral cord, etc.. The data set of this neural network is obtained from Mark Newman's network database [3]. This data had been compiled by Duncan Watts and Steven Strogatz [4] from original experimental data by White [66].

The network data, which is taken from Newman's database, includes 297 nodes

and 2148 weighted, directed edges (Figure 4.1). Newman noted that the nodes in the original data of White's were not consecutively numbered, so they had been renumbered to be consecutive. Furthermore, it is also stated that the original node numbers from Watts' data file are retained as the labels of the nodes and edge weights given by Watts. For simplicity, all edges are treated as undirected and unweighted for this thesis. Table 4.1 shows the analysis of the unweighted and undirected neural network.
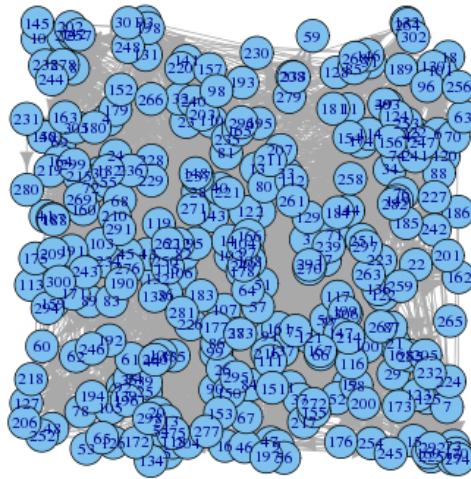
Figure 4.1. From [3]. Weighted, directed graph of neural network of c. elegans, numbered by Watts.

The artificial networks studied in this thesis have been generated with the same number of nodes and edges of unweighted and undirected neural network of c. elegans. For the construction of an ER random network model, the crucial value is the average degree $< k >= \frac{l}{N}$, and connection probability $p = \frac{L}{l}$, where l is the actual number of edges in the network and $L = N(N-1)$ is the maximum number of edges in a directed network with N nodes.

Table 4.1. Analysis of unweighted and undirected neural network of c. elegans.

# of nodes: N	297
Average node degree: $<k>$	14.47
Average shortest-path length:	2.46
Average clustering coefficient:	0.292
# of connected components:	1

WS graphs are generated according to the rule proposed by Watts and Strogatz [4]. They started with a regular N nodes ring graphs, in which each node is connected of its $2m$ nearest neighborhoods. Then, for each node, each link connected to a clockwise neighbor is rewired to a randomly chosen node with a probability p, and preserved with a probability $(1-p)$. Note that if $p=0$, the network is a regular ring, which has high clustering coefficient but a high average shortest path value. If $p=1$, the network is a random graph, which has very low average shortest path value but a low clustering coefficient. Whereas, WS network model, also called *small-world network*, is between a regular ring an random graph with $0 < p < 1$ having a high clustering coefficient and a low average shortest path value (Figure 4.2).

For constructing of a BA network, one should start with m_0 number of isolated nodes. At each time step, $t = 1, 2, \ldots, N - m_0$, a new node j with $m \leq m_0$ links is added to the network. The probability that a link will connect j to an existing node i is linearly proportional to the actual degree of i. Since every new node has m number of links, at time t, the network will have $N = m_0 + t$ nodes and $l = mt$ links. For large times, the average degree will be $<k> = 2m$, and the degree distribution will be scale-free $P(k) \sim k^{-\gamma}$.

The governing dynamics of the nodes in Equation 4.1 are the generalization of Kuramoto's globally coupled oscillators in Equation 2.37, where ε_{ij} are the coupling strengths between pairs of connected oscillators, a_{ij} are the elements of adjacency
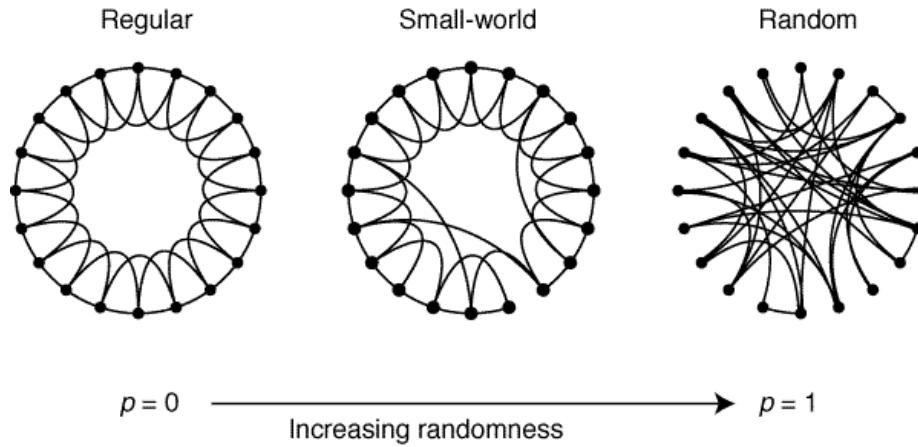
Figure 4.2. Form [4]. Illustration of small world network connectivity with respect to p.

matrix. The first problem when defining the Kuramoto model in complex networks is how to state the interaction dynamics properly [67]. The most important point is the preserving the heterogeneity of a complex network. Yet, there are several approaches, in this thesis, sum of the coming effects onto a node is divided by the maximum node degree in a network, k_{max}. This means that, if an oscillator has more connections, it has more chance to orient itself to its local environment. Equation 2.36 can be written as

$$\dot{\phi}_i = w_i + \frac{\varepsilon}{k_{max}} \sum_{j=1}^{N} a_{ij} \sin(\phi_j - \phi_i). \tag{4.1}$$

For statistical accuracy, in this study 20 graphs are generated for each network model according to the same construction rules. Heterogeneity of a network is measured via its minimum and maximum node degrees. As Table 4.2 demonstrates, among all the considered networks the most heterogeneous one is c. elegans' neural network and the least heterogeneous ones are WS networks. Note that if the rewiring probability p of WS network is small, the network is more homogeneous, and this network model approaches to the random one, ER as p increases.

Table 4.2. Averaged maximum and minimum node degrees of considered networks.

	$< k_{min} >$	$< k_{max} >$
CE	1	134
ER	5	26.45
BA	7	81.6
WS(p=0.1)	9.55	19.3
WS(p=0.2)	7.7	20.8
WS(p=0.3)	6.95	22.5
WS(p=0.4)	5.9	23.25
WS(p=0.5)	5.7	23.35
WS(p=0.6)	5.35	24.35
WS(p=0.7)	5.45	24.55
WS(p=0.8)	5.05	25.35
WS(p=0.9)	4.8	25.8

4.1.1.1. Synchronization of Identical Periodic Uniform Oscillators. As a first step for capturing the topological effects on synchronization, the nodes are assumed to be identical, $w_i = w = 1rad/sec$. Irrespective of initial phases and coupling strengths, identical periodic oscillators can adapt their phases to each other in the long run. The topology and coupling strengths dramatically affect how fast phase synchronized state is reached.

The coupling strength ε is changed between 0.05 and 0.5. The experiments are conducted for a duration 200 sec. The behavior of V(t) (Equation 3.1) in the unweighted and undirected neural network is demonstrated in Figure 4.3. As the coupling strength increases, the oscillators synchronize faster, but it should be noted that the final value of $V(t)$ is far from 0, whereas in the artificially created networks $V(t)$ almost equals to 0 as given in Table 4.3 and plotted in Figure 4.4.

Figure 4.4 shows the relevance of small-world property of a network for achieving collective behavior even if the common coupling is so small such as $\varepsilon = 0.05$. For such a small value, as the rewiring probability increases, the final value of $V(t)$ increases and approaches to the random ER network, as expected and Figure 4.2 demonstrates. And also one can observe that the hub structure, the outcome of scale-freeness, negatively affects the synchronizability. BA network has highest $V(t)$ value among all networks.

Final important note is about the difference between a "intelligently structured network" and artificial ones. One can observe that $V(t)$ approaches to zero with increase in the coupling strength for most of the artificial networks, as opposed to c. elegans' neural network. Even though it is more heterogeneous than the BA network, it allows better synchronizability. Although c. elegans has small-world properties, its performance in terms of phase locking is worse than the WS graph. As it is stated before, for some cases synchronization is not desired and special structure of c. elegans' network may hamper synchronization of the whole oscillators.
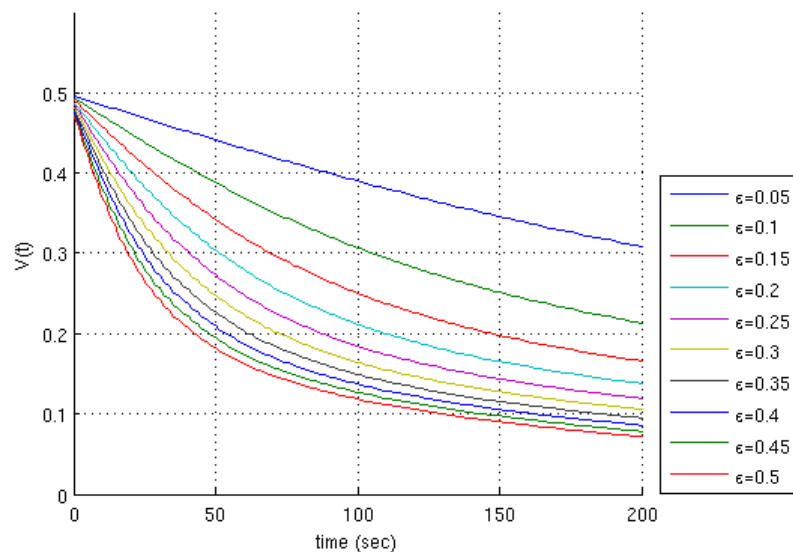
Figure 4.3. $V(t)$ with respect to varying ε in unweighted and undirected neural network of c. elegans.
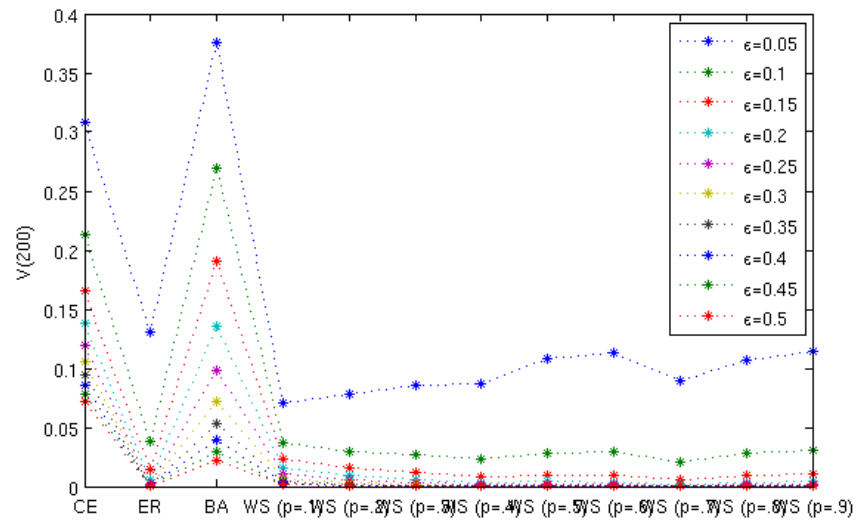
Figure 4.4. Final value of V(t) for different ε values in each network.

Table 4.3. Final value of V(t) for different ε values in each network.

	ε=0.05	ε=0.1	ε=0.15	ε=0.2	ε=0.25	ε=0.3	ε=0.35	ε=0.4	ε=0.45	ε=0.5
CE	0.3081	0.2127	0.1652	0.1376	0.1192	0.1056	0.09483	0.0858	0.0781	0.0714
ER	0.1303	0.0386	0.0139	0.0056	0.0024	0.0010	0.0004	0.0002	0.0001	5.13e-05
BA	0.3754	0.2699	0.1911	0.1360	0.0978	0.0713	0.0526	0.0392	0.0294	0.0223
WS(p=0.1)	0.0702	0.0365	0.0230	0.0151	0.0101	0.0069	0.0047	0.0033	0.0023	0.0016
WS(p=0.2)	0.0786	0.0288	0.0154	0.0087	0.0051	0.0030	0.0018	0.0011	0.0007	0.0004
WS(p=0.3)	0.0858	0.0272	0.0123	0.0060	0.0030	0.0015	0.0007	0.0004	0.0002	0.0001
WS(p=0.4)	0.0867	0.0225	0.0084	0.0034	0.0014	0.0006	0.0002	0.0001	5.88e-05	2.66e-05
WS(p=0.5)	0.1075	0.0278	0.0095	0.0038	0.0016	0.0007	0.0003	10.0001	6.67e-05	3.08e-05
WS(p=0.6)	0.1132	0.0288	0.0092	0.0033	0.0012	0.0005	0.0002	8.63e-05	3.67e-05	1.59e-05
WS(p=0.7)	0.0899	0.0206	0.0061	0.0020	0.0007	0.0002	0.0001	3.97e-05	1.53e-05	5.98e-06
WS(p=0.8)	0.1068	0.0284	0.0095	0.0036	0.0014	0.0006	0.0002	0.0001	5.24e-05	2.36-05
WS(p=0.9)	0.1145	0.0308	0.0102	0.0037	0.0015	0.0006	0.0002	0.0001	5.16e-05	2.30e-05

4.1.1.2. Synchronization of Nonidentical Periodic Uniform Oscillators. The second step in order to capture the topological effects to synchronization, the nodes are assumed to consist of nonidentical periodic oscillators. More specifically, the periodic oscillators that constitute the nodes have been chosen such that they differ from each other in terms of their natural frequencies. The initial phases are assigned uniformly distributed manner around π and the natural frequencies are assigned according to a Gaussian distribution with mean value $\mu = 1$ and variance $\sigma^2 = 0.01$ (Figure 4.5).
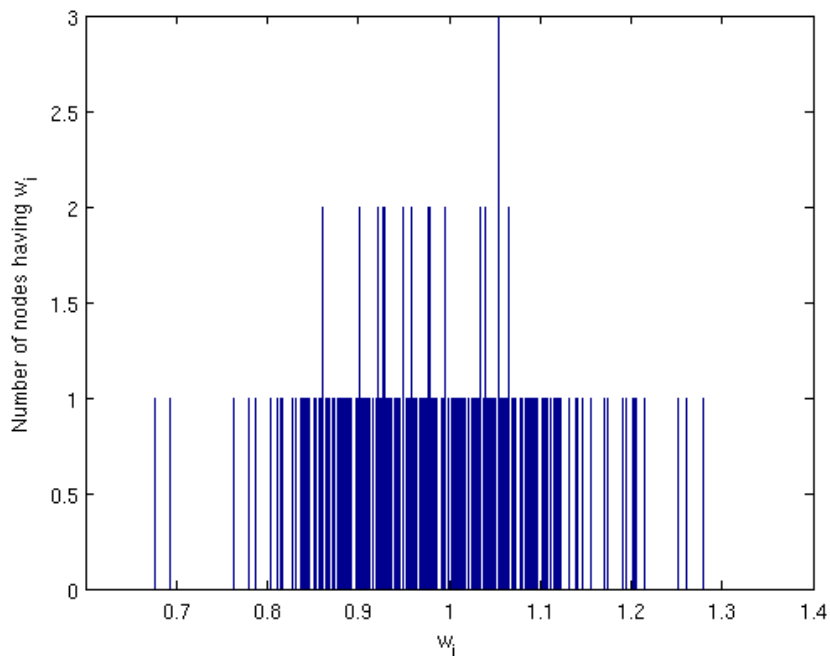
Figure 4.5. The histogram of the natural frequencies of 297 periodic oscillators distributed according to $\aleph(1,0.01)$.

Two Kuramoto oscillators represented in Equation 2.37 synchronize if and only if $\varepsilon > \varepsilon_c$. For Equation 2.37, the critical coupling strength equals to the difference between the natural frequencies of the oscillators. Kuramoto showed [24] that for relatively small N the critical coupling strength depends on the standard deviation of the Gauss distribution. To define a proper ε for complex networks, firstly a globally coupled network has been considered, in order to guarantee synchronization at least for such an all-to-all coupled case. It should be noted that a globally coupled network

has a homogeneous structure with $k_{max} = (N-1)$ which is identical for all vertices. It is observed that for $\varepsilon = 0.2 > \sigma = 0.1$ almost all nodes are frequency locked (Figure 4.6). Consequently, ε in Equation 4.1 has been taken as 0.2 in all other experiments and the sum of the effects coming from other nodes divided to k_{max} given in Table 4.2. It should be noted that due to technical limitations the experiments have been performed only for $t = 200$ sec.
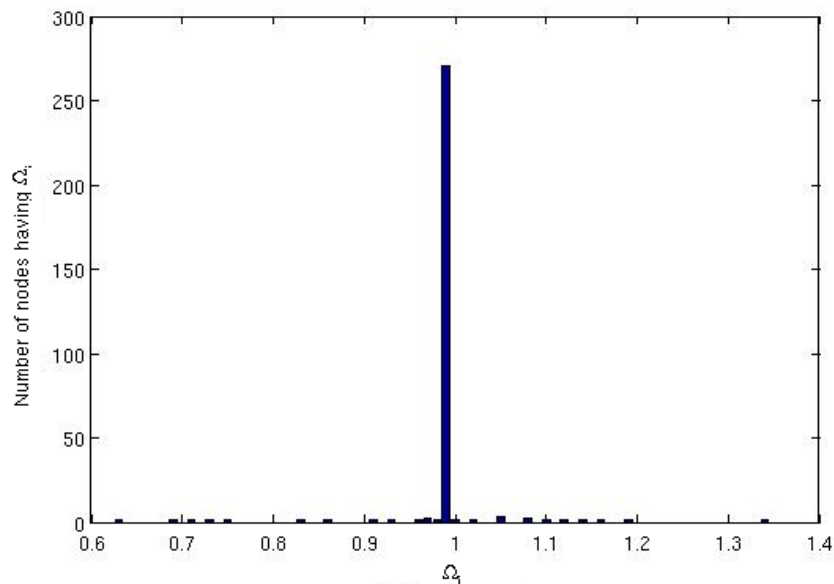
Figure 4.6. Final frequency distribution in an all-to-all coupled network with $\varepsilon = 0.2$. Number of nodes having the same frequency is 271 and number of occupied bins is 26.

Note that 282 of the randomly distributed natural frequencies of the oscillators are in different bins (Figure 4.5). It is expected that coupling will result in decrease in the number of occupied bins in the final observed frequency histogram. If the network topology provides optimal conditions for synchronization of the ensemble, like an all-to-all coupled structure, the number of occupied bars will be small. The sensitivity of the bin size is 10^{-3} which is also acceptable for numerical sensitivity of the simulations.

Figure 4.7 shows the final frequency distribution of the oscillators in the c. elegans' neural network. As expected, the number of occupied bins decreased to 201 as a

result of synchronization.
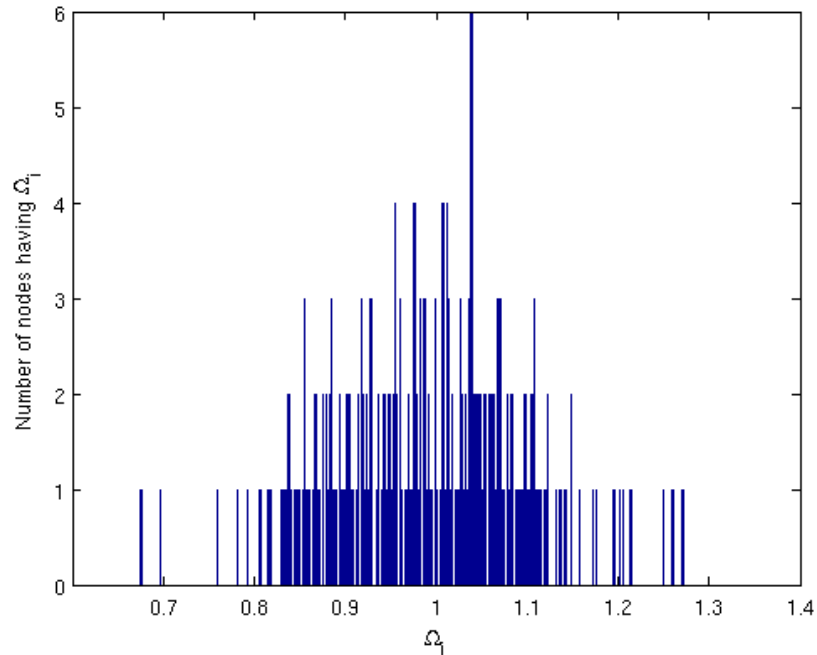
Figure 4.7. The final distribution of frequencies of the oscillators in c. elegans'
network.

The final view of the all networks is given in Table 4.4 and the histogram of the
final frequency distribution for some of the networks are shown in Figure 4.8. The ER
networks are much more homogeneous than the c. elegans' neural network, since the
average maximum degree is 26.45. As a result, the average number of occupied bins
for ER network slightly less than that of c. elegans. In the other more homogeneous
networks, the WS networks, the number of occupied bins is the least among other
models. Moreover, it is clear that for small p values, more oscillators synchronize
better. Increasing p randomizes the WS networks, causing the results to approach
the ER networks. It is meaningful to state that the small-world property, higher
clustering coefficient and lower average path length, allows synchronization. Among
all networks the BA network has the worst synchronizability. So it can be concluded
that hubs in a network hamper synchronization. These results do not contradict with

the ones obtained for the synchronization of identical periodic oscillators. Here again structural properties of c. elegans cause different outcomes than the artificial ones. For instance, [4] showed that the neural network of c. elegans has small-world property, but synchronization in this network is worse than the WS. Also, it allows synchronization more that the BA although it is more heterogeneous. This difference can be interpreted as an evidence for the effect of special structure of natural networks which must have evaluated in such a way that their structure allows optimal performance in some sense.

Table 4.4. Average number of occupied bins after 200 sec.

	# of occupied bins
CE	201
ER	200
BA	202.6
WS(p=0.1)	187.65
WS(p=0.2)	192.10
WS(p=0.3)	197.55
WS(p=0.4)	198.40
WS(p=0.5)	197.25
WS(p=0.6)	197.85
WS(p=0.7)	197.5
WS(p=0.8)	199.05
WS(p=0.9)	198
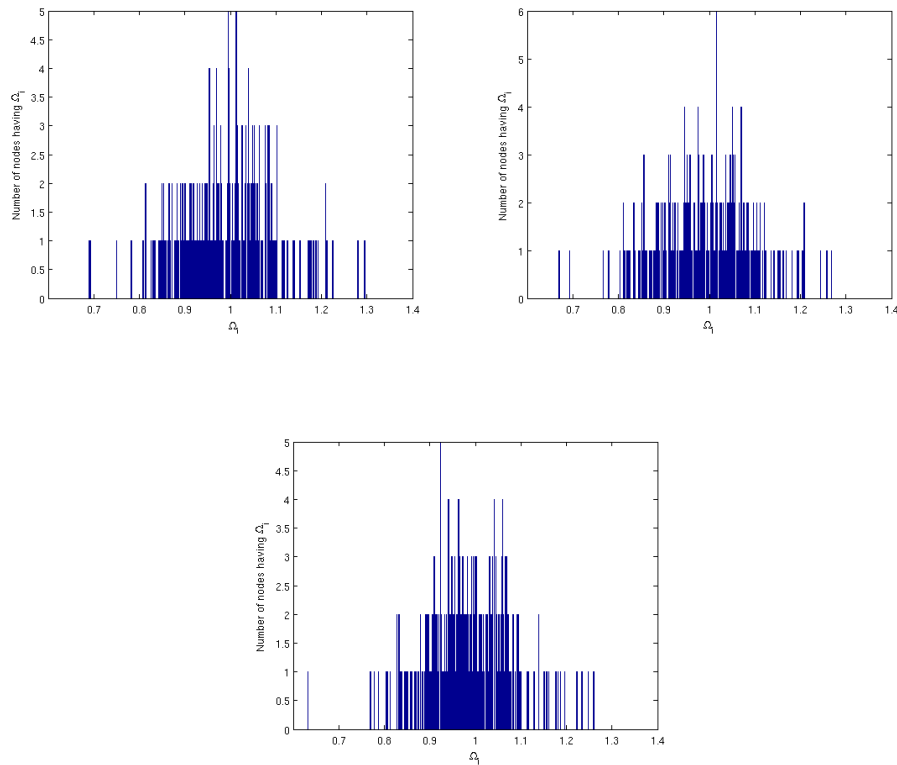
Figure 4.8. Final frequency distribution of (a) ER network (b) BA network (c) WS network for $p = 0.1$.

4.1.2. Synchronization of Periodic Uniform Oscillators with Similarity-Dependent Coupling Strengths

In this section coupling strengths will be formulated according to natural frequencies of the coupled oscillators. The impact of this formulation on the synchronization across an all-to-all coupled network will be investigated.

The oscillator dynamics are stated as in Equation 4.2 that is very similar to Equation 2.37 except for heterogeneous coupling strength $\varepsilon_{ij}(\Delta w_{ij})$, which is a function of the difference between the natural frequencies, and normalizing factor $N - 1$. This factor is taken as N by Kuramoto which does not make any difference for large

networks.

$$\dot{\phi_i} = w_i + \frac{1}{N-1} \sum_{j=1}^{N} \varepsilon_{ij}(\Delta w_{ij}) \sin(\phi_i - \phi_j) \qquad i = 1, ..., N \qquad (4.2)$$

The coupling strength $\varepsilon_{ij}(\Delta w_{ij})$ between the node i and node j has been formulated as a function of the difference of the natural frequencies in order to account for the similarity between node dynamics. ε_{ij} will take the higher values as two nodes are more similar in terms of their natural frequencies, which is an indicators of synchronizability. To calibrate and express the similarity numerically a Gaussian-distribution function is used as in Equation 4.3. This function takes its highest value when $|w_i - w_j| = 0$ and is zero when $|w_i - w_j| \to \infty$.

$$f(w_i - w_j) = \frac{1}{\sigma\sqrt{2\pi}} e^{\left(-\frac{(w_i - w_j)^2}{2\sigma^2}\right)} \qquad (4.3)$$

For a fair compression between the homogeneous coupling, where $\varepsilon_{ij} = \varepsilon$ for every i, j, and heterogeneous coupling, the average coupling strengths of both schemes need to be equal. A *scale factor* is obtained as follows

$$(N-1)\varepsilon = ScaleFactor_i \sum_{i \neq j} f'_{ij} \qquad (4.4)$$

where f'_{ij} is the normalized f_{ij} with the maximum value of $f_i = [f_{i1}, f_{i2}, ..., f_{iN}]^T$ vector. Finally $\varepsilon_{ij}(\Delta w_{ij})$ equals to

$$\varepsilon_{ij}(\Delta w_{ij}) = ScaleFactor_i f'_{ij}. \qquad (4.5)$$

To investigate the effect of heterogeneous coupling coefficients on synchronization, first let us start with an all-to-all coupled networks of 3 nonidentical uniform oscillators

with natural frequencies at $w_1 = 0.9, w_2 = 1, w_3 = 1.1$. If considered pairwise, the entrainment region is satisfied for $\varepsilon \geq 0.11$ for the first and the second oscillators and the second and third oscillators, as well. But as Figure 4.9 demonstrates that this coupling coefficient is not enough to synchronize all 3 oscillators, thus higher coefficients are needed.
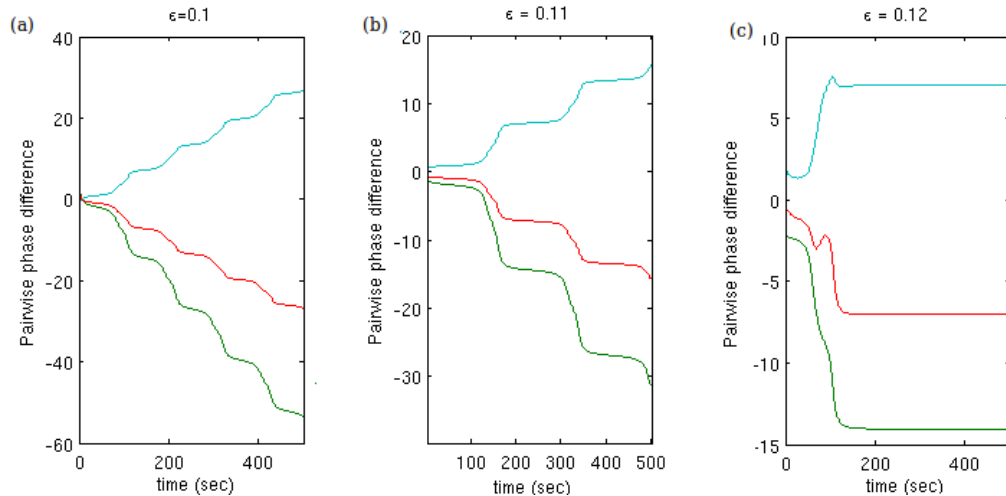
Figure 4.9. Behavior of pairwise phase differences of the all-to-all coupled 3 nonidentical uniform oscillators for (a) $\varepsilon = 0.1$; (b) $\varepsilon = 0.11$; (c) $\varepsilon = 0.12$.

On the other hand, if the weighted coupling strengths are considered as proposed above and demonstrated in Table 4.5, the oscillators can synchronize for smaller average coupling strengths,ε_{avg}, depending on the variance σ^2 in Equation 4.3. If the variance is small, the difference between the coupling strengths of one oscillator to the other is increased. Because this scheme of coupling strength assignment encourages the nodes to be more sensitive to the differences in the internal dynamics of the other nodes and weight the information coming from them. The effect of σ^2 on synchronization is obvious as Figure 4.10 shows. If the variance is small, the oscillators can synchronize for a small average coupling strength.

Next, the result of similarity-dependent coupling strengths scheme is studied on a larger network. This time an all-to-all coupled network of 10 nonidentical periodic
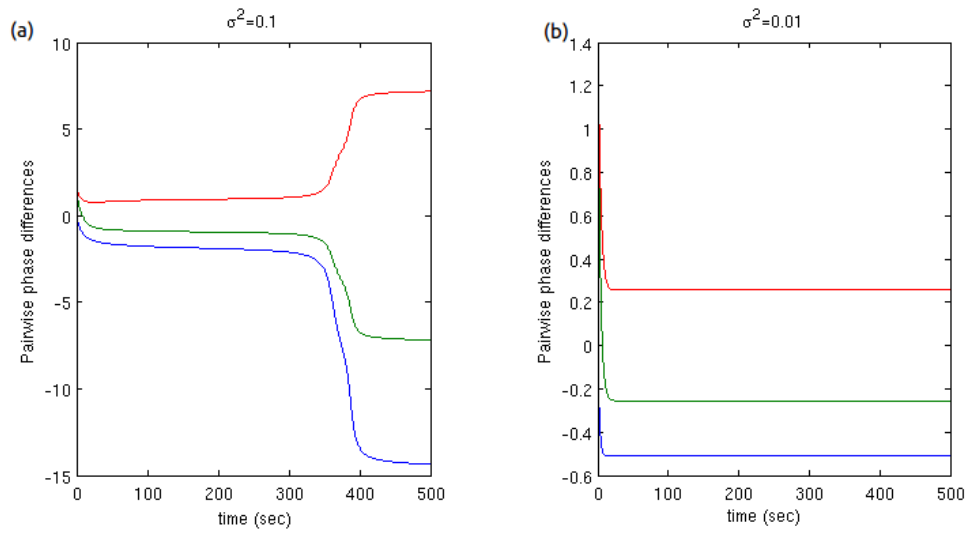
Figure 4.10. Behavior of pairwise phase differences of the all-to-all coupled network 3 nonidentical uniform oscillators for $\varepsilon_{avg} = 0.1$; (a) $\sigma^2 = 0.1$; (b) $\sigma^2 = 0.01$.
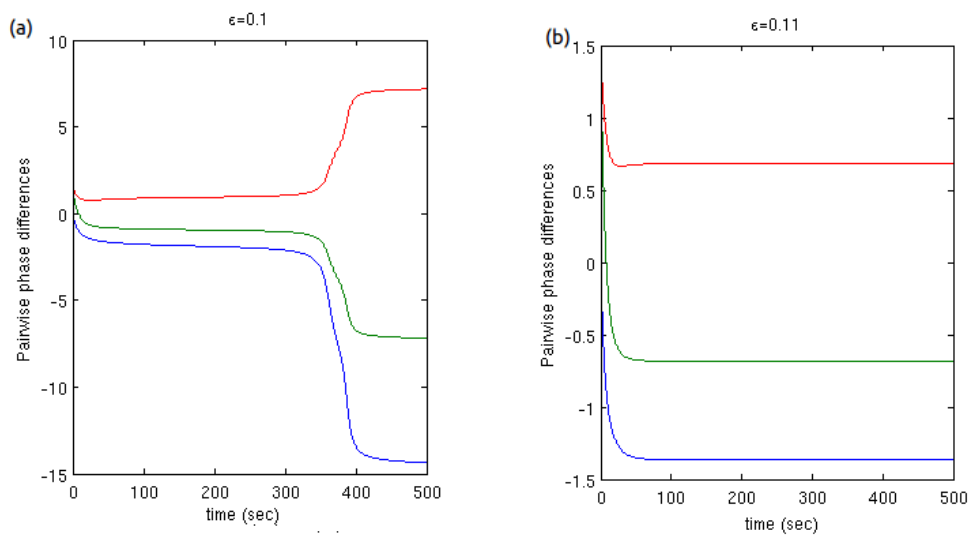
Figure 4.11. Behavior of pairwise phase differences of the all-to-all coupled network of 3 nonidentical uniform oscillators for the variance $\sigma^2 = 0.1$; (a) $\varepsilon_{avg} = 0.1$; (b) $\varepsilon_{avg} = 0.11$.

Table 4.5. Heterogeneous coupling strengths ε_{ij} depending on the variance σ^2 for the 3 oscillators for $\varepsilon_{avg} = 0.1$.

w_i	$\sigma^2 = 0.1$	$\sigma^2 = 0.01$
$w_1 = 0.9$	$\varepsilon_{12} = 0.1075$	$\varepsilon_{12} = 0.1635$
	$\varepsilon_{13} = 0.0925$	$\varepsilon_{13} = 0.0365$
$w_2 = 1$	$\varepsilon_{21} = 0.1$	$\varepsilon_{21} = 0.1$
	$\varepsilon_{23} = 0.1$	$\varepsilon_{23} = 0.1$
$w_3 = 1.1$	$\varepsilon_{31} = 0.0925$	$\varepsilon_{31} = 0.0365$
	$\varepsilon_{32} = 0.1075$	$\varepsilon_{32} = 0.1635$

oscillators are considered. Table 4.6 gives the first node's heterogeneous coupling coefficients $\varepsilon_{1j}(\Delta w_{1j})$ for the average coupling strength $\varepsilon_{avg} = 0.2$ and $\sigma = 0.1$ in Equation 4.3. As expected, the coupling strength between the most similar ones (first and fifth) is higher than the least similar ones (first and fifth). As Figure 4.12 demonstrates, the ensemble reaches phase synchronization for heterogeneous coupling strengths, whereas the first node could not synchronize properly for standard homogeneous coupling. Furthermore, if the variance is decreased, phase synchronization is obtained for smaller average coupling strengths.

4.1.3. Synchronization in Ensembles of Chaotic Oscillators Coupled via Mean Field

In this section, synchronization in an ensemble of N mean-field-coupled nonidentical Rössler oscillators is studied. Inspired by [18, 68] a different model is considered than the one in [69]. It is assumed that the effect of the rest of the oscillators on each individual oscillator is proportional to the difference between its output and the mean field. This difference is added to the system equation (Equation 4.6), where X stands

Table 4.6. Heterogeneous coupling strengths ε_{1j} for $\sigma^2 = 0.1$ where $\varepsilon_{avg} = 0.2$.

w_i	$\varepsilon_{1j}(\Delta w_{1j})$
1.2350	0
0.9384	0.1836
1.0748	0.2507
0.9808	0.2063
1.0889	0.2562
0.9235	0.1755
0.8598	0.1410
0.8578	0.1399
1.0488	0.2397
0.9823	0.2071

for mean field (Equation 2.38), that is the mean of the observed states x_i .

$$\dot{x}_i = -w_i y_i - z_i + \varepsilon(X - x_i)$$
$$\dot{y}_i = w_i x_i + 0.15 y_i$$
$$\dot{z}_i = 0.4 + z_i(x_i - 8.5) \qquad (4.6)$$

<u>4.1.3.1. Synchronization of Identical Chaotic Oscillators.</u> As stated in Section 2.3.2.1, mutually coupled identical oscillators can synchronize completely, which can be interpreted as if they forget their initial conditions and eventually converge to the same chaotic trajectory. One way of detecting synchronization in an ensemble is by observing the mean difference between the mean field and the oscillator (Equation 3.1), which approaches to zero as systems synchronize completely (as a result of tracking the same trajectory without any time delay).
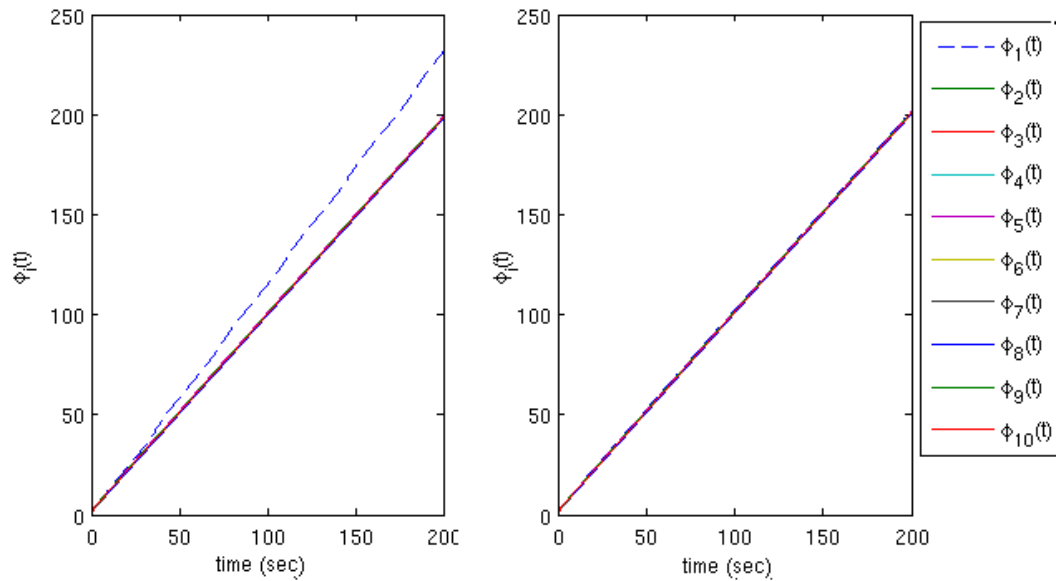
Figure 4.12. Phase dynamics of the all-to-all coupled network of 10 nonidentical uniform oscillators for $\varepsilon_{avg} = 0.2$; (a) homogeneous coupling (b) heterogeneous coupling with $\sigma = 0.1$.

Figure 4.14 shows how the ensemble deviation (Equation 3.1) behaves with varying coupling strength ε for $N = 6$ globally coupled identical Rössler oscillators (Equation 4.6) with $w_i = w = 1$. Obviously the systems reach complete synchronization as the coupling strength increases.

4.1.3.2. Synchronization of Nonidentical Chaotic Oscillators. In the phase synchronization of nonidentical oscillators, it is known that the observed frequencies of the oscillators become equal. If one plots the mean observed frequencies versus the individual mean natural frequencies, a synchronization plateau is observed.

Figure 4.15 shows how the synchronization plateau emerges as the coupling strength ε increases for $N = 6$ globally coupled nonidentical Rössler oscillators (Equation 4.6). As one can observe, all nodes start to oscillate at a common frequency for $\varepsilon = 0.175$. Table 4.7 shows the w_i parameters and variation of the mean observed
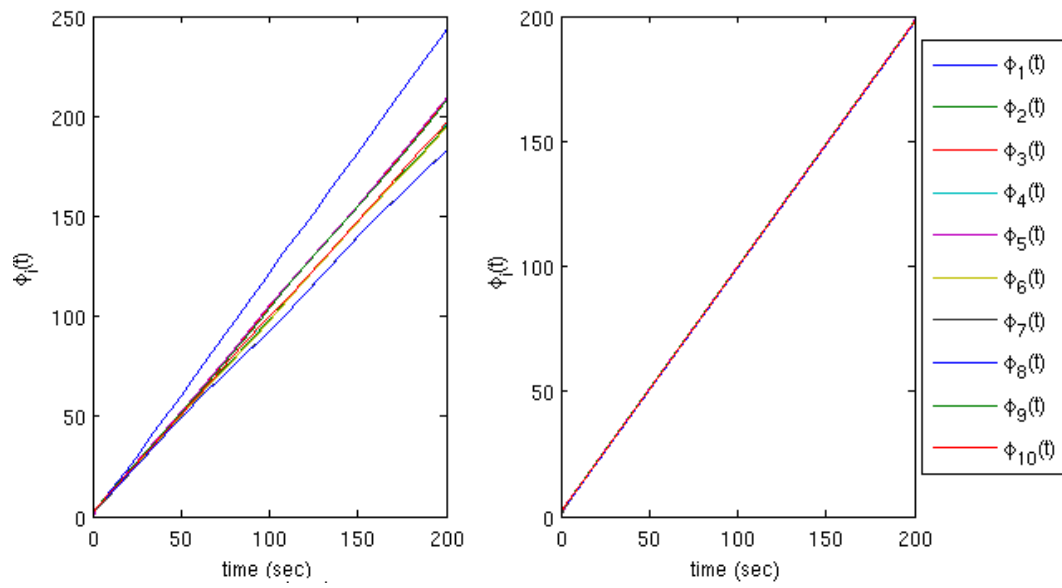
Figure 4.13. Phase dynamics of the all-to-all coupled 10 nonidentical uniform oscillators for $\varepsilon_{avg} = 0.15$; (a) homogeneous coupling (b) heterogeneous coupling with $\sigma = 0.01$.

(angular) frequencies Ω_i of the considered 6 Rössler oscillators.
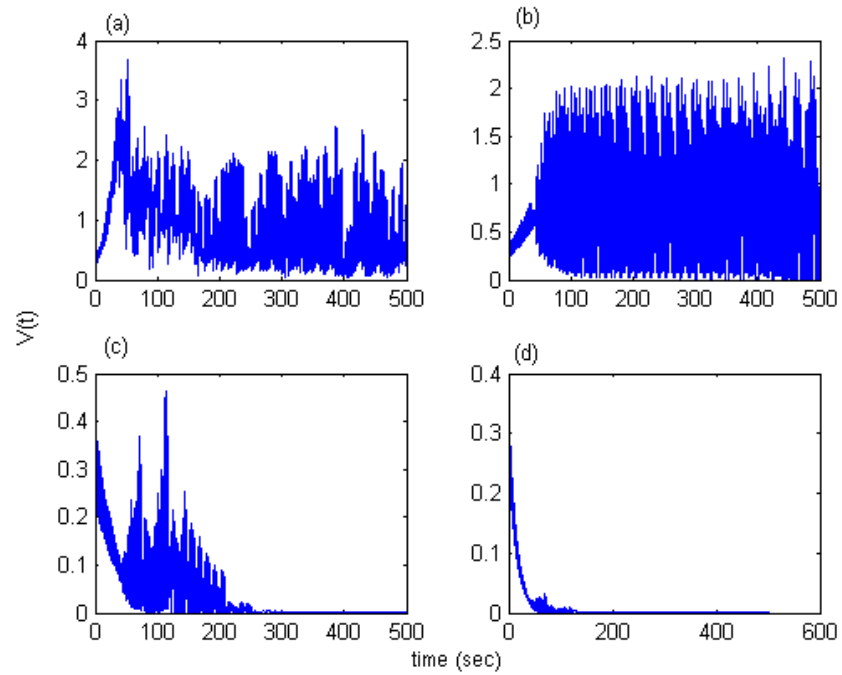
Figure 4.14. Behavior of $V(t)$ of the mean-fielded coupled identical Rössler oscillators

for (a) $\varepsilon = 0.025$; (b) $\varepsilon = 0.1$; (c) $\varepsilon = 0.2$; (d) $\varepsilon = 0.275$.
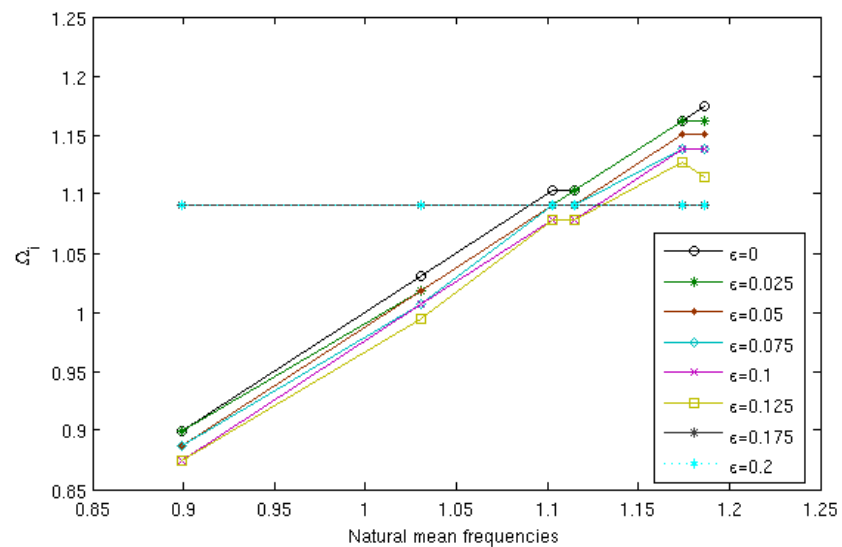
Figure 4.15. Emergence of phase synchronization in the ensemble of nonidentical

Rössler oscillators with respect to the coupling strength ε.

Table 4.7. w_i parameters and variation of the mean observed frequencies Ω_i of Rössler oscillators.

w_i		$\varepsilon = 0$	$\varepsilon = 0.025$	$\varepsilon = 0.05$	$\varepsilon = 0.8$	$\varepsilon = 0.1$	$\varepsilon = 0.125$	$\varepsilon = 0.15$	$\varepsilon = 0.175$	$\varepsilon = 0.2$
1.1407	Ω_1	1.1984	1.1505	1.1505	1.1505	1.1505	1.1505	1.1025	1.1025	1.1025
1.1300	Ω_2	1.1505	1.1505	1.1505	1.1505	1.1505	1.1505	1.1025	1.1025	1.1025
1.0671	Ω_3	1.1025	1.1025	1.1025	1.1025	1.1025	1.1025	1.0546	1.1025	1.1025
0.8793	Ω_4	0.9108	0.9108	0.9108	0.9108	0.8629	0.8629	0.8629	1.1025	1.1025
1.0717	Ω_5	1.1025	1.1025	1.1025	1.1025	1.1025	1.1025	1.0546	1.1025	1.1025
1.0000	Ω_6	1.0546	1.0067	1.0067	1.0067	1.0067	1.0067	1.0067	1.1025	1.1025

As discussed before, states of the chaotic oscillators become correlated as the coupling strength increases. [65] showed this correlation via mean field by presenting the phase portrait of $X = \frac{1}{N} \sum_{i=1}^{N} x_i$ and $Y = \frac{1}{N} \sum_{i=1}^{N} y_i$. Increasing correlation between the states manifests itself as a much more regular structure in this phase portrait (Figure 4.16).
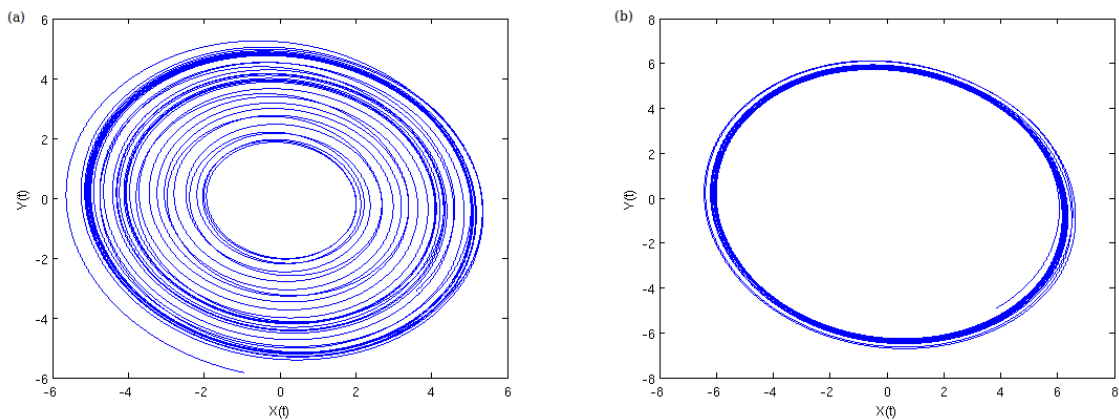
Figure 4.16. Phase portrait of X and Y (a) $\varepsilon = 0.175$; (b) $\varepsilon = 0.2$.

4.2. Synchronization Control

In this section, the effect and performance of different control methods for controlling the synchronization of globally coupled chaotic oscillators (Equation 4.6). Two different control techniques are considered: feeding back time-delayed mean field, and applying external periodic force.

4.2.1. Synchronization Control via Mean Field by Delay Feedback Control

Reference [55] has suggested two different forms for delayed feedback: differential method and direct method. In the differential method (Equation 4.7) the difference between delayed and current mean fields is fed back to one of the system variables, whereas in direct method (Equation 4.8), time-delayed mean field is fed back directly

to one of the system variables, with the amplitude K and delay time τ.

$$\dot{x}_i = -w_i y_i - z_i + \varepsilon(X + K[X_d - X] - x_i)$$
$$\dot{y}_i = w_i x_i + 0.15 y_i$$
$$\dot{z}_i = 0.4 + z_i(x_i - 8.5) \tag{4.7}$$

$$\dot{x}_i = -w_i y_i - z_i + \varepsilon(X + K X_d - x_i)$$
$$\dot{y}_i = w_i x_i + 0.15 y_i$$
$$\dot{z}_i = 0.4 + z_i(x_i - 8.5) \tag{4.8}$$

$$X_d(t) = X(t - \tau) \tag{4.9}$$

These feedback control techniques are applied to both an ensemble of identical Rössler oscillators (Section 4.1.3.1) and nonidentical Rössler oscillators (Section 4.1.3.2). In the former, the effect of the delayed mean field feedback on the complete synchronization state has been investigated. In the nonidentical ensemble, undergoing changes is the phase synchronization state of the ensemble has been studied.

4.2.1.1. Ensemble of Identical Chaotic Oscillators. In this section, it has been investigated whether feeding back the time-delayed mean field can affect the complete synchronization state. Depending on the control scheme, the time delay τ and the amplitude K, this feedback effect may change the time for achieving complete synchronization, settling time of $V(t)$, or may destroy the complete synchronization between the oscillators.

The coupling strength is assumed to be $\varepsilon = 0.2$ for the ensemble consisting of identical Rössler oscillators (Equation 4.6) with $w_i = w = 1$ as in Section 4.1.3.1 Figure

4.17 demonstrates the ensemble deviation, $V(t)$. As one can observe the ensemble synchronizes completely at $t = 250$ sec.
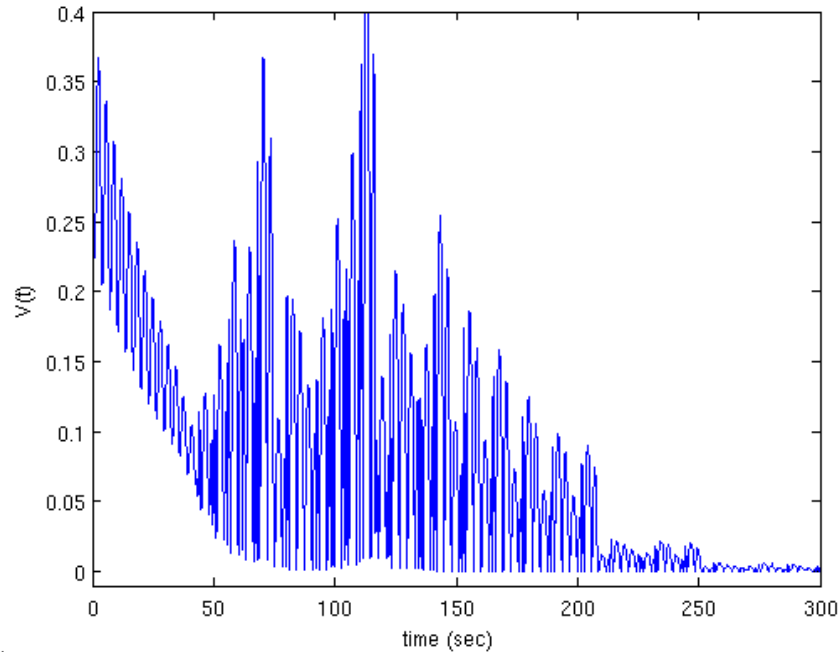
Figure 4.17. Behavior of $V(t)$ of the mean-field-coupled chaotic Rössler oscillators for $\varepsilon = 0.2$.

The differential feedback method (Equation 4.7) is rewritten for $w_i = w = 1$ as

$$\dot{x}_i = -y_i - z_i + \varepsilon(X + K[X_d - X] - x_i)$$
$$\dot{y}_i = x_i + 0.15y_i$$
$$\dot{z}_i = 0.4 + z_i(x_i - 8.5). \tag{4.10}$$

To observe the effects of the control input on the complete synchronization, the difference between the actual mean field and the delayed mean field is fed back to the x_i states of the oscillators at $t = 50$ sec, before compete synchronization is achieved, and $t = 300$ sec, after complete synchronization is achieved. With the former, it has been investigated if synchronization is achieved earlier than $t = 250$ sec. And with the

control action applied at $t = 300$ sec, the influence on the complete synchronization state of the system has been studied. Three different delay times are considered: (i) $\tau = T$; (ii) $\tau = t/2$, where $T = 24$ sec is the period of the mean-field calculated from the power spectrum of the mean-field; (iii) $\tau =< T_i >$ is the average mean natural frequencies of the oscillators. The difference between T and $< T_i >$ should be noted. The amplitude K is varied between $[-1, 1]$.

Table 4.8 shows the settling time of $V(t)$ for three different delay values and K. When $\tau = T$, the control signal accelerate the achievement of the complete synchronization state. Especially for $K > 0.5$, the system completely synchronizes as soon as the delayed mean field is fed back (Figure 4.18). It is important to note that the achievement of the synchronization is delayed by the control signal with positive small K values. In general, decrease in the settling time is also obtained by the delayed mean field for $\tau = T/2$, but it is not as effective as the one for $\tau = T$ (Figure 4.19). The time delayed feedback for $< T_i >$ generally shortens the settling time, but for large values of K the difference between oscillators is suppressed at first, then the collective behavior is totally destroyed (Figure 4.20).

The direct feedback method (Equation 4.8) is rewritten for $w_i = w = 1$ as

$$\dot{x}_i = -y_i - z_i + \varepsilon(X + KX(t - \tau) - x_i)$$
$$\dot{y}_i = x_i + 0.15y_i$$
$$\dot{z}_i = 0.4 + z_i(x_i - 8.5). \tag{4.11}$$

The delayed mean field is fed back directly to the x_i states of the oscillators at $t = 50$ sec and $t = 300$ sec, again. Time delay τ and feedback amplitude K are equal to the ones in differential feedback control technique in Equation 4.10).

Table 4.9 shows the effect of the direct feedback control method on the complete synchronization time. For all τ values, the control signal with $0 < K \leq 1$ does not

Table 4.8. The impact of differential time-delayed feedback applied at $t = 50$ sec on the synchronization time of the ensemble of identical Rössler oscillators.

K	$\tau = T$	$\tau = T/2$	$\tau =< T_i >$
-1	118	217	>300
-0.9	143	142	213
-0.8	248	265	108
-0.7	91	276	170
-0.6	82	104	97
-0.5	>300	>300	87
-0.4	204	123	117
-0.3	112	112	105
-0.2	124	276	178
-0.1	81	142	111
0.1	232	278	226
0.2	298	111	135
0.3	105	99	99
0.4	93	134	99
0.5	117	122	135
0.6	56	119	>300
0.7	57	108	>300
0.8	57	120	>300
0.9	57	131	>300
1	60	134	>300
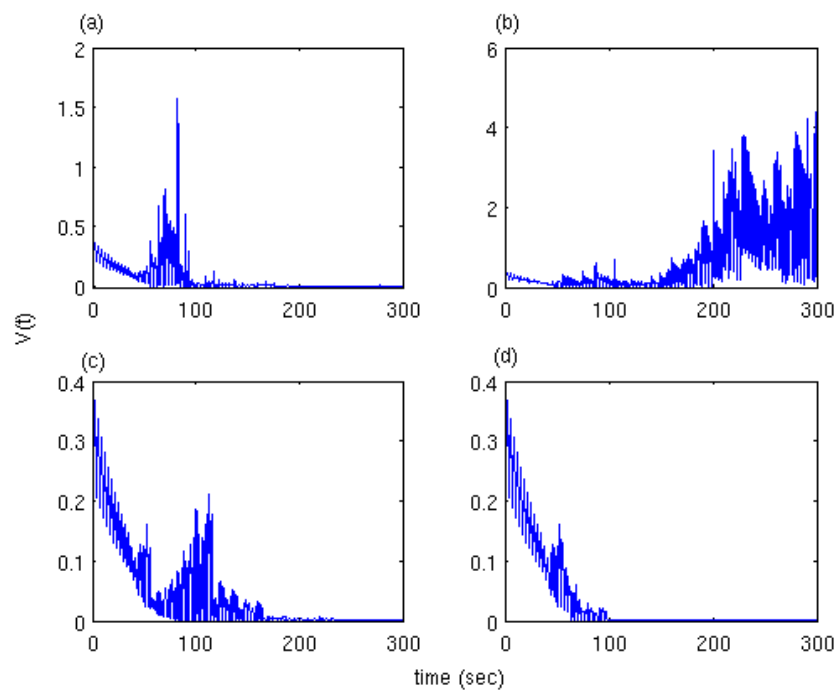
Figure 4.18. Behavior of $V(t)$ of Equation 4.10 for $\tau = T$. The control signal is applied at $t = 50$ sec. (a) $K = -1$; (b) $K = -0.5$; (c) $K = 0.5$; (d) $K = 1$.
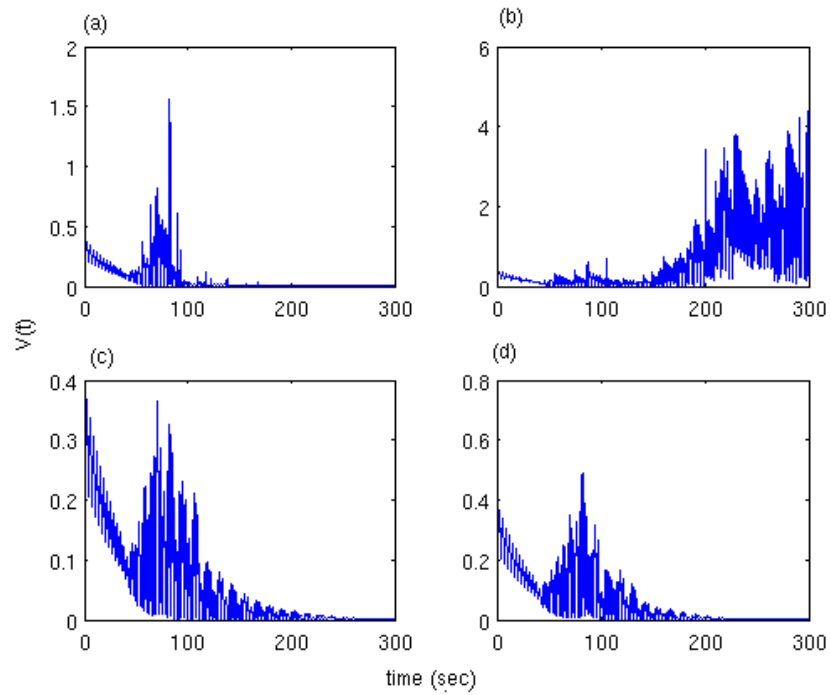
Figure 4.19. Behavior of $V(t)$ of Equation 4.10 for $\tau = T/2$. The control signal is applied at $t = 50$ sec. (a) $K = -1$; (b) $K = -0.5$; (c) $K = 0.5$; (d) $K = 1$.
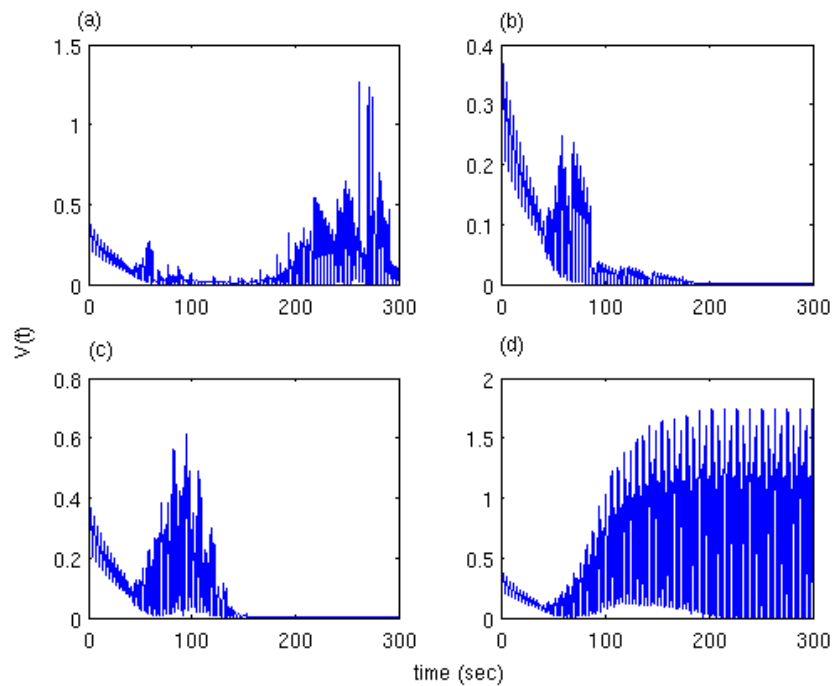
Figure 4.20. Behavior of $V(t)$ of Equation 4.10 for $\tau = < T_i >$. The control signal is applied at $t = 50$ sec. (a) $K = -1$; (b) $K = -0.5$; (c) $K = 0.5$; (d) $K = 1$.

significantly affect the settling time, even more, the amplitude of $V(t)$ during the transition is greater than the one without control (Figure 4.21-4.20). Thus, it can be stated that the direct feedback method with positive amplitude has a negative effect on achieving complete synchronization in such a system. On the other hand, for $-1 < K < 0$ the ensemble completely synchronizes faster. Especially for $\tau = T/2$ and $\tau =< T_i >$ complete synchronization is achieved as soon as the control signal is applied.
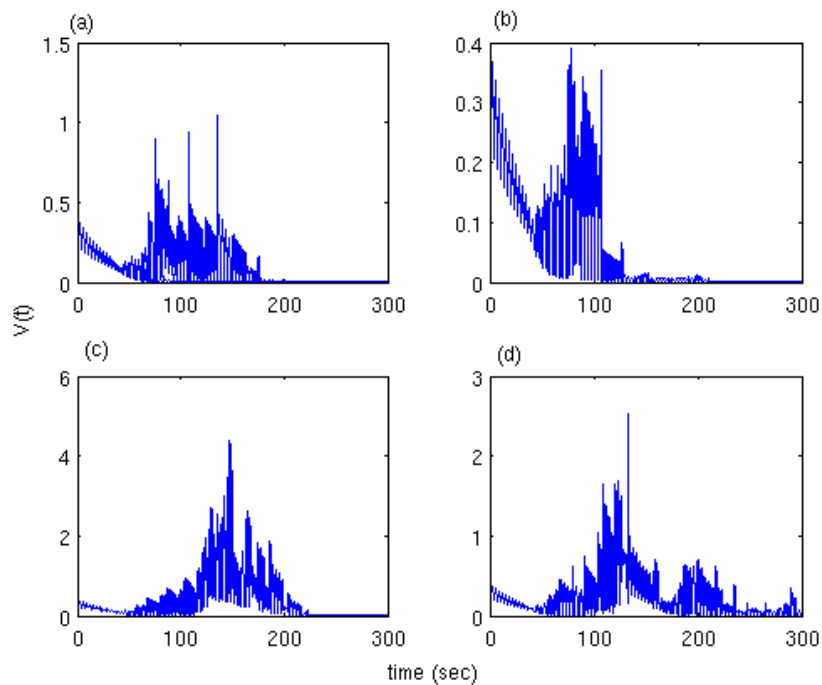
Figure 4.21. Behavior of $V(t)$ of Equation 4.11 for $\tau = T$. The control signal is applied at $t = 50$ sec. (a) $K = -1$; (b) $K = -0.5$; (c) $K = 0.5$; (d) $K = 1$.

Both of the delayed mean field feedback control methods do not affect the synchronous behavior of the identical oscillators when they applied after the systems reaches synchronization, $t = 300$ sec. Figure 4.24 and 4.25 demonstrate an example for $K = 0.5$. The reason can be the regular oscillations of the mean field and tracking the same chaotic trajectory by the oscillators. Figure 4.24 and Figure 4.25 show how ensemble deviation differs for different values of τ and K.

Table 4.9. The impact of direct time-delayed feedback applied at $t = 50$ sec on the synchronization time of the ensemble of identical Rössler oscillators.

	Settling time (sec)		
K	$\tau = T$	$\tau = T/2$	$\tau = < T_i >$
-1	171	70	70
-0.9	162	70	69
-0.8	97	70	66
-0.7	122	63	63
-0.6	159	57	57
-0.5	108	57	57
-0.4	216	57	57
-0.3	233	66	66
-0.2	>300	81	81
-0.1	130	118	139
0.1	>300	283	243
0.2	284	62	>300
0.3	254	194	110
0.4	>300	>300	124
0.5	223	116	>300
0.6	163	>300	>300
0.7	145	181	>300
0.8	290	>300	219
0.9	>300	>300	135
1	295	202	261
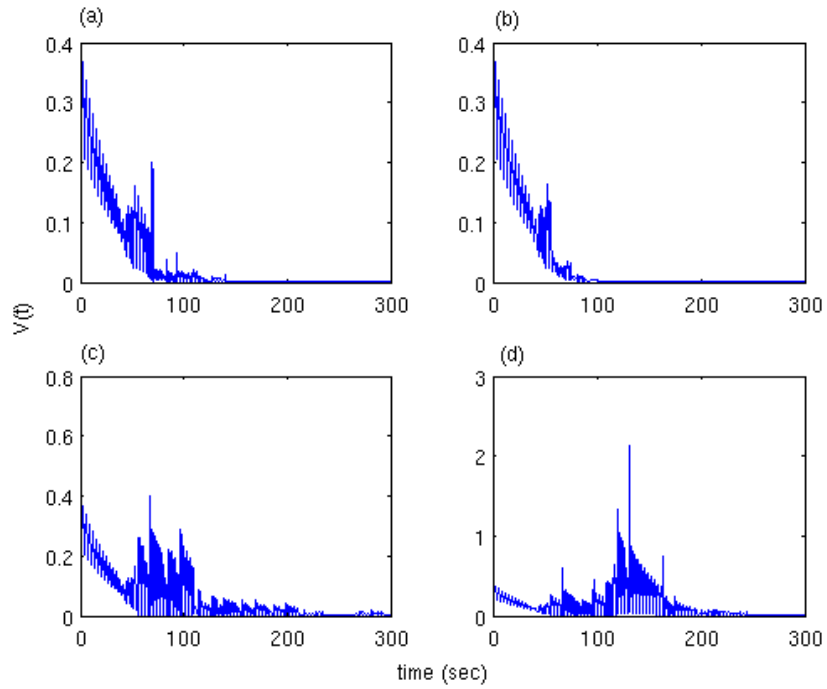
Figure 4.22. Behavior of $V(t)$ of Equation 4.11 for $\tau = T/2$. The control signal is applied at $t = 50$ sec. (a) $K = -1$; (b) $K = -0.5$; (c) $K = 0.5$; (d) $K = 1$.
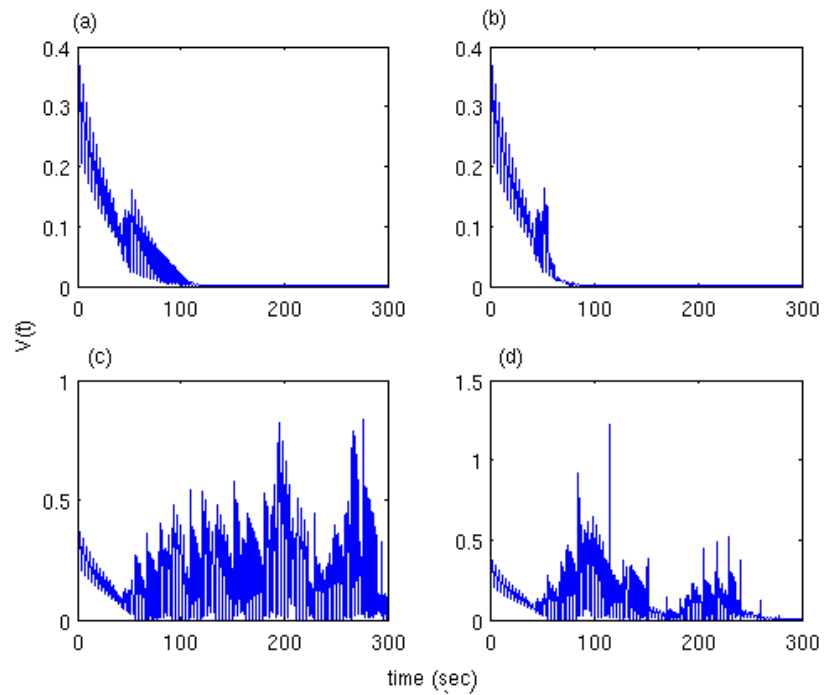
Figure 4.23. Behavior of $V(t)$ of Equation 4.11 for $\tau = <T_i>$. The control signal is applied at $t = 50$ sec. (a) $K = -1$; (b) $K = -0.5$; (c) $K = 0.5$; (d) $K = 1$.
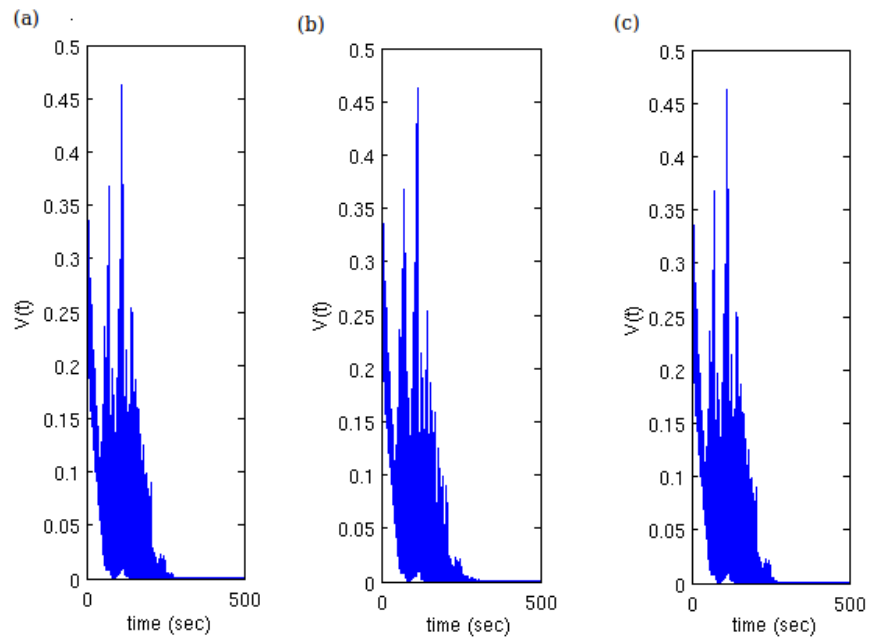
Figure 4.24. Behavior of $V(t)$ of Equation 3.1 for $K = 0.5$ (a) $\tau = T$; (b) $\tau = T/2$; (c)$\tau = < T_i >$.
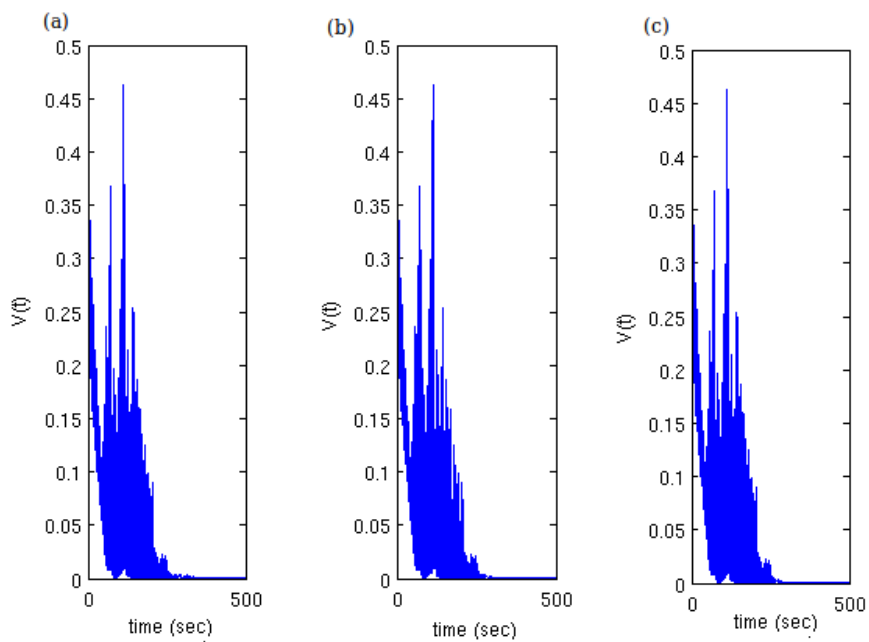
Figure 4.25. Behavior of $V(t)$ of Equation 4.11 for $K = 0.5$ (a) $\tau = T$; (b) $\tau = T/2$; (c)$\tau = < T_i >$.

4.2.1.2. Ensemble of Nonidentical Chaotic Oscillators. In this section, it is investi-
gated whether the delayed feedback of the mean field has any effect on the phase
synchronization of an ensemble of 6 nonidentical Rössler oscillators. As one can re-
member, in the phase synchronization state, the chaotic oscillators oscillate with the
same mean angular frequency while their amplitudes remain uncorrelated. The consid-
ered feedback effects may introduce correlation between the amplitudes of the coupled
chaotic oscillators, or suppress, even destroy the phase synchronization.

Here again two different feedback control methods, Equation 4.7 and Equation 4.8
are applied to the ensemble in Section 4.1.3.2, and the coupling coefficients are assumed
to be $\varepsilon = 0.2$. The amplitude K is varied between $[-1, 1]$ and five different delay times
are considered: (i) $\tau = T$; (ii) $\tau = T/2$, where T equals to the mean-period of the mean
field of the phase synchronized ensemble for $\varepsilon = 0.2$; (iii) $\tau = < T_i >$, the averaged
mean natural frequencies of the oscillators; (iv) $\tau = T_6$, mean natural frequency of the
6th oscillators; (v) $\tau = T_1$ mean natural frequency of the 1th oscillators.

To measure the time-delayed feedback effect on correlation between the phase
synchronized oscillators, the Pearson's correlation coefficient (Equation 3.2) is extended
for an ensemble of chaotic oscillators by taking the mean of the pairwise correlations of
the x_i states of the Rössler oscillators. It should be remembered that if the amplitudes
of two coupled nonidentical chaotic oscillators are correlated, they track the same
chaotic trajectory with a time lag, which is the lag synchronization. Furthermore, if
they are highly correlated (zero time lag), the observed states will approach each other
and the $y = x$ line, as well (Figure 4.26). The control effect on the state relations,
correlation coefficient with control $corr_f(x_i, x_j)$ is divided by the correlation coefficient
without control $corr(x_i, x_j)$ (Equation 4.12), i.e. $CorrelationFactor > 1$ provides
stronger correlation between the states.

$$CorrelationFactor = \frac{1}{N(N-1)} \sum_{i=1}^{N} \sum_{j=1(i \neq j)} \frac{|corr_f(x_i, x_j)|}{|corr(x_i, x_j)|} \qquad (4.12)$$
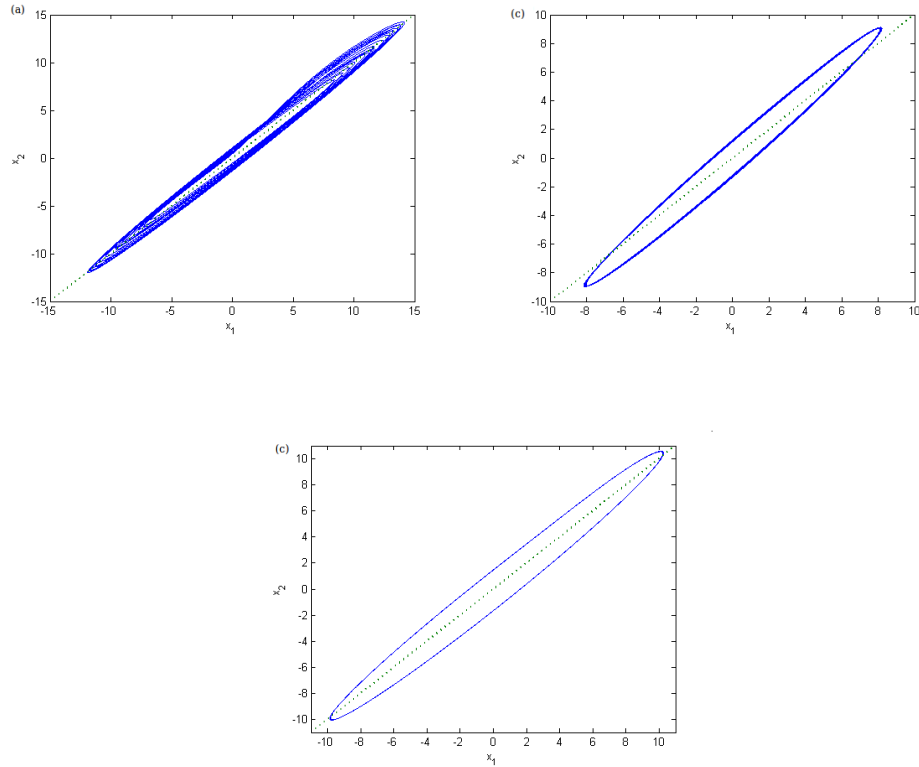
Figure 4.26. Plot of x_1 and x_2 (a) correlation factor is 1.6297 (b) correlation factor is 0.6357 (c) correlation factor is 1.

Figure 4.27, 4.28 and the tables in Appendix A demonstrate the importance of the control method, choice of K and τ. At the first sight, it is seen that the direct feedback control has a richer impact, such that in differential feedback control for $K > 0$ and $\tau \in \{T, T/2, < T_i >, T_6\}$ makes a slight difference in the phase and amplitude relation of the ensemble. Whereas, for direct feedback control the amplitudes of the oscillators become more correlated for $K > 0$ and any τ. Furthermore, the direct feedback control method, except for $\tau = T_1$, preserves the common frequency of the ensemble which is achieved without any control input.

One important point is the possibility of obtaining more correlated amplitudes by destroying the phase synchronization, which is relevant for differential feedback method. For example, in Figure 4.27 although the correlation factor reaches its some of the highest values for $K = -1, K = -0.8$ and $\tau = T$, but phase synchronization is

destroyed since all of the mean observed frequencies of the oscillators are not identical (Table A.1). Another important fact about the same control method is the effect of τ on the synchronization frequency and correlation factor. For instance, different state correlations are obtained for the same synchronization frequency for different K and $\tau \in \{T_6, T_1\}$.

As a conclusion, one can say that desired behavior and common frequency of the ensemble can be achieved by choosing the control technique, its amplitude and delay time. Directly applied delayed mean field with the positive amplitudes provides better collective behavior in the ensemble by reinforcing the phase synchronization, whereas differentially applied delayed mean field does not have any significant impact for the same amplitude range. On the other hand, the same control method suppresses the synchronization. For some cases, differentially applied delayed mean field brings less correlated amplitudes but phase synchronized oscillators, or an unsynchronized ensemble but highly correlated pairs.
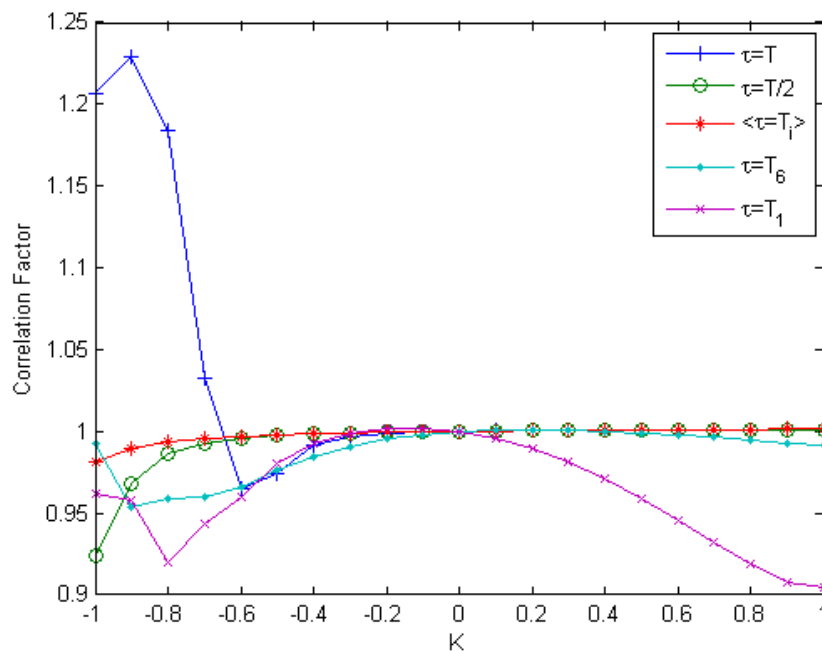
Figure 4.27. Correlation factor of Equation 4.7 versus K for different delay values τ.
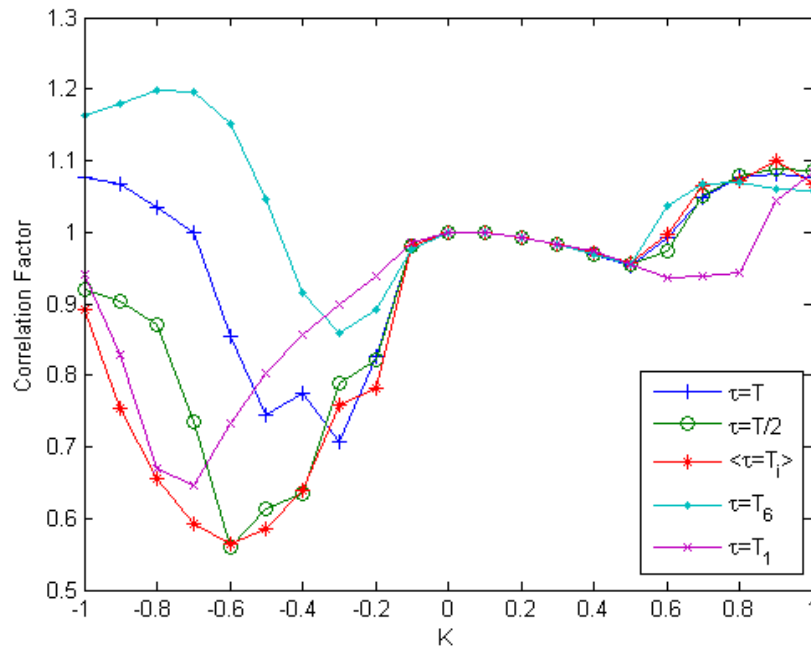
Figure 4.28. Correlation factor of Equation 4.8 versus K for different delay values τ.

4.2.2. Synchronization Control via Mean Field by External Periodic Input

The second control technique to be concerned is controlling globally coupled oscillators via externally forced mean field. Being exposed to external forcing of an ensemble of coupled oscillators is common in physics, chemistry and biology in which mutual synchronization competes with forced synchronization [70], in particular the situation is relevant for modeling of neuronal rhythms in the case when an ensemble of interacting neurons is influenced by rhythms from other brain regions [62]. In this thesis, two different system equations are investigated to capture the external effect. In Equation 4.13 the external force is applied to the mean field of the ensemble. The next one is Equation 4.14, where each of the external periodic force $sin(v_i)$ is able to

entrain the ith oscillator in the absence of the mean field effect.

$$\dot{x}_i = -w_i y_i - z_i + \varepsilon(X + C sin(vt) - x_i)$$
$$\dot{y}_i = w_i x_i + 0.15 y_i$$
$$\dot{z}_i = 0.4 + z_i(x_i - 8.5) \tag{4.13}$$

$$\dot{x}_i = -w_i y_i - z_i + \varepsilon(X - x_i) + C sin(v_i t)$$
$$\dot{y}_i = w_i x_i + 0.15 y_i$$
$$\dot{z}_i = 0.4 + z_i(x_i - 8.5) \tag{4.14}$$

Here again, periodic external actions are applied to both an ensemble of identical Rössler oscillators (Section 4.1.3.1) and nonidentical Rössler oscillators (Section 4.1.3.2), to investigate the effect on the complete synchronization and phase synchronization, respectively.

4.2.2.1. Ensemble of Identical Chaotic Oscillators. In this section, the effect of periodic external force on the ensemble of 6 identical all-to-all coupled chaotic Rössler oscillators is studied. It is observed that complete synchronization is achieved for $\varepsilon = 0.2$ at $t = 250$ sec (Section 4.1.3.1). In order to understand the effect of these periodic external actions on synchronization of the identical Rössler oscillators (Equation 4.15, Equation 4.16), an external force is applied to an unsynchronized ensemble with $\varepsilon = 0.1$, and to a synchronized ensemble with $\varepsilon = 0.2$. Four different external force frequencies are considered: (i) the frequency of the period-one UPO,$v = 1.0134$; (ii) the frequency of the period-two UPO, $v = 0.5067$; (iii) the frequency of the period-three UPO, $v = 0.3324$; (iv) the mean frequency of the identical oscillators, $v = 1.0546$. The

rewritten system equations are as follows

$$\dot{x}_i = -y_i - z_i + \varepsilon(X + Csin(vt) - x_i)$$
$$\dot{y}_i = x_i + 0.15y_i$$
$$\dot{z}_i = 0.4 + z_i(x_i - 8.5), \tag{4.15}$$

$$\dot{x}_i = -y_i - z_i + \varepsilon(X - x_i) + Csin(v_it)$$
$$\dot{y}_i = x_i + 0.15y_i$$
$$\dot{z}_i = 0.4 + z_i(x_i - 8.5). \tag{4.16}$$

Figure 4.29 and Figure 4.30 show the correlation factors (Equation 4.12). As Figure 4.29 shows for Equation 4.15, states become more correlated, especially when the frequency of the external force equals to mean frequency of the oscillators. None of the periodic external forces applied to the mean-field provide the necessary conditions for a fully synchronized ensemble. On the other hand, as Figure 4.30 demonstrates, the complete synchronization is achieved with the second method in Equation 4.16 for some C and τ values, where the correlation factor is 1.0304. Even in the worst case, the number of pairwise completely synchronized oscillators (Figure 4.31) is greater than the unforced ensemble. Note that if the frequency of the external force is equal to one of the considered UPO frequencies, synchronization is enhanced better.

Finally, the external force has no effect when it is applied to the fully synchronized ensemble coupled with $\varepsilon = 0.2$. Correlation factor values for the considered external force frequencies and action amplitudes of four different cases are given in Appendix B.

4.2.2.2. Ensemble of Nonidentical Chaotic Oscillators. In this section, the effect of periodic external force to the ensemble of 6 nonidentical all-to-all coupled chaotic Rössler
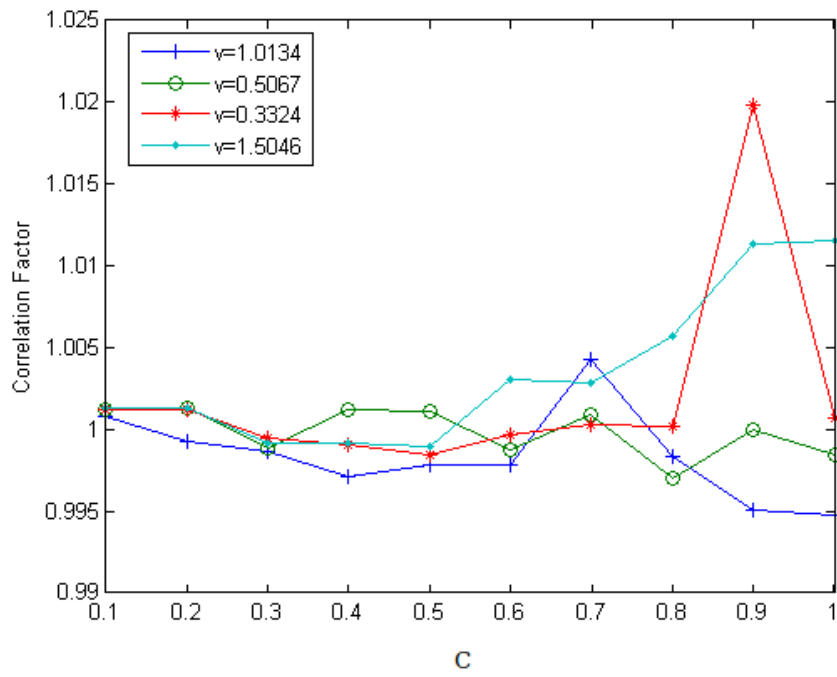
Figure 4.29. Correlation factor for Equation 4.15 where $\varepsilon = 0.1$ versus amplitude C.
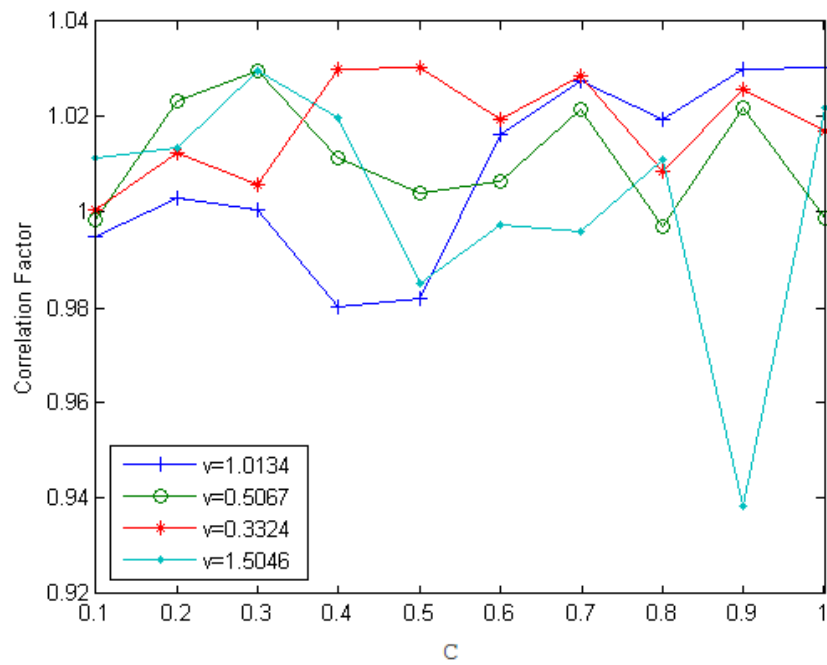
Figure 4.30. Correlation factor for Equation 4.16 where $\varepsilon = 0.1$ versus amplitude C.
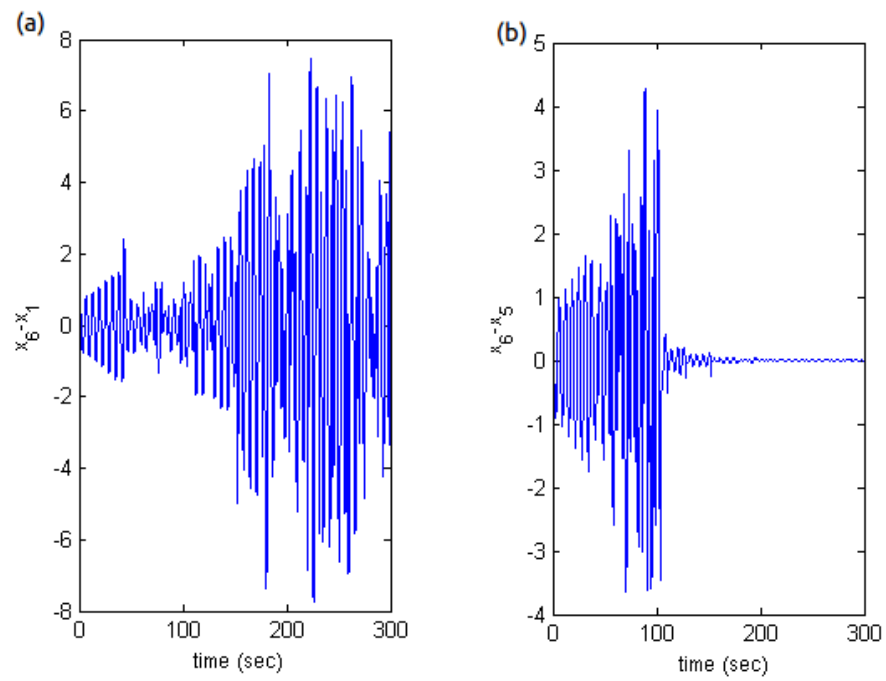
Figure 4.31. State differences for Equation 4.16 where $v = 0.3324$ and $C = 0.9$ (a) $x_6 - x_1$; (b) $x_6 - x_5$.

oscillators is studied. Their w_i parameters, mean natural frequencies and the mean observed frequencies in the phase synchronization state for $\varepsilon = 0.2$ are given in Table 4.7. The external force is applied to the ensemble after the phase synchronization is achieved, at $t = 150$ sec.

In the first approach, represented in Equation 4.13, the periodic force is applied to the mean field with five different frequencies: (i) $v = 1.08$; (ii) $v = 1.18$; (iii) $v = 1.1$; (iv) $v = 0.91$ (mean natural frequency of a randomly chosen oscillator); (v) $v = 1.03$ (period one UPO of a randomly chosen oscillator). As Figure 4.32 shows if the frequencies of the external input is chosen close to the synchronization frequency of the ensemble ($\Omega = 1.1205$), e.g. $v = 1.1$ and $v = 1.08$, the states of the oscillators become more correlated. As the difference between the frequency of the external force and the phase synchronization frequency, the external action suppresses the synchronization. It should be noted that the application of the external periodic force directly to the mean-field (Equation 4.13) does not change the common phase synchronization frequency of the ensemble or break it up.

In the second approach (Equation 4.14), the purpose is to investigate whether the application of any external action in the entrainment region of the oscillator can destroy the synchronization in the ensemble. An external periodic force $sin(v_i t)$ is applied to the corresponding i^{th} oscillator in ensemble after phase synchronization is achieved. The mean observed frequencies Ω_i of the chaotic oscillators are given in Table 4.10 for various amplitudes C. As one can see, the 4th oscillator leaves the group at $C = 0.2$ and then the 6th oscillator leaves. As C coefficient increases, some of the oscillators start to oscillate with some other mean observed frequencies and the correlation between the states is decreased (Figure 4.33). Here, the required minimum value of C to separate one of the oscillators from the ensemble is greater than the one for entraining a single oscillator, because of the mean-field coupling which restrains the group from breaking up.
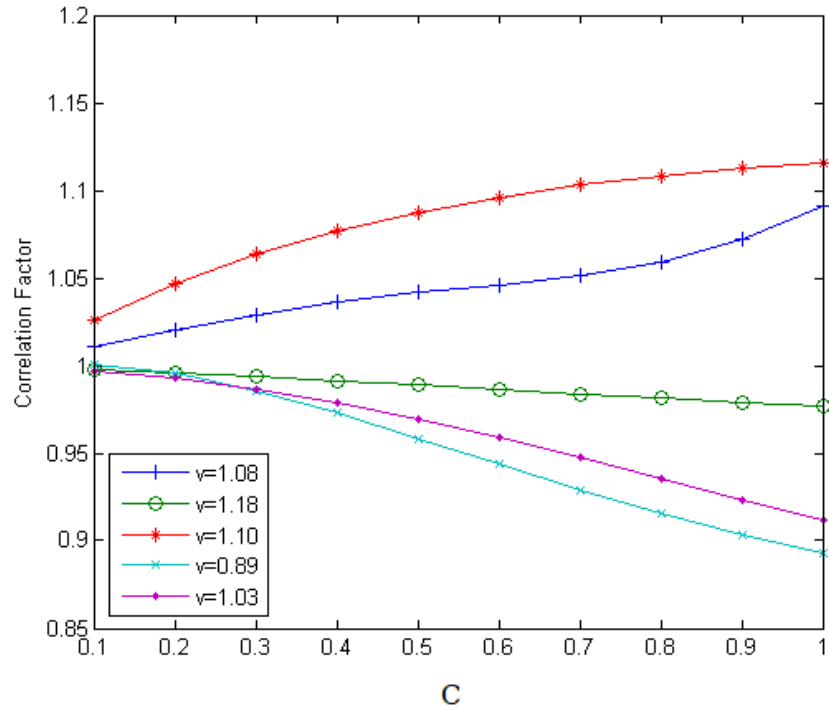
Figure 4.32. Correlation factor of Equation 4.13 versus C for various v.
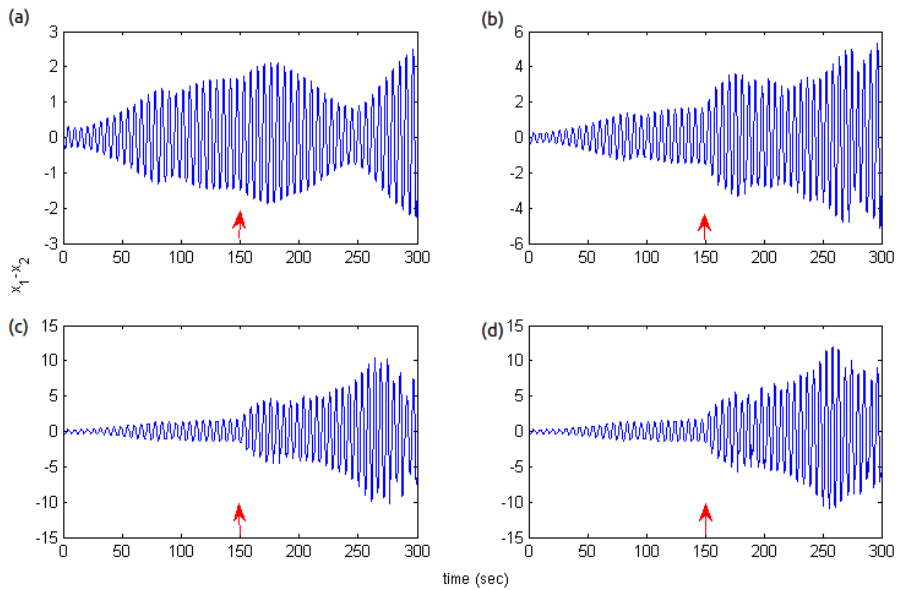
Figure 4.33. State difference between the 1st and 2nd oscillators; (a) $C = 0.2$; (b) $C = 0.5$; (c) $C = 0.8$; (d) $C = 1.0$. External force applied at $t = 150$ sec (red arrow).

Table 4.10. Final mean observed frequencies Ω_i of the oscillators in Equation 4.14 with the external force $sin(v_i t)$ for different coupling strengths.

	$v_1 = 1.145$	$v_2 = 1.14$	$v_3 = 1.1$	$v_4 = 0.9$	$v_5 = 1.1$	$v_6 = 1$
C	Ω_1	Ω_2	Ω_3	Ω_4	Ω_5	Ω_6
0.1	1.1025	1.1025	1.1025	1.1025	1.1025	1.1025
0.2	1.1025	1.1025	1.1025	0.9108	1.1025	1.1025
0.3	1.1025	1.1025	1.1025	1.1025	1.1025	1.1025
0.4	1.1025	1.1025	1.1025	0.9108	1.1025	1.0067
0.5	1.1025	1.1025	1.1025	0.9108	1.1025	1.0067
0.6	1.0546	1.1505	1.1025	0.9108	1.1025	1.0067
0.7	1.1505	1.1505	1.1025	0.9108	1.1025	1.0067
0.8	1.1505	1.1505	1.1025	0.9108	1.1025	1.0067
0.9	1.1505	1.1505	1.1025	0.9108	1.1025	1.0067
1.0	1.1505	1.1505	1.1025	0.9108	1.1025	1.0067

5. DISCUSSION AND CONCLUSION

Throughout this thesis, synchronization of several types of oscillators in several different network schemes, coupled according to different principles is studied. Synchronization control and the possibility of influencing the synchronous behavior of an ensemble are examined.

5.1. Synchronization in Complex Networks

Synchronization of periodic uniform oscillators has been investigated in complex networks with different structural properties. For this purpose, a model of c. elegans' neural network is compared with artificially generated networks, such as Erdös-Rényi networks, Watts-Strogatz networks and Barabasi-Albert networks. It can be stated that small-world property allows synchronization, whereas, the scale-free degree distribution and existence of hubs in a network hampers synchronization. Compared with the artificial ones, the specific structure of a natural network, the neural network of c. elegans, demonstrates itself. Since it is a natural network, it is far from a random graph. Although it has the highest maximum node degree value, it synchronizes better than a scale-free network. Despite of having small-world property, it is not a "pure" small-world network, thus it performs different than a Watts-Strogatz'. Considering the relatively poor synchronizability of the neural network of c. elegans, it is meaningful to conclude that "functionality" does not mean "synchronizability" . It should be remembered that synchronization may be harmful in some cases and evaluation of a natural is based upon optimal functionality in some sense.

It should be noted that, no analytical approach is provided for quantifying synchronization in general complex networks. In this thesis, the number of occupied bins of the histogram of observed frequencies has been used to analyze the synchronization of nonidentical oscillators in complex networks. Here, there is a fine border separating the numerical errors and true analysis for defining the bin size. It is observed that a bin

size of 10^{-3} or 10^{-4} does not make any difference, but this method loses its validity for larger bin sizes. A better analysis could be "node tracking", looking at nodes individually to observe how the form clusters by adjusting their frequencies, which would allow us to detect the synchronization regions. But of course this method is not applicable to large networks, such as brain. As known, researchers use macroscopic measurements for such large networks.

For a further investigation of synchronization in complex networks, weighted and directed couplings can be studied. Also, different types of oscillators can be considered. But apart from these, the most important contribution would be developing analytical tools qualifying synchronizability of complex networks. Also representation of topological features on the coupling strength would be valuable.

5.2. Synchronization of Periodic Uniform Oscillators with Similarity-Dependent Coupling Strengths

Similarity dependent coupling is the most important contribution of this thesis. It is an obvious fact that similars tend to interact more. In this thesis, a special application of this idea has been tested in an ensemble of uniform periodic oscillators, where "similarity " is defined in terms of the difference between the parameters which directly effect synchronizability. When the coupling strengths are chosen as an increasing function of similarity, which is measured in terms of natural frequency difference for our case, it is observed that the overall synchronizability of the network is improved compared to occurrence of clusters uniform coupling strengths. It can be stated that similarity-dependent coupling suppresses individual differences between the oscillators and provides an easily-adapted group.

Certainly, more studies are needed to support this hypothesis. Firstly, larger network sizes and different network topologies need to be studied. Here, node tracking may reveal some effects of structural network properties (such as community and motif formations) on synchronization. Secondly, different types of oscillators should be con-

sidered, i.e. nonuniform periodic ones and chaotic oscillators. For chaotic oscillators, defining similarity for the mean frequencies or for certain UPOs may introduce some other interesting facts.

In this thesis, it has been assumed that the information of natural frequencies is available. However, in most of real situations individual oscillators may not have a priori knowledge about each other's natural frequencies. A more realistic approach can be obtained by assigning the coupling strengths depending on observed frequencies. For such a purpose adequate phase observers may be needed.

Some researchers investigated the effect of physical distance between the nodes on synchronization in complex networks. In this thesis, an all-to-all coupled network is studied, where physical distance has no meaning. But, from our perspective, physical distance may not affect the coupling strength not only by rescaling it, but also by introducing a certain time delay. Formulating couplings strength as a function of this delay may release some other real world phenomena.

5.3. Synchronization of All-to-All Coupled Chaotic Oscillators and Its Control

Synchronization of mean-field-coupled chaotic oscillators has been studied. In an ensemble of identical chaotic oscillators, one can talk of complete synchronization. Identical oscillators have the same mean frequency, but due to the dependence on initial conditions they follow different chaotic attractors. If the coupling strength is strong enough, these oscillators forget their initial conditions and are all locked to a common chaotic attractor, the synchronization subset of the whole system. On the contrary, if an ensemble consists of nonidentical chaotic oscillators, the mean field coupling provides phase synchronization while the amplitudes of the oscillators remain uncorrelated. For stronger coupling strengths the amplitudes become correlated, and if the oscillators initially have slight differences they may completely synchronize.

Next, two different control techniques have been examined for influencing synchronization in these ensembles. In the first method, time delayed mean field is applied to the ensemble both directly and differentially. It is seen that feeding back the time-delayed mean field to an ensemble of identical chaotic oscillators may shorten the time for achieving complete synchronization or to hamper the evolution of the collective behavior. On the other hand, time delayed mean field does not affect the ensemble if it is applied to the systems after achieving complete synchronization, where the mean field oscillations becomes regular. If time delayed mean field is fed back to an ensemble of nonidentical chaotic oscillators after achieving phase synchronization, its effect becomes more crucial. In such a case delayed mean field may increase the correlation between the oscillators, change the synchronization frequency of the ensemble or destroy the phase synchronization.

The second control method is applying external periodic forces to ensembles of identical and nonidentical mean-field-coupled chaotic Rössler systems. In this thesis, two different methods are considered. In the first one, an external periodic force is applied to the mean field. In the second one, the external periodic force is applied directly to the oscillator. Firstly, if an unsynchronized ensemble of identical oscillators is considered, the application of the external for with a frequency equals to the mean observed frequency of the oscillators enhances the synchronization by increasing the number of completely synchronized pairs. Furthermore, if the coupled oscillators are directly entrained by the external force with a frequency equals to the frequency of a UPO of the chaotic oscillators, and then complete synchronization is accomplished. Both of the external forcing methods do not induce any change in a completely synchronized group.

Then phase synchronization of an ensemble of nonidentical chaotic oscillators is studied. If the mean field is forced by an external periodic action with a frequency close to the mean observed frequency of synchronized oscillators, the correlation between the states increases. On the other hand, if the applied frequency is relatively far from the mean observed frequency, phase synchronization remains but the state correlations

decrease. When the periodic external forces are chosen among the ones that can entrain each of the considered oscillators without any mean field coupling and applied directly to the relevant oscillators, phase synchronization of ensemble is destroyed.

The tools used for analysis of synchronization should be mentioned. The power spectral density analysis is used to calculate the mean frequencies of the chaotic oscillators. In an ensemble of identical chaotic (or periodic) oscillators, the difference between the mean field and the output states of the oscillators, ensemble deviation, is investigated for how the state relations evolve as time goes by. Furthermore, the state relations of the coupled nonidentical chaotic oscillators are examined. As can be remembered the phase synchronization between the nonidentical chaotic oscillators is a "weak" synchronization, i.e. the amplitudes remains uncorrelated. But increase in the coupling strengths or applications of appropriate control inputs have been studied introduces correlations between the states. The correlation coefficient, which is a strong statistical tool, has been used to measure this quantity. It should be noted only a few researchers have used correlation factor for detecting synchronization. Of course, as all the synchronization analysis tools do, there are several problems in this method. Depending on structural differences, synchronized chaotic systems may track different chaotic attractors or may not follow each other with a certain lag. Thus comparison of the correlation coefficients may not give an exact idea about the amplitude relations. Phase dynamics of the oscillators can be considered as a better analysis tool. But defining phase of a chaotic oscillator is restricted by the geometry of the flow in the state space, and for many cases it is difficult to defining a surface transversally crossed by all the trajectories. Furthermore, irregular fluctuations of the phase of such an oscillator may hamper the analysis. As an alternative analysis tool, which has not been used in this thesis, Lyapunov exponents can be suggested.

Finally, the user interface designed for the experiments of synchronization in complex networks has limited features. Peopled are welcome to improve this interface and provide a "toolbox" which allows students and researchers to analyze synchronization of various types of oscillators in complex networks and control this collective behavior.

Such a toolbox will accelerate the undergoing researches and will help to understand basis of the synchronization phenomena .

APPENDIX A: DELAYED FEEDBACK CONTROL EXPERIMENTS

Table A.1. Mean observed frequencies of the oscillators in Equation 4.7 for $\tau = T$.

K	Ω_1	Ω_2	Ω_3	Ω_4	Ω_5	Ω_6
-1.0	1.1984	1.1505	1.1984	0.9587	1.1984	1.1984
-0.9	0.9587	0.9587	0.9587	0.9587	0.9587	0.9587
-0.8	1.1505	1.1505	1.1984	0.9587	1.1984	1.1984
-0.7	1.1984	1.1984	1.1984	1.1984	1.1984	1.1984
-0.6	1.1505	1.1505	1.1505	1.1505	1.1505	1.1505
-0.5	1.1025	1.1025	1.1025	1.1025	1.1025	1.1025
-0.4	1.1025	1.1025	1.1025	1.1025	1.1025	1.1025
-0.3	1.1025	1.1025	1.1025	1.1025	1.1025	1.1025
-0.2	1.1025	1.1025	1.1025	1.1025	1.1025	1.1025
-0.1	1.1025	1.1025	1.1025	1.1025	1.1025	1.1025
0.0	1.1025	1.1025	1.1025	1.1025	1.1025	1.1025
0.1	1.1025	1.1025	1.1025	1.1025	1.1025	1.1025
0.2	1.1025	1.1025	1.1025	1.1025	1.1025	1.1025
0.3	1.1025	1.1025	1.1025	1.1025	1.1025	1.1025
0.4	1.1025	1.1025	1.1025	1.1025	1.1025	1.1025
0.5	1.1025	1.1025	1.1025	1.1025	1.1025	1.1025
0.6	1.1025	1.1025	1.1025	1.1025	1.1025	1.1025
0.7	1.1025	1.1025	1.1025	1.1025	1.1025	1.1025
0.8	1.1025	1.1025	1.1025	1.1025	1.1025	1.1025
0.9	1.1025	1.1025	1.1025	1.1025	1.1025	1.1025
1.0	1.1025	1.1025	1.1025	1.1025	1.1025	1.1025

Table A.2. Mean observed frequencies of the oscillators in Equation 4.7 for $\tau = T/2$.

K	Ω_1	Ω_2	Ω_3	Ω_4	Ω_5	Ω_6
-1.0	1.1025	1.1025	1.1025	1.1025	1.1025	1.1025
-0.9	1.1025	1.1025	1.1025	1.1025	1.1025	1.1025
-0.8	1.1025	1.1025	1.1025	1.1025	1.1025	1.1025
-0.7	1.1025	1.1025	1.1025	1.1025	1.1025	1.1025
-0.6	1.1025	1.1025	1.1025	1.1025	1.1025	1.1025
-0.5	1.1025	1.1025	1.1025	1.1025	1.1025	1.1025
-0.4	1.1025	1.1025	1.1025	1.1025	1.1025	1.1025
-0.3	1.1025	1.1025	1.1025	1.1025	1.1025	1.1025
-0.2	1.1025	1.1025	1.1025	1.1025	1.1025	1.1025
-0.1	1.1025	1.1025	1.1025	1.1025	1.1025	1.1025
0.0	1.1025	1.1025	1.1025	1.1025	1.1025	1.1025
0.1	1.1025	1.1025	1.1025	1.1025	1.1025	1.1025
0.2	1.1025	1.1025	1.1025	1.1025	1.1025	1.1025
0.3	1.1025	1.1025	1.1025	1.1025	1.1025	1.1025
0.4	1.1025	1.1025	1.1025	1.1025	1.1025	1.1025
0.5	1.1025	1.1025	1.1025	1.1025	1.1025	1.1025
0.6	1.1025	1.1025	1.1025	1.1025	1.1025	1.1025
0.7	1.1025	1.1025	1.1025	1.1025	1.1025	1.1025
0.8	1.1025	1.1025	1.1025	1.1025	1.1025	1.1025
0.9	1.1025	1.1025	1.1025	1.1025	1.1025	1.1025
1.0	1.1025	1.1025	1.1025	1.1025	1.1025	1.1025

Table A.3. Mean observed frequencies of the oscillators in Equation 4.7 for $\tau = <T_i>$.

K	Ω_1	Ω_2	Ω_3	Ω_4	Ω_5	Ω_6
-1.0	1.1025	1.1025	1.1025	1.1025	1.1025	1.1025
-0.9	1.1025	1.1025	1.1025	1.1025	1.1025	1.1025
-0.8	1.1025	1.1025	1.1025	1.1025	1.1025	1.1025
-0.7	1.1025	1.1025	1.1025	1.1025	1.1025	1.1025
-0.6	1.1025	1.1025	1.1025	1.1025	1.1025	1.1025
-0.5	1.1025	1.1025	1.1025	1.1025	1.1025	1.1025
-0.4	1.1025	1.1025	1.1025	1.1025	1.1025	1.1025
-0.3	1.1025	1.1025	1.1025	1.1025	1.1025	1.1025
-0.2	1.1025	1.1025	1.1025	1.1025	1.1025	1.1025
-0.1	1.1025	1.1025	1.1025	1.1025	1.1025	1.1025
0.0	1.1025	1.1025	1.1025	1.1025	1.1025	1.1025
0.1	1.1025	1.1025	1.1025	1.1025	1.1025	1.1025
0.2	1.1025	1.1025	1.1025	1.1025	1.1025	1.1025
0.3	1.1025	1.1025	1.1025	1.1025	1.1025	1.1025
0.4	1.1025	1.1025	1.1025	1.1025	1.1025	1.1025
0.5	1.1025	1.1025	1.1025	1.1025	1.1025	1.1025
0.6	1.1025	1.1025	1.1025	1.1025	1.1025	1.1025
0.7	1.1025	1.1025	1.1025	1.1025	1.1025	1.1025
0.8	1.1025	1.1025	1.1025	1.1025	1.1025	1.1025
0.9	1.1025	1.1025	1.1025	1.1025	1.1025	1.1025
1.0	1.1025	1.1025	1.1025	1.1025	1.1025	1.1025

Table A.4. Mean observed frequencies of the oscillators in Equation 4.7 $\tau = T_6$.

K	Ω_1	Ω_2	Ω_3	Ω_4	Ω_5	Ω_6
-1.0	1.1505	1.1505	1.1505	1.1505	1.1505	1.1505
-0.9	1.1505	1.1505	1.1505	1.1505	1.1505	1.1505
-0.8	1.1505	1.1505	1.1505	1.1505	1.1505	1.1505
-0.7	1.1505	1.1505	1.1505	1.1505	1.1505	1.1505
-0.6	1.1025	1.1025	1.1025	1.1025	1.1025	1.1025
-0.5	1.1025	1.1025	1.1025	1.1025	1.1025	1.1025
-0.4	1.1025	1.1025	1.1025	1.1025	1.1025	1.1025
-0.3	1.1025	1.1025	1.1025	1.1025	1.1025	1.1025
-0.2	1.1025	1.1025	1.1025	1.1025	1.1025	1.1025
-0.1	1.1025	1.1025	1.1025	1.1025	1.1025	1.1025
0.0	1.1025	1.1025	1.1025	1.1025	1.1025	1.1025
0.1	1.1025	1.1025	1.1025	1.1025	1.1025	1.1025
0.2	1.1025	1.1025	1.1025	1.1025	1.1025	1.1025
0.3	1.1025	1.1025	1.1025	1.1025	1.1025	1.1025
0.4	1.1025	1.1025	1.1025	1.1025	1.1025	1.1025
0.5	1.1025	1.1025	1.1025	1.1025	1.1025	1.1025
0.6	1.1025	1.1025	1.1025	1.1025	1.1025	1.1025
0.7	1.0546	1.0546	1.0546	1.0546	1.0546	1.0546
0.8	1.0546	1.0546	1.0546	1.0546	1.0546	1.0546
0.9	1.0546	1.0546	1.0546	1.0546	1.0546	1.0546
1.0	1.0546	1.0546	1.0546	1.0546	1.0546	1.0546

Table A.5. Mean observed frequencies of the oscillators in Equation 4.7 where $\tau = T_1$.

K	Ω_1	Ω_2	Ω_3	Ω_4	Ω_5	Ω_6
-1.0	1.0546	1.0546	1.0546	1.0546	1.0546	1.0546
-0.9	1.0546	1.0546	1.0546	1.0546	1.0546	1.0546
-0.8	1.0546	1.0546	1.0546	1.0546	1.0546	1.0546
-0.7	1.0546	1.0546	1.0546	1.0546	1.0546	1.0546
-0.6	1.0546	1.0546	1.0546	1.0546	1.0546	1.0546
-0.5	1.0546	1.0546	1.0546	1.0546	1.0546	1.0546
-0.4	1.1025	1.1025	1.1025	1.1025	1.1025	1.1025
-0.3	1.1025	1.1025	1.1025	1.1025	1.1025	1.1025
-0.2	1.1025	1.1025	1.1025	1.1025	1.1025	1.1025
-0.1	1.1025	1.1025	1.1025	1.1025	1.1025	1.1025
0.0	1.1025	1.1025	1.1025	1.1025	1.1025	1.1025
0.1	1.1025	1.1025	1.1025	1.1025	1.1025	1.1025
0.2	1.1025	1.1025	1.1025	1.1025	1.1025	1.1025
0.3	1.1025	1.1025	1.1025	1.1025	1.1025	1.1025
0.4	1.1025	1.1025	1.1025	1.1025	1.1025	1.1025
0.5	1.1025	1.1025	1.1025	1.1025	1.1025	1.1025
0.6	1.1025	1.1025	1.1025	1.1025	1.1025	1.1025
0.7	1.1025	1.1025	1.1025	1.1025	1.1025	1.1025
0.8	1.1025	1.1025	1.1025	1.1025	1.1025	1.1025
0.9	1.1025	1.1025	1.1025	1.1025	1.1025	1.1025
1.0	1.1025	1.1025	1.1025	1.1025	1.1025	1.1025

Table A.6. Mean observed frequencies of the oscillators in Equation 4.8 where $\tau = T$.

K	Ω_1	Ω_2	Ω_3	Ω_4	Ω_5	Ω_6
-1.0	1.1984	1.1984	1.1984	1.1984	1.1984	1.1984
-0.9	1.1984	1.1984	1.1984	1.1984	1.1984	1.1505
-0.8	1.1505	1.1505	1.1505	1.1505	1.1505	1.1505
-0.7	1.1505	1.1505	1.1505	1.1505	1.1505	1.0067
-0.6	1.1505	1.1505	1.1505	1.1505	1.1505	1.0067
-0.5	1.1505	1.1505	1.1505	1.1505	1.1505	1.0067
-0.4	1.1505	1.1505	1.0546	1.1505	1.0546	1.0546
-0.3	1.1025	1.1025	1.0546	1.0546	1.0546	1.0546
-0.2	1.1025	1.1025	1.0546	1.0546	1.0546	1.0546
-0.1	1.1025	1.1025	1.1025	1.1025	1.1025	1.1025
0.0	1.1025	1.1025	1.1025	1.1025	1.1025	1.1025
0.1	1.1025	1.1025	1.1025	1.1025	1.1025	1.1025
0.2	1.1025	1.1025	1.1025	1.1025	1.1025	1.1025
0.3	1.1025	1.1025	1.1025	1.1025	1.1025	1.1025
0.4	1.1025	1.1025	1.1025	1.1025	1.1025	1.1025
0.5	1.1025	1.1025	1.1025	1.1025	1.1025	1.1025
0.6	1.1025	1.1025	1.1025	1.1025	1.1025	1.1025
0.7	1.1025	1.1025	1.1025	1.1025	1.1025	1.1025
0.8	1.1025	1.1025	1.1025	1.1025	1.1025	1.1025
0.9	1.1025	1.1025	1.1025	1.1025	1.1025	1.1025
1.0	1.1025	1.1025	1.1025	1.1025	1.1025	1.1025

Table A.7. Mean observed frequencies of the oscillators in Equation 4.8 where $\tau = T/2$.

K	Ω_1	Ω_2	Ω_3	Ω_4	Ω_5	Ω_6
-1.0	1.1984	1.1984	0.9587	0.9587	0.9587	0.9587
-0.9	1.1505	1.1505	0.9587	0.9587	0.9587	0.9587
-0.8	1.1505	1.1505	1.0067	0.9587	1.0067	0.9587
-0.7	1.1505	1.1505	1.0067	0.9587	1.0067	0.9587
-0.6	1.1505	1.1505	1.0546	0.8629	1.0546	1.0067
-0.5	1.1505	1.1505	1.0546	0.8629	1.0546	1.0067
-0.4	1.1025	1.1025	1.0546	1.0546	1.0546	1.0067
-0.3	1.1025	1.1025	1.0546	1.0546	1.0546	1.0546
-0.2	1.1025	1.0546	1.0546	1.0546	1.0546	1.0546
-0.1	1.1025	1.1025	1.1025	1.1025	1.1025	1.1025
0.0	1.1025	1.1025	1.1025	1.1025	1.1025	1.1025
0.1	1.1025	1.1025	1.1025	1.1025	1.1025	1.1025
0.2	1.1025	1.1025	1.1025	1.1025	1.1025	1.1025
0.3	1.1025	1.1025	1.1025	1.1025	1.1025	1.1025
0.4	1.1025	1.1025	1.1025	1.1025	1.1025	1.1025
0.5	1.1025	1.1025	1.1025	1.1025	1.1025	1.1025
0.6	1.1025	1.1025	1.1025	1.1025	1.1025	1.1025
0.7	1.1025	1.1025	1.1025	1.1025	1.1025	1.1025
0.8	1.1025	1.1025	1.1025	1.1025	1.1025	1.1025
0.9	1.1025	1.1025	1.1025	1.1025	1.1025	1.1025
1.0	1.1025	1.1025	1.1025	1.1025	1.1025	1.1025

Table A.8. Mean observed frequencies of the oscillators in Equation 4.8 where $\tau =< T_i >$.

K	Ω_1	Ω_2	Ω_3	Ω_4	Ω_5	Ω_6
-1.0	1.1505	1.1025	1.0067	0.8629	1.0546	0.9587
-0.9	1.1505	1.1025	1.0546	0.8629	1.0546	0.9587
-0.8	1.1505	1.1505	1.0546	0.8629	1.0546	0.9587
-0.7	1.1505	1.1505	1.0546	0.8629	1.0546	0.9587
-0.6	1.1025	1.1025	1.0546	0.8629	1.0546	1.0067
-0.5	1.1025	1.1025	1.0546	0.8629	1.0546	1.0067
-0.4	1.1025	1.1025	1.0546	1.1025	1.0546	1.0546
-0.3	1.1025	1.1025	1.0546	1.0546	1.0546	1.0546
-0.2	1.0546	1.0546	1.0546	1.0546	1.0546	1.0546
-0.1	1.1025	1.1025	1.1025	1.1025	1.1025	1.1025
0.0	1.1025	1.1025	1.1025	1.1025	1.1025	1.1025
0.1	1.1025	1.1025	1.1025	1.1025	1.1025	1.1025
0.2	1.1025	1.1025	1.1025	1.1025	1.1025	1.1025
0.3	1.1025	1.1025	1.1025	1.1025	1.1025	1.1025
0.4	1.1025	1.1025	1.1025	1.1025	1.1025	1.1025
0.5	1.1025	1.1025	1.1025	1.1025	1.1025	1.1025
0.6	1.1025	1.1025	1.1025	1.1025	1.1025	1.1025
0.7	1.1025	1.1025	1.1025	1.1025	1.1025	1.1025
0.8	1.1025	1.1025	1.1025	1.1025	1.1025	1.1025
0.9	1.1025	1.1025	1.1025	1.1025	1.1025	1.1025
1.0	1.1025	1.1025	1.1025	1.1025	1.1025	1.1025

Table A.9. Mean observed frequencies of the oscillators in Equation 4.8 where $\tau = T_6$.

K	Ω_1	Ω_2	Ω_3	Ω_4	Ω_5	Ω_6
-1.0	1.1505	1.1505	1.1984	0.8629	1.1984	1.1984
-0.9	1.1505	1.1505	1.1505	0.8629	1.1505	1.1505
-0.8	1.1505	1.1505	1.1505	0.8629	1.1505	1.1505
-0.7	1.1505	1.1505	1.1505	0.8629	1.1505	1.1505
-0.6	1.1505	1.1505	1.1505	0.8629	1.1505	1.1505
-0.5	1.1505	1.1505	1.1025	1.1025	1.1025	1.1025
-0.4	1.1025	1.1025	1.1025	1.1025	1.1025	1.1025
-0.3	1.1025	1.1025	1.0546	1.1025	1.0546	1.1025
-0.2	1.1025	1.1025	1.0546	1.0546	1.0546	1.0546
-0.1	1.1025	1.1025	1.1025	1.1025	1.1025	1.1025
0.0	1.1025	1.1025	1.1025	1.1025	1.1025	1.1025
0.1	1.1025	1.1025	1.1025	1.1025	1.1025	1.1025
0.2	1.1025	1.1025	1.1025	1.1025	1.1025	1.1025
0.3	1.1025	1.1025	1.1025	1.1025	1.1025	1.1025
0.4	1.1025	1.1025	1.1025	1.1025	1.1025	1.1025
0.5	1.1025	1.1025	1.1025	1.1025	1.1025	1.1025
0.6	1.1025	1.1025	1.1025	1.1025	1.1025	1.1025
0.7	1.1025	1.1025	1.1025	1.1025	1.1025	1.1025
0.8	1.1025	1.1025	1.1025	1.1025	1.1025	1.1025
0.9	1.1025	1.1025	1.1025	1.1025	1.1025	1.1025
1.0	1.1025	1.1025	1.1025	1.1025	1.1025	1.1025

Table A.10. Mean observed frequencies of the oscillators in Equation 4.8 where $\tau = T_1$.

K	Ω_1	Ω_2	Ω_3	Ω_4	Ω_5	Ω_6
-1.0	0.9587	0.9587	0.9587	0.8629	0.9587	0.9587
-0.9	1.0067	1.1025	1.0067	0.8629	1.0067	0.9587
-0.8	1.1025	1.1025	1.0067	0.8629	1.0067	0.9587
-0.7	1.1025	1.1025	1.0546	0.8629	1.0546	0.9587
-0.6	1.0546	1.0546	1.0546	0.8629	1.0546	0.9587
-0.5	1.0546	1.0546	1.0546	1.0546	1.0546	1.0546
-0.4	1.0546	1.0546	1.0546	1.0546	1.0546	1.0546
-0.3	1.0546	1.0546	1.0546	1.0546	1.0546	1.0546
-0.2	1.0546	1.0546	1.0546	1.0546	1.0546	1.0546
-0.1	1.1025	1.1025	1.1025	1.1025	1.1025	1.1025
0.0	1.1025	1.1025	1.1025	1.1025	1.1025	1.1025
0.1	1.1025	1.1025	1.1025	1.1025	1.1025	1.1025
0.2	1.1025	1.1025	1.1025	1.1025	1.1025	1.1025
0.3	1.1025	1.1025	1.1025	1.1025	1.1025	1.1025
0.4	1.1025	1.1025	1.1025	1.1025	1.1025	1.1025
0.5	1.1025	1.1025	1.1025	1.1025	1.1025	1.1025
0.6	1.1025	1.1025	1.1025	1.1025	1.1025	1.1025
0.7	1.1025	1.1025	1.1025	1.1025	1.1025	1.1025
0.8	1.1505	1.1505	1.1505	1.1505	1.1505	1.1505
0.9	1.1505	1.1505	1.1505	1.1505	1.1505	1.1505
1.0	1.1505	1.1505	1.1505	1.1505	1.1505	1.1505

APPENDIX B: EXTERNAL FORCE CONTROL EXPERIMENTS

Table B.1. Correlation coefficients for Equation 4.13 where $\varepsilon = 0.1$.

C	$v = 1.0134$	$v = 0.5067$	$v = 0.3324$	$v = 1.5046$
0.1	0.9948	0.9984	1.0007	1.0115
0.2	1.0029	1.0235	1.0124	1.0134
0.3	1.0005	1.0298	1.0058	1.0295
0.4	0.9801	1.0116	1.0301	1.0200
0.5	0.9821	1.0040	1.0305	0.9850
0.6	1.0164	1.0065	1.0195	0.9974
0.7	1.0275	1.0217	1.0287	0.9959
0.8	1.0196	0.9971	1.0085	1.0112
0.9	1.0302	1.0219	1.0258	0.9384
1.0	1.0304	0.9989	1.0170	1.0220

Table B.2. Correlation coefficients for Equation 4.14 where $\varepsilon = 0.1$.

K	$v = 1.0134$	$v = 0.5067$	$v = 0.3324$	$v = 1.5046$
0.1	1.0008	1.0012	1.0012	1.0013
0.2	0.9992	1.0013	1.0012	1.0013
0.3	0.9987	0.9989	0.9995	0.9992
0.4	0.9971	1.0012	0.9990	0.9992
0.5	0.9979	1.0011	0.9984	0.9990
0.6	0.9978	0.9988	0.9996	1.0031
0.7	1.0043	1.0009	1.0003	1.0028
0.8	0.9984	0.9970	1.0002	1.0057
0.9	0.9951	0.9999	1.0198	1.0113
1.0	0.9948	0.9984	1.0007	1.0115

Table B.3. Correlation coefficients for Equation 4.13 where $\varepsilon = 0.2$.

K	$v = 1.0134$	$v = 0.5067$	$v = 0.3324$	$v = 1.5046$
0.1	1	1	1	1
0.2	1	1	1	1
0.3	1	1	1	1
0.4	1	1	1	1
0.5	1	1	1	1
0.6	1	1	1	1
0.7	1	1	1	1
0.8	1	1	1	1
0.9	1	1	1	1
1.0	1	1	1	1

Table B.4. Correlation coefficients for Equation 4.14 where $\varepsilon = 0.2$.

C	$v = 1.0134$	$v = 0.5067$	$v = 0.3324$	$v = 1.5046$
0.1	1	1	1	1
0.2	1	1	1	1
0.3	1	1	1	1
0.4	1	1	1	1
0.5	1	1	1	1
0.6	1	1	1	1
0.7	1	1	1	1
0.8	1	1	1	1
0.9	1	1	1	1
1.0	1	1	1	1

APPENDIX C: MANUAL FOR THE INTERFACE

Algorithm Settings category includes the followings:

- SelectAlgorithm:
  (i) ExtForceSync: Algorithm for externally forced oscillators
  (ii) 2MutualSync: Algorithm for 2 mutually coupled oscillators
  (iii) AlltoAllSync: Algorithm for N coupled oscillators. If this option is selected, user can edit the topology settings and coupling matrix.
- Coupling Strength: Defines common coupling strength between the oscillators
- Node Type:
  (i) Firefly
  (ii) ChaoticRösslerOscillator
  (iii) ChaoticLorenzOscillator
  (iv) Specify: For combining the oscillators mentioned above. If this option is chosen, a predefined "config.txt" file including the nodes identity numbers, type numbers and their parameters.
- NaturalFreqWn & Params
  (i) Rand: For assigning random natural frequencies of fireflies and allowed parameters of the chaotic oscillators. User should define the mean and variance of the Gaussian distribution.
  (ii) Defined: For assigning predefined natural frequencies and parameters. User can choose one of the variables existing in MATLAB's workspace.
  (iii) SetWn: The box must be filled to confirm the parameters.
  (iv) Show W: To show the assigned parameters in the main figure
- CreateConfig: For creating a configuration file in order to specify node types
- UpdateConfig: For updating the configuration file in order to specify node types

Topology Settings category includes the followings:

- ChooseTopology:
  - (i) Ring1: A ring topology for coupling with one of the nearest neighbors.
  - (ii) Ring2: A ring topology for coupling with two nearest neighbors.
  - (iii) MeanField: A globally coupled network.
  - (iv) UserDefined: A user defined graph existing in the workspace under the name "AdjMat".
- # of Nodes: For defining the network size.

Coupling Matrix category includes the followings:

- Coupling Matrix: A table demonstrates the coupling matrix of the considered network with respect to the node numbers.
- Set C.M.: If the user desired to edit the displayed coupling matrix, this box must be filled.
- Set C.M.: After editing the coupling matrix, user must press this button to confirm. If it proceeds properly, the node colors will change.
- EffectType: To specify how the interacting nodes effect from each other
  - (i) SelfDeg: Normalizing to total effect to one oscillator according to the degree of this oscillator
  - (ii) MaxDeg: Normalizing to total effect to one oscillator according to the maximum degree of the network
  - (iii) MeanDeg: Normalizing to total effect to one oscillator according to the mean degree of the network
  - (iv) Similarity: For similarity dependent coupling approach

Analysis category includes the following:

- Power Spectrum: For power spectral distribution analysis of the results

Simulation category includes the followings:

- Sim Time(sec): Defining the total simulation time in terms of seconds
- Play: The button for starting simulation

Please note that user should type "global PlotPoints" in the command window of MATLAB to call the time solution to the work space.

Error messages pop up for the following cases:

- Wrong Parameter Dimension: Parameter vector must be a Nx1 vector.
- Wrong Coupling Matrix Dimension: Coupling matrix must be a NxN matrix.
- Unspecified Parameters: User must fill the "SetWn" box.
- Unspecified Topology: If AlltoAllSync option is chosen, topology type must be selected.
- Unspecified Effect Type: Effect type must be chosen in any case.

REFERENCES

1. Pikovsky, A., M. Rosenblum and J. Kurths, *Synchronization: A Universal Concept in Nonlinear Sciences*, Cambridge University Press, New York, NY, USA, 2001.

2. Zaks, M. A., E. H. Park, M. Rosenblum and J. Kurths, "Alternating Locking Rations in Imperfect Phase Synchronization", *Physical Review Letters*, Vol. 82, pp. 4228–4231, 1999.

3. Newman, M., "Network Data: Neural Network", Jun. 2011, `http://www-personal.umich.edu/ mejn/netdata/`, accessed at Decembre 2011.

4. Watts, D. J. and S. Strogatz, "Collective Dynamics of 'Small-World' Networks", *Nature*, Vol. 393, pp. 440–442, 1998.

5. Boccaletti, S., V. Latora, Y. Moreno, M. Chaves and D.-U. Hwang, "Complex Networks: Structure and Dynamics", *Physics Reports*, Vol. 424, pp. 175–308, 2006.

6. Fell, J. and N. Axmacher, "The Role of Phase Synchronization in Memory Processes", *Nature Review Neuroscience*, Vol. 12, pp. 105–118, 12.

7. Fries, P., "A Mechanism for Cognitive Dynamics: Neuronal Communication through Neuronal Coherence", *TRENDS in Cognitive Sciences*, Vol. 9, No. 10, pp. 474–480, 2001.

8. Schnitzler, A. and J. Gross, "Normal and Pathological Oscillatory Communication in the Brain", *Nature Review Neuroscience*, Vol. 6, No. 4, pp. 285–296, 2005.

9. Erdos, P. and A. Renyi, "On Random Graphs", *Publicationes Mathematicae*, Vol. 6, pp. 290–297, 1959.

10. Barabasi, A. L. and R. Albert, "Emergence of Scaling in Random Networks", *Science*, Vol. 286, pp. 509–512, 1999.

11. Strogatz, S., *Sync: The Emerging Science of Spontaneous Order*, Hyperion, New York, NY, USA, 2003.

12. Appleton, E. V., "The Automatic Synchronzation of Triode Oscillator", *Mathematical Proceedings of the Cambridge Philosophical Society.*, Vol. 21, pp. 231–248, 1922.

13. van der Pol, B., "Forced Oscillations in a Circuit with Nonlinear Resistance", *Philosophical Magazine*, Vol. 3, pp. 64–80, 1927.

14. Lumsden, P. J., "Rhythms in Plant Life", Jan. 2001, `http://www.encyclopedia.com/doc/1G2-3408000265.html`, accessed at Marc 2012.

15. Czeisler, C. A., J. F. Duffy, T. L. Shanahan, E. N. Brown, J. F. Mitchell, D. W. Rimmer, J. M. Ronda, E. J. Silva, J. S. Allan, J. S. Emens, D. J. Dijk and R. E. Kronauter, "Stability, Precision, and Near 24-hour Period of Human Circadian Pacemaker", *Science*, Vol. 284, pp. 2177–2181, 1999.

16. Buck, J. B. E., "Mechanism of Rhythmic Synchronous Flashing of Fireflies", *Science*, Vol. 159, pp. 1319–1327, 1968.

17. Walker, T. J., "Acoustic Synchrony: Two Mechanisms in the Snowy Tree Cricket.", *Science*, Vol. 166, pp. 891–894, 1969.

18. Garica-Ojalvo, J., M. Elowitz and S. Strogatz, "Modeling a Multicellular Clock: Repressilators Coupled by Quorum Sensing", *PNAS*, Vol. 101, pp. 10955–10960, 2004.

19. Néda, Z., "Tumultuous Applause Can Transform Itself Into Waves of Synchronized

Clappling", *Nature*, Vol. 403, No. 6772, pp. 849–850, 2000.

20. Aschoff, J., *Vertebrate Circadian Systems*, Springer, Berlin, 1982.

21. Sturis, J., "Entrainment of Pulsatile Insluin Secretion by Oscillatory Glucose Infusion", *The Journal of Clinical Investigation*, Vol. 87, pp. 439–445, 1991.

22. Buckzek, C., "Laser Injection Locking", *Proceedings of the IEEE,*, Vol. 61, No. 10, pp. 1411–1431, 1973.

23. Buck, J., "Control of Flashing in Fireflies", *Journal of Comparative Physiology A*, Vol. 144, pp. 277–286, 1981.

24. Kuramoto, Y., *Chemical Oscillations, Waves and Turbulence*, Springer, Berlin.

25. Adler, R., "A Study of Locking Phenomena In Oscillators", *Proceedings of the IRE*, Vol. 34, No. 6, pp. 351–357, 1946.

26. Winfree, A. T., *The Geometry of Biological Time*, Springer-Verlang, Berlin, Germany, 1980.

27. Wiener, N., *Cybernetics: Or Control and Communication in the Animal and the Machine*, John Wiley & Sons, New York, NY, USA, 1948.

28. Boccaletti, S., J. Kurths, G. Osipov, D. L. Valladares and C. S. Zhou, "The Synchronization of Chaotic Systems", *Physics Reports*, Vol. 366, pp. 1–101, 2002.

29. McClintonick, M. K., "Menstrual Synchrony and Suppression", *Nature*, Vol. 229, pp. 244–245, 1971.

30. Richard, P., B. M. Bakker, B. Teusink, K. Van Dam and H. V. Westerhoff, "Acetaldehyde Mediates the Synchronization of Sustained Glycolytic Oscillations in Population of Yeast Cells", *European Journal of Biochemistry*, Vol. 235, pp. 238–

241, 1996.

31. Fujisaka, H., "Stability Theory of Synchronized Motion in Coupled-Oscillator Systems", *Progress of Theoretical Physics*, Vol. 69, No. 1, pp. 32–47, 1983.

32. Pecora, L., "Synchronization in Chaotic Systems", *Physical Review Letters*, Vol. 64, pp. 821–824, 1990.

33. Rosenblum, M., P. A. and J. Kurths, "Phase Synchronization of Chaotic Oscillators", *Physical Review Letters*, Vol. 76, p. 1804, 1996.

34. Rosa Jr., E., E. Ott and M. H. Hess, "Transition to Phase Synchronization of Chaos", *Physical Review Letters*, Vol. 80, No. 8, pp. 1642–1645, 1998.

35. Rosenblum, M., P. A. and J. Kurths, "From Phase to Lag Synchronization in Coupled Chaotic Oscillators", *Physical Review Letters*, Vol. 78, pp. 4193–4196, 1997.

36. Rulkov, N. F., M. M. Sushchik, L. S. Tsimring and H. D. I. Abarbanel, "Generalized Synchronization of Chaos in Directionally Coupled Chaotic Systems", *Physical Review E.*, Vol. 51, No. 2, pp. 980–994, 1995.

37. Fermat, R. and G. Solis-Perales, "On the Chaos Synchronization Phenomena", *Physical Review A.*, Vol. 262, No. 1, pp. 50–60, 1999.

38. Stefanski, A., *Determining Thresholds of Complete Synchronization and Application*, World Scientefic Publishing, Singapore, 2009.

39. Kapitaniak, T., "Synchronization of Chaos Using Continious Control", *Physical Review E.*, Vol. 50, pp. 1642–1644, 1994.

40. Amritkar, R. E. and N. Gupte, "Synchronization of Chaotic Orbits: The Effect of a Finite Time Step", *Physical Review E.*, Vol. 47, pp. 3889–3895, 1993.

41. Kocarev, L. and U. Parlitz, "General Approach for Chaotic Synchronization with Applications to Communication", *Physical Review Letters*, Vol. 74, pp. 5028–5031, 1995.

42. Güémez, J. and M. A. Matrias, "Modified Method for Synchronizing and Cascading Chaotic Systems", *Physical Review E*, Vol. 52, pp. 2145–R2148, 1995.

43. Balmforth, N., C. Tresser, P. A. Worfolk and C. W. Wu, "Master-Slave Synchronization and the Lorenz Equations", *Chaos*, Vol. 7, No. 3, pp. 392–394, 1997.

44. Pazo, D., M. A. Zaks and J. Kurths, "Role of Unstable Periodic Orbits in Phase and Lag Synchronization between Coupled Chaotic Oscillators", *Chaos*, Vol. 13, No. 1, pp. 309–318, 2003.

45. A., P., M. Rosenblum and J. Kurths, "Phase Synchronization in Regular and Chaotic Systems", *International Journal of Bifurcation and Chaos*, Vol. 10, No. 10, pp. 2291–2305, 2000.

46. A., P., M. A. Zaks, M. Rosenblum, G. Osipov and J. Kurths, "Phase Synchronization of Chaotic Oscillators in Terms of Periodic Orbits", *Chaos*, Vol. 7, No. 4, pp. 680–687, 1997.

47. Parlitz, U., L. Junge, W. Lauterborn and L. Kocarev, "Experimental Observation of Phase Synchronization", *Physical Review E.*, Vol. 54, No. 2, pp. 2115–2118, 1996.

48. Rosa Jr., E., W. B. Pardo, C. M. Ticos, J. A. Walkenstein and M. Monti, "Phase Synchronization of Chaos in a Plasma Discharge Tube", *International Journal of Bifurcation and Chaos*, Vol. 10, No. 11, pp. 2551–2564, 2000.

49. Park, E. H., M. A. Zaks and J. Kurths, "Phase Synchronization in the Forced Lorenz System", *Physical Review E.*, Vol. 60, pp. 6627–6638, 1999.

50. *Generalized Synchronization, Predictability and Equivalence of Unidirectionally Coupled Systems*, Vol. 76, 1996.

51. Barreto, E. and P. So, "Mechanisims for the Development of Unstable Dimension Variability and the Breakdown of Shadowing in Coupled Chaotic Systems", *Physical Review Letters*, Vol. 85, No. 12, pp. 2490–2493, 2000.

52. Pyragas, K., O. V. Popovych and P. A. Tass, "Controlling Synchrony in Oscillatory Networks with a Separate Stimulation-Registration Setup", *Europhysics Letters*, Vol. 80, p. 40002, 2007.

53. Tass, P. A., *Phase Resetting in Medicine and Biology: Stochastic Modelling and Data Analysis*, Springer, Berlin, Germany, 1999.

54. Tass, P. A., "A Model of Desynchronizing Deep Brain Stimulation with a Demand-Controlled Coordinated Reset of Neural Subpopulations", *Biological Cybernetics*, Vol. 89, pp. 81–88, 2003.

55. Rosenblum, M. and P. A., "Controlling Synchrony in an Ensemble of Globally Coupled Oscillators", *Physical Review Letters*, Vol. 92, No. 11, p. 114102, 2004.

56. Rosenblum, M. and A. Pikovsky, "Delayed Feedback Control of Collective Synchrony: An Approach to Suppression of Pathological Brain Rhythms", *Physical Review E.*, Vol. 70, p. 041904, 2004.

57. Popovych, O. V., C. Hauptmann and P. A. Tass, "Desynchronization and Decoupling of Interacting Oscillators by Nonlinear Delayed Feedback", *International Journal of Bifurcation and Chaos*, Vol. 16, p. 1977, 2006.

58. Lynch, S., *Dynamical Systems with Applications Using Maple*, Springer-Birkhäuser, Boston, USA, 2010.

59. Pyragas, K., "Continuous Control of Chaos by Self-Controlling Feedback", *Phys.*

Lett. A., Vol. 170, pp. 421–427, 1992.

60. Pyragas, K., *Control of Dynamical Systems via Time-Delayed Feedback and Unstable Controller*, pp. 221–256, Kluwer Academic Publishers, Netherlands, 2003.

61. Hövel, P., M. A. Dahlem and E. Schöll, "Control of Synchronization in Coupled Neural Systems by Time-Delayed Feedback", *International Journal of Bifurcation and Chaos*, Vol. 20, No. 3, pp. 813–825, 2010.

62. Baibolatov, Y., M. Rosenblum, Z. Z. Zhanabaev, M. Kyzgarina and A. Pikovsky, "Periodically Forced Ensemble of Nonlinearly Coupled Oscillattors: From Partial to Full Synchrony", *Physical Review E.*, Vol. 80, p. 046211, 2009.

63. Belykh, V. N., G. Osipov, N. Kucklander, B. Blasius and J. Kurths, "Automatic Control of Phase Synchronization in Coupled Complex Oscillators", *Physica D*, Vol. 200, pp. 81–104, 2005.

64. Pikovsky, A., M. Rosenblum, G. Osipov and J. Kurths, "Phase Synchronization of Chaotic Oscillators by External Driving", *Physica D*, Vol. 104, pp. 219–238, 1997.

65. Pikovsky, A. and S. Ruffo, "Finite-Size Effects in a Population of Interacting Oscillators", *Physical Review E.*, Vol. 59, No. 2, pp. 1633–1636, 1999.

66. White, J. G., E. Southgate, J. N. Thomson and S. Brenner, "The Structure of the Nervous System of the Nematode Caenorhabditis Elegans", *Philosophical Transactions of the Royal Society B*, Vol. 314, pp. 1–340, 1986.

67. Arenas, A., A. Diaz-Guilera, J. Kurths, Y. Moreno and C. S. Zhou, "Synchronization in Complex Networks", *Physics Reports*, Vol. 469, pp. 93–153, 2008.

68. Osipov, G., A. Pikovsky, M. Rosenblum and J. Kurths, "Phase Synchronization Effects in a Lattice of Nonidentical Rossler Oscillators", *Physical Review E.*, Vol. 55, pp. 2353–2361, 1997.

69. Pikovsky, A., M. Rosenblum and J. Kurths, "Synchronization in a Population of Globally Coupled Chaotic Oscillators", *Europhysics Letters*, Vol. 34, No. 3, pp. 165–170, 1996.

70. Childs, L. M. and S. Strogatz, "Stability Diagram for the Forced Kuramoto Model", *Chaos*, Vol. 18, No. 4, p. 043128, 2008.